Università degli Studi dell'Insubria

Scuola di Dottorato dell'Università degli Studi dell'Insubria

Dottorato di Ricerca in Medicina Sperimentale e
Traslazionale – XXXII CICLO

The Peptide Transporters of teleost fish, an emerging model in translational research: functional characterization and comparative study of SLC15A1a (PepT1a) and SLC15A1b (PepT1b) transporters

Tutor: Prof.ssa Elena Bossi

Coordinatore: Prof.ssa Daniela Negrini

Tesi di Dottorato di:
Francesca Vacca
Matr: 730378

Anno Accademico 2018-2019

Index

Scientific Production

The data reported in this Ph.D. thesis have been published in following papers:

- *"Identification and characterization of the Atlantic Salmon Peptide Transporter 1a"*- A Gomes & **F Vacca**, R Cinquetti, K Murashita, A Barca, E Bossi, I Rønnestad, T Verri. American Journal of Physiology-Cell Physiology, published on-line 30 October 2019, Doi 10.1152/ajpcell.00360.2019, PubMed ID 31664857.

- *"The Peptide Transporter 1a of the zebrafish Danio rerio, an emerging model in nutrigenomics and nutrition research: molecular characterization, functional properties and expression analysis"* – **F Vacca** & A Barca, AS Gomes, A Mazzei, B Piccinni, R Cinquetti, G Del Vecchio, A Romano, I Rønnestad, E Bossi, T Verri. Genes & Nutrition, accepted; in press. Doi 10.1186/s12263-019-0657-3.

The national and international conferences in which the data have been presented are the following:

- **F Vacca**, R Cinquetti, AS Gomes, I Rønnestad, T Verri, E Bossi. *Molecular modification and functional studies of two PepT1 isoforms of Salmo salar: new insights of PepT1a*, 11th Meeting of Young Researchers in Physiology, 25-27 May 2017 Firenze, Italy. Session- communication: cell physiology II. **Oral communication**.

- **F Vacca**, R Cinquetti, AS Gomes, I Rønnestad, A Barca, T Verri, E Bossi. *Comparison of the electrophysiological properties of the two paralogues of Salmo salar oligopeptide transporter PepT1: new insights from PepT1a vs. PepT1b*, 10th Conference SFB-Transmembrane Transporter in health and disease, 6-9 September 2017, Vienna, Austria. **Poster**.

- AS Gomes, K Murashita, **F Vacca**, E Bossi, T Verri, AE O Jordal, A Aksnes, I Rønnestad. *Sensing and transport of peptides in the gastro-intestinal tract of Atlantic salmon*. World Aquaculture 2017, 28 June 2017, Cape Town, South Africa. Oral communication, presenter: Ana S Gomes.

- AS Gomes, T Verri, E Bossi, **F Vacca,** R Cinquetti, A Barca, K Murashita, AE O Jordal, A Aksnes, I Rønnestad. *Transport and sensing of di- and tripeptides in the gastrointestinal tract of post-smolt Atlantic salmon.* Aquaculture Europe 2017, 17-20 October 2017, Dubrovnik, Croatia. **Poster**.

- **F Vacca**, R Cinquetti, AS Gomes, I Rønnestad, A Barca, T Verri, E Bossi. *Salmo salar oligopeptide transporters PepT1a and PepT1b: a comparative electrophysiological characterization of the transport of lysine-containing peptides***,** 12th Meeting of Young Researchers in Physiology, 3-4 May 2018 Anacapri, Italy. Session- communication: cell physiology II. **Oral communication**.

- **F Vacca**, AS Gomes, R Cinquetti, K Murashita, FG Imperiali, A Barca, T Verri, I Rønnestad, E Bossi. *Salmo salar oligopeptide transporters PepT1a and PepT1b: a comparative electrophysiological characterization of partial and complete transport cycle,* Europhysiology, 14-16 September 2018, London, UK. Abstract book https://www.physoc.org/events/europhysiology2018/#tab-04, session A- Poster Communications: Epithelia & Membrane Transport, pp 162P-163P. **Poster**.

- **F Vacca**, AS Gomes, R Cinquetti, K Murashita, FG Imperiali, A Barca, T Verri, I Rønnestad, E Bossi. *A comparative electrophysiological analysis on the transport cycle of PepT1a and PepT1b, two di/tripeptide transporters from the Atlantic salmon Salmo salar*, 69th SIF National Congress Italian Physiological Society, 19-21 September 2018 Florence, Italy. Abstract book, poster session II: Metabolism, Nutrition and System Physiology, pp 225. **Poster**. Selected for Pitch Contest: **Oral communication**.

- AS Gomes, I Rønnestad, K Murashita, **F Vacca**, R Cinquetti, A Barca, A Aksnes, E Bossi, T Verri. *Comparative characterization of the Atlantic salmon (Salmo salar L.) di/tripeptide transporters PepT1a and PepT1b*, Experimental Biology 2019, 6-9 April 2019, Orange County Convention Center Orlando, Florida, USA. Program book, topic Category: Comparative Section Osmoregulation Endocrine And Metabolic Physiology, pp. 243.

- **F Vacca**, R Cinquetti, AS Gomes, I Rønnestad, A Barca, T Verri, E Bossi. *Functional characterization of partial and complete transport cycle of the newly cloned Atlantic salmon (Salmo salar) PepT2 (Slc15a2) di/tripeptide transporter*, 13th Meeting of Young Researchers in Physiology, 10-12 May 2019 Anacapri, Italy. Session-communication: cardiovascular and cellular physiology. **Oral communication**.

- **F Vacca**, AS Gomes, R Cinquetti, A Barca, T Verri, K Murashita, I Rønnestad, E Bossi. *Comparative electrophysiological characterization of Slc15a1 transporters,*

PepT1a and PepT1b, of two teleost fishes, Joint Workshop- Membrane proteins: Structure Function and Regulation, organized on behalf of the Groups "Membrane" and "Proteine" belonging to the SIB (Società Italiana di Biochimica e Biologia Molecolare), 27-28 June 2019, University of Calabria, "University Club". **Oral communication** and Selected for Travel Fellowship.

- **F Vacca**, E Bossi, AS Gomes, R Cinquetti, A Barca, T Verri, K Murashita, I Rønnestad. *Functional analysis, properties and kinetics of a PepT2-type di/tripeptide transporter of the Atlantic salmon (Salmo salar) highly expressed in midgut and hindgut,* 70th SIF National Congress Italian Physiological Society and Congress Federation of European Physiological Societies, 10-13 September 2019, Bologna, Italy. (2019) Abstracts. Acta Physiologica 227: e13366 Doi 10.1111/apha.13366, pp. 5. Abstract selected: **Oral communication**.

- **F Vacca**, E Bossi, AS Gomes, R Cinquetti, A Barca, T Verri, K Murashita, I Rønnestad*., Slc15a1 transporters in teleosts fish: PepT1a and PepT1b, comparative functional studies.* 70th SIF National Congress Italian Physiological Society and Congress Federation of European Physiological Societies, 10-13 September 2019, Bologna, Italy. (2019) Abstracts. Acta Physiologica 227: e13366 Doi 10.1111/apha.13366, pp. 50. Oral communication, presenter: Elena Bossi.

- T Verri, E Bossi, A Barca, G Del Vecchio, A Mazzei, G Piccinno, **F Vacca**, R Cinquetti, K Murashita, AS Gomes, I Rønnestad, *Diversity in proton movement and coupling to substrate in vertebrate PepT1 proteins: a 'phylogenetic' approach.* 70th SIF National Congress Italian Physiological Society and Congress Federation of European Physiological Societies, 10-13 September 2019, Bologna, Italy. Abstracts. Acta Physiologica 227: e13366 Doi 10.1111/apha.13366, pp. 52. Oral communication, presenter: Tiziano Verri.

- G Piccinno, G Del Vecchio, A Barca, A Mazzei, **F Vacca**, R Cinquetti, K Murashita, AS Gomes, E Bossi, I Rønnestad, T Verri, *SoLute Carrier (SLC) genes expression along the rostro-caudal axis of adult teleost fish gut: a publicly available datasets analysis.* 70th SIF National Congress Italian Physiological Society and Congress Federation of European Physiological Societies, 10-13 September 2019, Bologna, Italy. Abstracts. Acta Physiologica 227: e13366 Doi 10.1111/apha.13366, pp. 112. **Poster**.

- E Bossi, D Zanella, **F Vacca**, C Roseti, R Gornati, G Bernardini, *To cross or not to cross: some, but not all, metal nanoparticles enter cells by plasma membrane direct crossing.* Nano Day IV, 11-14 December 2019, Milan, Italy. Abstract book ISBN 978-88-943573-8-7, pp. 86. Oral communication, presenter: Elena Bossi.

Preface

Translational research is the process that applies knowledge from basic biology to techniques and devices in order to solve critical medical issues. Increasingly, in the last decades, the aim of basic and translational research is to identify specific cellular and animal models for every single process, physiological or pathological, under study. To find out the adequate animal model, one of the best approaches is to study the orthologues of human genes in different species. Small differences in sequences correlated to significant differences in functionality provide fundamental information for structure-function studies. This aspect is particularly important in detailing the molecular basis of disease and disorders, gathering insights on genotype-phenotype interaction i.e. on the relationship between sequence and function of a given gene. The increase in the number of fully sequenced genomes offers important advances in comparative genomics and in translational research. The finding that in zebrafish genome there are orthologues for most human genes is particularly important. In fact, zebrafish are for many aspects an outstanding model organism for high-throughput phenotyping and modeling human disease and disorders. However, while the biological sequences (nucleic acid or amino acidic sequences) from species can be rapidly analyzed and compared with each other, information on the biological role of a given gene product can be compared only after a detailed functional characterization. With this in mind, the research work of this thesis has the aim to understand and compare the function of proteins belonging to the SoLute Carrier family 15 member A1 SLC15A1 (PepT1) in some fish orthologues. The intestinal transporter PepT1 represents a major route of peptides and drug intake. It can mediate the uptake of a large number of molecules (more than 8000 compounds), such as peptide like

molecules and bacterial peptides. Besides the important role of PepT1 in the nutrient uptake and sensing, the study of the functional properties of this transporter is of great importance not only for the involvement in pathological states, but also for its double role in therapeutic approaches. The development of drugs that target the intestinal peptide transporter PepT1 has become one of the main challenges to circumvent the reduced oral bioavailability, which is one of the principal causes of prodrugs failure in preclinical and clinical studies. Due to its high expression in intestinal inflammatory diseases and in some cancer cells, PepT1 has been also suggested as possible target of newly developed nano delivery system like functionalized nanoparticles (NPs).

Chapter 1. Introduction

Comparative approaches: from comparative genomics to translational research

The advances in genomics and next-generation sequencing have provided new opportunities for comparative studies by the constant and rapid increasing in the number of fully sequenced genomes. The comparative approach is required and useful in many fields of basic and translational research.

New insights into evolutionary, genetic, biochemical, metabolic, and physiological pathways are gained by the comparison of entire genomes from different species. Comparative genomics allows to better understand how species have evolved and to determine the function of genes and noncoding regions of the genome. Numerous functions of human genes have been identified by examining their counterparts in organism models.

Moreover, the abundance of genomic information is a great value in translational and biomedical research, particularly in the comprehension of the molecular basis of human genetic disorders. For instance, animal models can be chosen to monitor pathogenesis of human diseases based on explicit gene homology. The gene homology is being increasingly leveraged to create functional disease models in animals that can help to understand newly identified human pathogenic mutations or altered metabolic pathway in order to develop of new clinical tools for the diagnosis, for drug discovery and to test the efficacy of emerging therapies (Phillips and Westerfield, 2014).

Fish species as models in environmental and comparative genomics

In recent years, several fish species have played important roles in deepening the knowledge of the vertebrate genome evolution. These studies yielded a great number of information on the structure of human genes and provided precious insights into the molecular basis of human genetic and disorders.

Fish represent the most heterogeneous group of vertebrates; they are divided into three major superclasses i.e. Agnatha, Chondrichthyes and Osteichthyes. This latter superclass consists of a large and diverse subclass called Actinopterygii, representing around 95 % of all existing fish species and whose majority (almost 99 %) is grouped in the infraclass called teleost fish (Volff, 2005).

With more than 30.000 species identified so far (www.fishbase.org), teleost fish exhibit extraordinary diversity in morphology, lifestyle and physiology. This biodiversity is largely due to peculiar features in their genome (Volff, 2005; Ravi and Venkatesh, 2008). During Actinopterygian lineage evolution, a round of whole genome duplication led to extensive paralogy among fish genes. Paralogue genes have been maintained in teleost genome, thus providing the driving force behind the diversification of gene functions and the generation of diversity among fish species. Fish offer interesting physiological models of response and adaptation to an astonishing range of environmental conditions. In aquatic habitat, the intimate physiological contact between fish internal fluid compartments and external environment potentially induces a high sensitivity of organisms to different water-borne parameters such as: oxygen level, temperature, salinity and even pollutants. So, the environmental genomics largely employ fish as model to study the organism-environment interface though genomic approaches (Cossins and Crawford, 2005).

While the studies on environmental genomics are useful to better understand the molecular basis of the adaptive strategies in fish lineage, the studies on

comparative genomics allow to detail the evolution in vertebrate genome and the function of individual genes.

An interesting application of teleost fish model in environmental and comparative genomics is represented by the studies on the SoLute Carrier superfamily (SLC), that includes genes for passive transporters, ion-coupled transporters and exchangers, which have an important role as 'metabolic gates' of cells and mediate the transport of a wide range of essential nutrients and metabolites and drugs (Zhang et al., 2019). According to their biological significance, the SLC members are conserved throughout evolution, thus the comparative approach is a good tool to investigate the relation between structural features and functional properties of these transporters. Moreover, the major part of these proteins has been recently highlighted for their importance as pharmacological targets (Cesar-Razquin et al., 2015). In recent years, structural data were obtained by crystal structure and molecular models of SLC homologues from a great variety of eukaryotes and prokaryotes. These structures provided templates useful in clarifying the substrate specificity of the human SLC members (Colas et al., 2016). On a functional perspective, studies about features of teleost transporter revealed extraordinary assortment of molecular and functional properties, reflecting peculiar protein adaptations to the physiology of the species and/or to the environments in which they live. The information obtained from teleost fish models are a good tool to clarify how human transporters work and what are their essential roles in human physiology (Romano et al., 2014). Notably, recent studies on mammals suggested that some intestinal SLC transporters important in nutrient uptake, have also the role of nutrient sensors (Zietek and Daniel, 2015; Daniel and Zietek, 2015). In fish, the intestine is a multifunctional organ not only involved in nutrient absorption but also with other physiological role like osmoregulation, acid-base regulation and nutrient sensing etc. The study and characterization of role of intestinal SLC proteins is of great importance for fish nutrition, but also

for human health. In the last decades, the increase in the number of databank sequences has revealed progressively that teleost fish SLC genes are duplicated (Verri et al., 2017). The presence of duplicated genes provides novel opportunities for refining the investigations on regulation and function of distinct paralogues.

The identification of fish orthologues of some mammalian genes highlighted that many aspects of developmental pathways, organ system and physiological mechanism are conserved (Roest Crollius and Weissenbach, 2005). For instance, the basic mechanism involving central and peripheral signaling in the controlling appetite has been preserved along the vertebrate evolution, in particular between teleost fish and mammals (Soengas et al., 2018). All these aspects made teleost fish attractive models for investigating the physiology of appetite control under an evolutionary perspective.

Fish as models for understanding the vertebrate endocrine regulation of feeding

Fish and mammals differ in many aspects of their physiology, particularly in terms of metabolic rates, growth patterns and energy storage. Fish show low metabolic rate since they are poikilotherms and do not expend energy to maintain a constant body temperature (van de Pol et al., 2017); many species have indeterminate growth (Volkoff et al., 2009), while others present energy-demanding foraging behavior to survive during periods of low food availability (Ronnestad et al., 2017). In addition to physiological function differences, mammals and fish differ in brain and gastrointestinal tract morphologies. These organs are involved mainly in homeostatic and hedonic regulation of food intake. Despite this, the regulation of food intake is well conserved between teleost and mammals since they share similar endocrine signals, mainly hormones and neuropeptides (Soengas et al., 2018).

The homeostatic energy supply in vertebrate is guaranteed by several neuroendocrine pathways regulated by a dual signal component: a short term and a long term signaling (**Figure 1.1**).

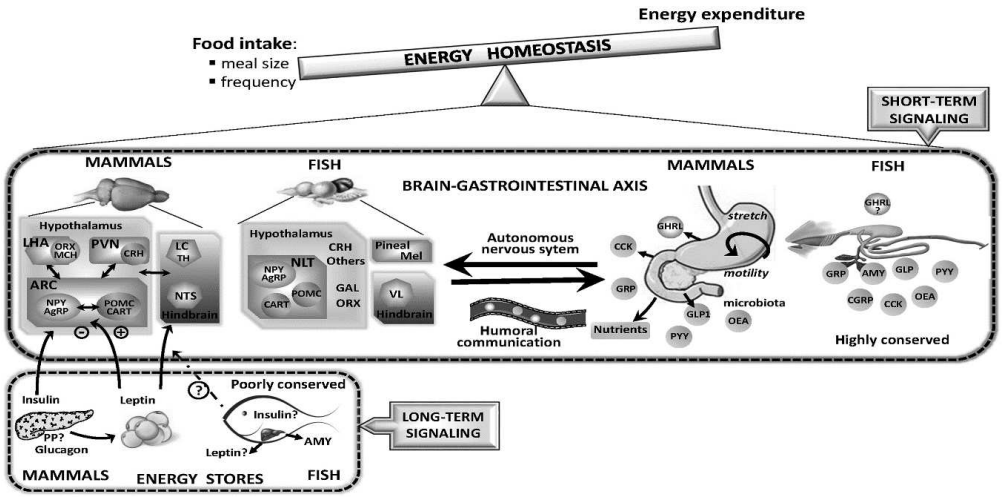

Figure 1.1 Schematic model summarizing the short- and long-term control of energy homeostasis integrating central and peripheral signals in mammals and fish (Soengas et al., 2019).

The short-term control of food intake is mediated by central and peripheral signals that take place between brain and gastrointestinal tract (Soengas et al., 2018). The major components of short-term signaling from gastrointestinal tract are represented by nutrients and appetite-regulating hormones. Both these signals send nutritional information to the control areas in the brain through afferent nerves or via systemic circulation. In gastrointestinal tract, the nutrient sensing mechanisms lead to the modulation of the secretion of appetite-regulating hormones by enteroendocrine cells.

Several appetite regulatory hormones were isolated in some teleost fish species and they showed similar structures and modes of action to their mammalian

counterparts. Among the hormones that induce appetite and food consumption (orexigenic function), ghrelin (GHRL) is produced in the stomach of fish (as in mammals) or in the intestine of some stomach less species (Ronnestad et al., 2017). Several studies, conducted on fish, suggested that ghrelin is an appetite stimulator (Amole and Unniappan, 2009; Hatef et al., 2015; Tian et al., 2015) and a modulator of digestive processes and glucose homeostasis (Blanco et al., 2017).

The counterpart of mammalian peptides with food-intake limiting function (anoxigenic function) have been also identified in fish. Some of them are cholecystokinin (CCK), gastric-releasing peptide (GRP), peptide tyrosine tyrosine (PYY) and glucagone like peptides (GLP-1 and GLP-2). Although in fish little is known about the detailed mechanisms underlying the physiological roles of all these peptides, recent results supported the conservation of anorexigenic function of these hormones in the teleost lineage (Ronnestad et al., 2017).

The short-term signals from the gut to the brain interact with long-term signals that modulate the sensitivity of brain responses to gastrointestinal satiation signaling (Cummings and Overduin, 2007). In mammals, the long-term signals are primarily humoral. The adiposity hormones, leptin and insulin, communicate with the brain in modulating fat stores to the brain and regulate short-term food intake to achieve long-term energy balance (Yamada et al., 2006).

As opposed to mammals which have a single leptin gene expressed in subcutaneous fat, many fish species have several leptin gene paralogues expressed mostly in liver and intestine (Ronnestad et al., 2017). The presence of multiple leptin paralogues in teleosts may underline such a variety of different functional properties of leptin in fish (Soengas et al., 2018). While some findings suggested that leptin is involved in mobilization of lipid stores in fish, emerging data suggest that leptin might be important in other metabolic processes, such as glucose homeostasis (Michel et al., 2016), and coordination of energy

metabolism and somatic growth (Won et al., 2016; Ronnestad et al., 2017). In mammals, insulin is an adiposity signal that conveys fat store information to the brain. It has anabolic functions at the periphery and catabolic effects in the hypothalamus (Havel, 2001). Whereas the anorexigenic action of insulin and its mechanism of action are clear in mammals, the effects of insulin treatment on food intake in fish are contradictory (Delgado et al., 2017).

The regulation of food intake, gastrointestinal physiology and nutrient metabolism is also mediated by gut microbiota that refers to the population of microorganisms residing in the intestine. Among the possible mechanisms in which microbiota acts on the regulation of appetite, is reported the production of certain compounds e.g. short-chain fatty acids (SCFAs). These molecules may affect the secretion of appetite-regulating hormones by enteroendocrine cells (Alcock et al., 2014). The microbiota was shown to influence behavior, feeding, digestive functions and metabolism in fish in a species-specific manner (Volkoff, 2019).

The dysbiosis, i.e. imbalances in the microbiota, was shown to contribute to etiology of several diseases. The role of microbiota was reported in intestinal inflammatory disorders such as Inflammatory Bowel Disease (IBD) (Belkaid and Hand, 2014); in several autoimmune diseases (Belkaid and Hand, 2014); in Type II Diabetes and Metabolic Syndrome (Belkaid and Hand, 2014); in cancer (Belkaid and Hand, 2014); in obesity (Cuevas-Sierra et al., 2019) and eating disorders (Ruusunen et al., 2019).

Although gut microbiota of mammal and fish are different, Valenzuela and colleagues (Valenzuela et al., 2018) showed that germ free zebrafish larvae could be colonized by human gut microorganism. This result together with the similar role of microbiota on fish and mammal biology (Teame et al., 2019; Bates et al., 2007), open an interesting area to study host-microbiota interactions using zebrafish as a model (Teame et al., 2019).

Fish as models in translational research: spotlight on zebrafish

Among teleost fish, zebrafish (*Danio rerio*) have become the most used laboratory model for their main features, such as: small size, the ease of breeding, optical clarity of embryos, well-characterized extrauterine development, quick maturation, reaching larval stage by 72 hours post-fertilization, and ease of genetic manipulation. All these features make zebrafish very suitable and increasingly used to study developmental biology, and gene function (Bradford et al., 2017). In addition, zebrafish have been recognized to be valuable vertebrate models for studying human disease and associated therapeutics (Deveau et al., 2017; Liu et al., 2016).

The zebrafish genome contains orthologues for many human genes, as reported by the ninth assembly of the zebrafish genome (Zv9), published on 17 April 2013 (Howe et al., 2013). The comparison with the human reference genome showed that 71,4% of human genes have at least one zebrafish orthologue, 2.601 genes of which (82%) have morbidity descriptions listed in OMIM (Online Mendelian Inheritance in Man) (Howe et al., 2013). Moreover, the advance in functional genomics techniques, in both forward and reverse genetics approaches, has enabled the systematic linkage between genotype and phenotype, revealing a lot of genes in zebrafish involved in cell metabolism, morphogenesis, tissue homeostasis, organogenesis and cancer progression (Fuentes et al., 2018).

After the identification of human orthologues of annotated protein-coding genes in zebrafish, the usefulness of zebrafish as a disease model for translational research has increased dramatically. CRISPR/Cas9 technology has revolutionized genome editing, representing the most important advances in zebrafish disease modelling (Patton and Tobin, 2019). The major advantage offered by the technique is the generation of site-specific mutation in genome that can be performed in a tissue-specific manner. The precision gene editing in

zebrafish provides a powerful platform to improve the knowledge on gene-phenotype relation (Tessadori et al., 2018) and gene-gene (and even gene-environment) interactions in human disorders (Patton and Tobin, 2019; Farr et al., 2018). Moreover, it enables the rapid testing of candidate disease genes identified through human genetics (Ton et al., 2018).

The zebrafish has also emerged as a particularly useful system for studying the tissue inflammation and infection. Notably, zebrafish has been recently used as a model to study intestinal inflammation for its transparent body (Teame et al., 2019). Oehlers and coworkers successfully used zebrafish to study the susceptibility genes and host-microbe interactions in IBD (Oehlers et al., 2011a; Oehlers et al., 2011b).

A fascinating area in recent and rapid expansion that shows zebrafish as powerful model organism, is the study on the role of metabolism in obesity, disease (including dyslipidaemia, diabetes and fatty liver disease), and tumor.

A major strength of studying obesity in zebrafish is the ability to use fluorescent probe to identify genes involved in defects of lipid metabolism *in vivo* (Farber et al., 2001). Several obesity models were developed in zebrafish using changes in diet or genetic manipulations such as modifications of genes encoding appetite hormones or metabolic pathways (Zang et al., 2018). Taken together, diet-induced and genetic-induced models provided an *in vivo* system in which it is possible to study the environmental, physiological and genetic basis of obesity and to screen new developed drugs to treat obesity (Zang et al., 2018).

For diabetes modelling, although an appropriate model to study diabetes long term effect is still lacking in zebrafish, the disease complications such as diabetic retinopathy (Jung et al., 2016) and changes in bone metabolism (Carnovali et al., 2016) were investigated using long immersion of larval or adult zebrafish in glucose solutions. This approach allowed to generate a zebrafish model of chronic hyperglycemia.

To investigate cancer progression, zebrafish have emerged as powerful platform due to the close resemblance at molecular and anatomical level between zebrafish models of cancer and human tumors. Different techniques develop zebrafish models of cancer either by exposure to carcinogens or due to genetic mutation of tumor suppressor genes or introduction of an oncogene (Santoriello and Zon, 2012). Dysregulation of metabolism is a central driver of several diseases and cancer types. In tumor progression the metabolism reprogramming is well-known and established hallmark event (Hanahan and Weinberg, 2011); the most well-described metabolic change is the Warburg effect in which cancer cells increase glucose uptake and glycolytic activity (Vander Heiden et al., 2009). Several studies suggested the efficacy of zebrafish tumor models to yield new insights on the molecular mechanisms of the Warburg effect (Sandoval et al., 2017; Shtraizent et al., 2017). Recently, zebrafish models of melanoma revealed that the Warburg effect is a cancer "archetype" (i.e. co-opted cellular state) that emerges during the tumor progression (Baron et al., 2018).

Emerging studies that used zebrafish as a model system are focused on the integration of metabolomics and transcriptomics methodologies to illuminate the mechanism underlying metabolic dysfunction of disease and metabolic reprogramming of tumor (Salmi et al., 2019).

In the field of drug discovery and development, the tissue-specific distribution of molecules is important for disease treatment. In this regard, the body transparence of zebrafish gives more benefits in pharmacokinetics study, particularly in investigating the drug distributions in the context of the whole animal. By the screening of a large panel of fluorescent molecules, Yao and coworkers found 15 molecules that showed a tissues-specific distribution in zebrafish larvae (Yao et al., 2017). Among these molecules, two structurally similar chemotherapeutic compounds, doxorubicin and epirubicin, were observed to have distinct distribution preferences. Notably, the liver-specific distribution of epirubicin was associated with a greater antiproliferative effect in

a zebrafish model of hepatic hyperplasia (Yao et al., 2017). This and many other studies suggest that zebrafish is a powerful model in drugs discovery and development. Moreover, these studies provided a novel approach for understanding how to minimize off-target toxicities and may have important implications for drug efficacy (Patton and Tobin, 2019).

SoLute Carrier transporters (SLC)

The cells control the movement of many substrates across plasma and inner membranes by membrane integral proteins: channels, pumps and transporters. Their roles are importing and exporting molecules, including water, ions, nutrients, vitamins, cofactors, and many drugs across the lipid bilayer. All these roles are fundamental for cellular homeostasis. Transport proteins can be involved in active and passive transport system which generate ion gradients across membranes, employing different energy-coupling mechanisms. These systems are defined as primary- or secondary-active transport systems. ATP-binding cassette (ABC) transporters and ion pumps (ATPases) are primary-active. Ion pumps hydrolyze ATP to pump ions as Na^+, K^+, H^+, Ca^{2+} against their electrochemical gradient across the lipid bilayer, in/out of cells or organelles. Ion gradients are used to drive uphill transport processes across biological membranes. On the other hand, passive transporters (facilitated transporters) allow passage of solutes according to their gradient. In 2004, the definition of SLC (SoLute Carrier) was introduced to define the genes encoding passive transporters and secondary active transporters: ion coupled symporters and antiporters. A membrane protein has been assigned to a specific SLC family if it has at least 20-25% amino acid sequence identity to other members of that family (Hediger et al., 2004). The SLC classification was then used for solute carriers of all kingdoms, from animals to bacteria.

After the G-protein-coupled receptors (GPCRs), SLCs are the second-largest family of membrane proteins in the human genome (Hoglund et al., 2011). The HUGO (HUman Genome Organisation) Gene Nomenclature Committee (HGNC) provides a list of transporter families of the SLC gene series (www.genenames.org). According to the current counting (www.bioparadigms.org), human SLC genes include over 400 members, distributed in 65 subfamilies based on their sequence similarity (Hediger et al., 2013) (www.bioparadigms.org). In line with the classification of the human genes, teleost fish genes for SLC-type transporters have been collected preliminarily in the GenBank database (Dec 2010–Mar 2011) and classified in more than 50 families (Verri et al., 2012). The most relevant species are zebrafish with 304 genes identified, followed by Atlantic salmon (*Salmo salar*) with 53 genes. According to the whole-genome duplication, several SLC genes are duplicated in teleost fish. Moreover, in salmonids genome, where independent events of polyploidization were detected (Volff, 2005), probably more than two copies of the same SLC gene could be found.

Despite their non-uniform distribution, SLC are globally expressed throughout the body and in human are highly expressed in kidney, brain, liver, gut, and heart, where they mediate the transport of a wide spectrum of essential nutrients and metabolites across cellular or subcellular compartments, consistently with the tissue metabolic characteristics. The transported substrates include glucose, amino acids and small peptides, fatty acids and lipids, vitamins, neurotransmitters, inorganic/metal ions and many other solutes. Current research focuses on the roles of SLC transporters in nutrient and metabolic sensing, regulation, and drug development (Zhang et al., 2019).

SoLute Carrier 15 family (SLC15)

The digestion and uptake of dietary proteins in the intestinal lumen are mainly in the form of free amino acids and small peptides. After intestinal absorption, the amino acids and small peptides reach the systemic circulation to be delivered to various tissues as energy metabolites or resources for protein synthesis. While free amino acids are absorbed via several kinds of SLC transporters (Broer, 2008), the di- and tripeptides are solely transported by the SoLute Carrier 15 family (SLC15) (Spanier, 2014), also referred to as the Proton coupled Oligopeptide Transporters family (POT) (Paulsen and Skurray, 1994) or Peptide Transport Family (PTR). Originally discovered in bacteria (Hagting et al., 1994), members of the SLC15 family were found in all kingdoms of life, with the exception of the Archaea (Newstead, 2017a).

The SLC15 family includes four known members in vertebrates (Daniel and Kottra, 2004). PepT1 and PepT2 (encoded by SLC15A1 and SLC15A2 genes, respectively) are oligopeptide transporters. Pht1 and Pht2 (encoded by SLC15A4 and SLC15A3 genes, respectively) are peptide/histidine transporters. Finally, a putative fifth member of SLC15 family is reported, the SLC15A5, which is partially known in sequence but unknown in function (Sreedharan et al., 2011).

While many studies evaluated the implications of PepT1 and PepT2 in biological processes, few investigations are focused on the peptide/histidine transporters up to now.

Primary sites of the functional expression of PepT1 and PepT2 are the intestine and kidney, respectively. Additionally, other localization sites have been identified, including bile duct epithelium, pancreas and liver for PepT1, and brain, lung and mammary gland for PepT2 (Viennois et al., 2018). In the apical surface of epithelial cells, PepT1 represents the low-affinity/high-capacity system and it is the main route for dietary peptide uptake. PepT2 on the other hand represents the high affinity/low-capacity variant, thought to mediate more

selective transport. PepT1 and PepT2 are proton coupled symporters, thus their function is strictly dependent on the transmembrane proton electrochemical gradient. PepT1 and PepT2 mediate the uptake of a large number of substrates (400 different dipeptides, 8000 different tripeptides) (Brandsch et al., 2008; Vig et al., 2006) and many peptidomimetic compounds, β-lactam antibiotics, selected ACE inhibitors and renin inhibitors, as well as antiviral and anticancer drugs (Spanier and Rohm, 2018; Brodin et al., 2002).

Pht1 and Pht2 were initially cloned from the brain (Yamashita et al., 1997; Sakata et al., 2001), but they resulted to be expressed in a variety of tissues including spleen and thymus, intestinal segments, eye and lung (Viennois et al., 2018). Pht1 and Pht2 were identified subcellularly rather than in the plasma membrane, thus they are considered endosomal/lysosomal transporters (Song et al., 2018). Due to their subcellular localization, the driving force, the transport mode and the substrate specificity have not been analyzed systematically for these two transporters. The functional characterization of the rat Pht1 transporter (Yamashita et al., 1997) and of the human Pht1 transporter (Bhardwaj et al., 2006) showed an increasing in the uptake of substrate in the presence of a proton gradient. This observed pH dependence suggested that the peptide/histidine transporters have a similar electrogenic mode of operation as it occurs for the PepT-type proteins (Daniel and Kottra, 2004). Nevertheless, even though Pht1 and Pht2 can transport di- and tripeptides, it is unknown whether they can transport the same wide substrate spectrum of PepT1 and PepT2. In contrast to oligopeptide transporters, Pht1 and Pht2 are reported to accept free L-histidine as substrate and currently they are considered the high affinity transporters for histidine and histidine-containing dipeptides, such as carnosine (β-alanine-L-histidine) and carnosine-like molecules (Yamashita et al., 1997; Sakata et al., 2001).

Among the SoLute Carrier 15 family, PepT1 transporter is deeply studied in human and mammalian models, as well as one of the best characterized

transporters in teleost fish due to its major physiological role in protein absorption, nutrition and body growth, ultimately (Verri et al., 2017).

SLC15A1 (PepT1)

PepT1 gene cloning and tissue expression

In 1994, the complementary DNA coding for the rabbit PepT1 was cloned screening an intestinal cDNA library, expressed in *Xenopus laevis* oocytes and used for uptake studies of ^{14}C-labelled glycyl-sarcosine (Fei et al., 1994). Subsequently, PepT1 was isolated by expression and genomic cloning from other mammalian species such as human (Liang et al., 1995), rat (Saito et al., 1995), mouse (Fei et al., 2000), sheep, cow, pig (Chen et al., 1999) and macaque (Zhang et al., 2004a).

The first teleost fish PepT1 transporter was cloned from zebrafish in 2003 (Verri et al., 2003). The electrophysiological characterization in *X. laevis* oocytes showed that zebrafish PepT1 was able to mediate substrate transport as a low affinity/high capacity system (Verri et al., 2003). Later, cDNA sequences of PepT1 transporters were cloned and functionally characterized from European see bass (*Dicentrachus labrax*) (Sangaletti et al., 2009), Atlantic salmon (*Salmo salar*) (Ronnestad et al., 2010) and Antarctic icefish (*Chionodraco hamatus*) (Rizzello et al., 2013), providing the basis of functional comparison among teleost fish orthologues and among teleost and mammalian orthologues. Although detailed kinetic characterization in *X. laevis* oocytes was carried out only for few PepT1 proteins in fish, the presence of a low affinity type peptide transporter was described in intestinal brush border membrane of both omnivorous (Reshkin and Ahearn, 1991) and carnivorous teleost species (Maffia et al., 1997; Verri et al., 2000; Nordrum et al., 2000; Bakke et al., 2000). Additionally, the PepT1-

related nucleotide sequences of many teleost species became available in databank as annotated or predicted by computational analysis (Romano et al., 2014).

The analyses on fully completed genomes of zebrafish and pufferfish (*Tetraodon nigroviridis*) allowed Goncalves and coworkers to identify another PepT1-like gene, thus providing the first evidence of the presence of two PepT1 genes in teleost fish genome (Goncalves et al., 2007). The two genes were named *slc15a1a* and *slc15a1b*, and their encoded proteins were designated as PepT1a and PepT1b, respectively. According to the designation reported by Romano et al. in 2014, the characterized transport activity in functional studies reported in many papers has been generally indicated as "PepT1", nevertheless it must be actually ascribed to PepT1b proteins. Consequently, functional data deriving from PepT1a transport proteins are still lacking (Romano et al., 2014).

In mammals, PepT1 is mainly expressed in enterocytes of small intestine and in renal proximal tubular cells of the S1 segments. Furthermore, PepT1 expression is also detected in the pancreas, bile duct, liver (Daniel, 2004; Daniel and Kottra, 2004; Gilbert et al., 2008; Smith et al., 2013) and a little or no expression is found in healthy distal colonic epithelium (Wuensch et al., 2013).

In teleost fish, PepT1 is principally expressed in the intestine with very low extent in kidney, liver, spleen and other organs and tissues (Romano et al., 2014). The primary targets of PepT1 expression in intestine are the pyloric caeca, if present, and foregut (Wang et al., 2017). However, patterns of expression along the intestine are diverse across multiple fish species (Romano et al., 2014). As a matter of fact, PepT1 expression is confined at the most proximal portions in zebrafish, carps and pufferfish; is uniform in proximal and distal regions in cods and killifish; decreases from proximal to distal intestine portions in salmon, trout, sea bass and sea bream (Romano et al., 2014; Verri et al., 2017). Moreover, the spatiotemporal mRNA expression of PepT1 in intestine varies largely during ontogeny (Verri et al., 2003; Liu et al., 2013) and in

response to different solicitations such as nutritional states (Bucking and Schulte, 2012; Ronnestad et al., 2010; Liu et al., 2013; Con et al., 2017), dietary challenges (Goncalves et al., 2007; Liu et al., 2013) and environmental conditions (Bucking and Schulte, 2012; Con et al., 2017).

In 2012 Burking and Schulte detected for the first time that the expression of PepT1a and PepT1b mRNAs occurred contemporarily in mummichog (*Fundulus heteroclitus*) intestine but this result was environmental-specific. The expression analysis revealed that while both paralogues were expressed in freshwater fish, only PepT1b expression was detectable in seawater acclimated fish (Bucking and Schulte, 2012). Also, it has been shown that fasting and re-feeding induced changes in expression of both paralogues in mummichog, showing: up-regulation after short-term fasting (following 3 days of fasting), down-regulation after prolonged fasting (following 21 days) and up-regulation (above pre-fasted levels) after resumption of feeding (following 7 days of re-feeding) (Bucking and Schulte, 2012).

Regarding the intestinal tract distribution of PepT1a and PepT1b, their expression was uniform in mummichog, while Huang and coworkers reported that PepT1a-to-PepT1b ratio was inverted, passing from proximal to mid intestine in Nile tilapia (*Oreochromis niloticus*) (Huang et al., 2015).

A more recent study on Mozambique tilapia (*Oreochromis mossambicus*) intestine showed that both PepT1 genes were expressed in anterior and middle tracts of freshwater and seawater acclimated fish (Con et al., 2017). After 6 hours of feeding, the regulation of expression along the intestine changed according to the environmental conditions: in freshwater fish it was shown an upregulation about 5-fold higher in anterior tract that in the middle intestine, whereas in saltwater fish the expression was almost equal between the two analyzed tracts (Con et al., 2017).

Expression patterns differ largely from species to species, making the unique identification of the PepT1a-to-PepT1b ratio difficult. All the previously

reported studies revealed the plasticity of PepT1a and PepT1b expression as response to dietary challenges and environmental salinity conditions. Overall, these data suggest that the PepT1a transporter might be expressed and operate at intestinal level in parallel or coupled to the PepT1b transporter (Verri et al., 2017).

Hence, to understand the role of each transporter in fish physiology, different steps need to be taken, namely the assessment of their local distribution along the intestine, their expression patterns in the different tissues and organs and their transport properties.

Molecular structure of PepT1 transport proteins

PepT1 proteins display a high degree of homology across species (e.g. about 60% similarity at protein level between rabbit PepT1 and zebrafish PepT1b). The length of the protein is about of 700 amino acids in higher vertebrates (human and rabbit PepT1 are proteins of 708 and 707 amino acids, respectively) and it is usually longer in most of the lower vertebrates, such as in teleost fish where PepT1 transporter consists of 718 amino acids for zebrafish, 728 amino acids for European sea bass and 734 amino acids for Atlantic salmon (Wang et al., 2017).

The membrane topology of PepT1 was proposed for the first time in studies on the rabbit transporter (Fei et al., 1994). The classical hydropathy plot suggested that PepT1 consists of 12 transmembrane domains (TMDs) with a long extracellular domain (ECD) between TMD 9 and 10. This consensus model was partly confirmed for human PepT1 by epitope tagging analyses (Covitz et al., 1998). The structural features of PepT1 are highly conserved among vertebrates (**Figure 1.2**) and include: 12 TMDs with intracellular both C- and N- termini; a conserved motif (ExxERFxYY) located at the TMD 1; two PTR2 family

proton/oligopeptide symporter signatures; a large extracellular loop between TMD 9 and TMD 10 and several putative glycosylation and phosphorylation sites.

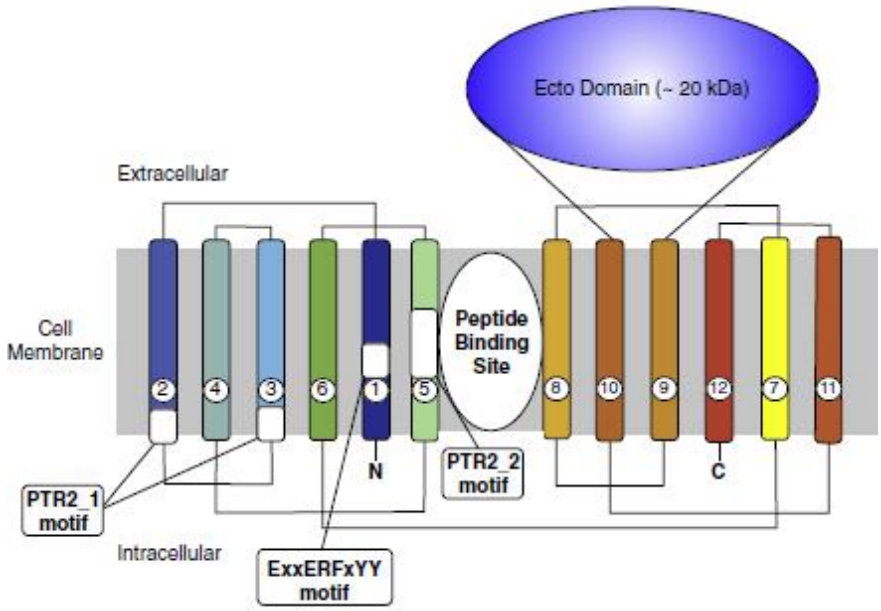

Figure 1.2 Topology diagram of human PepT1 with transmembrane helices colored blue to red including the position of the extracellular domain between TMD 9 and 10. The locations of the conserved sequence motifs within the TMDs are shown (Newstead, 2015).

Before the crystallization of PepT1 homologue (Newstead et al., 2011), several groups proposed a putative structure model of PepT1 based on computer modelling methods (Bolger et al., 1998; Yeung et al., 1998; Lee et al., 1999; Meredith and Price, 2006; Pedretti et al., 2008).

Although there is no three-dimensional protein structure of a vertebrate peptide transporter available yet, many structural features can be deduced from crystallized bacterial homologues.

The full structure of a proton dependent oligopeptide transporter was determined by X-ray crystallography only from prokaryotic and plant POT

family members (Parker and Newstead, 2014; Sun et al., 2014). The atomic resolution structure of transmembrane domains in various crystalized conformations allowed to obtain an insight on the distinct states of transport cycle (Newstead, 2015). All bacterial structures revealed the canonical 12 TMDs arranged equally into an N- and C-terminal bundle and two additional transmembrane helices, A and B, that form a hairpin-like structure inserted between TMD 6 and 7 (Newstead et al., 2011). POT transporters were proposed to transport substrates via the rocker-switch mechanism. The N- and C- bundles form a "V" shaped transporter that oscillates back and forth from an outward to an inward facing state along the pseudo two-fold symmetry axis running perpendicular to the membrane plane (Colas et al., 2016). To transport di- and tripeptides across the membrane, the transporter must undergoes to conformational changes (**Figure 1.3**), which comprise 4 states. An outward open state (step 1 in **Figure 1.3**) in which the transporter is ready to interact with substrate and driving ion(s). An outward open state with substrate and driving ion(s) bound (step 2) that switches the transporter into an occluded state (step 3) which is followed by an inward open conformation and by the release of the substrates and ion(s) into the cell (step 4). Finally, the empty transporter reorients to outward-facing state (step 4→1).

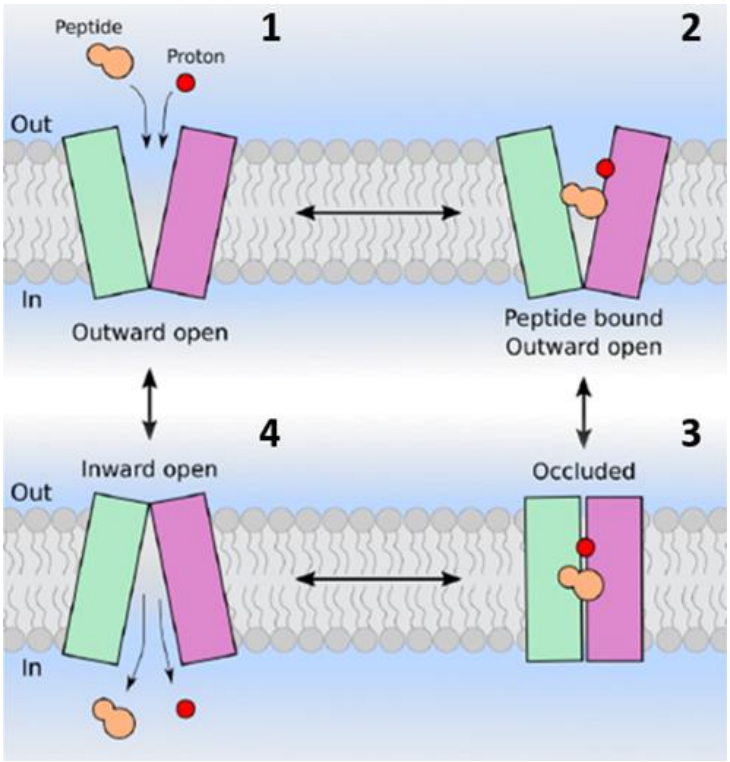

Figure 1.3 Schematic representation of the POT alternate access transport mechanism (rocker-switch mechanism).

The first crystal structure was determined in 2011, from the bacterium *Shewanella oniedensis* (PepTSo) (Newstead et al., 2011). PepTSo was crystalized in the asymmetric inward-occluded conformation revealing two gates, the extracellular gate (formed by TMDs 1, 2, 7 and 8) and the intracellular gate (formed by TMDs 4, 5, 10 and 11). The gates are responsible of controlling the access to the central cavity where peptide-binding site is located. The interaction between these gates occur through residues that are conserved across the POT family proteins. These residues are involved in two salt bridge interactions positioned above and below the main peptide binding site. The structures of *Streptococcus thermophilus* (PepTSt) (Solcan et al., 2012) and *Geobacillus kaustophilus* (GkPOT)

(Doki et al., 2013) were captured in the inward open state revealing the residues involved in salt bridge interactions that appeared to mediate the opening and closure of the extracellular and intracellular gates in response to proton and peptide binding.

The closed state of the intracellular gate is stabilized by the salt bridge interaction that is made by highly conserved residues, a lysine on TMD 4 and a glutamate on TMD 10. On the extracellular gate, the residues involved in the interaction are less conserved. In PepTSt and GkPOT the interaction is through an arginine on TMD 1 to a conserved glutamate on TMD 7. In PepTSo and in "mammalian-like" bacterial POT members, the interaction involves a conserved histidine on TMD 2 combined with an arginine-aspartate salt bridge on TMD 1 and TMD 7 (Newstead, 2017; Parker et al., 2017). A further highly conserved domain in the POT family is represented by the ExxER motif on TMD 1 that plays a key role in proton binding (Newstead, 2017; Longo et al., 2018).

While the structural differences observed in crystallographic models provide information about the structural basis for mechanism of POT transporters, many mechanistic details remain uncharacterized. In fact, the absence of outward- facing experimental models prevent to elucidate the conformational transitions occurring between the inward- and outward-facing states.

Through multiscale molecular dynamic (MD) simulations from the high resolution crystal structure of a "mammalian-like" bacterial POT family transporter from *Xanthomonas campestris*, PepTXc, Parker and collaborators revealed that the binding of proton to the histidine on TMD 2 facilitates the reorientation of the transporter from the inward- to outward- facing state (Parker et al., 2017). Based on these results, Parker and coworkers proposed a model of the alternating access for proton coupled peptide transport by the "mammalian-like" POT proteins (**Figure 1.4**).

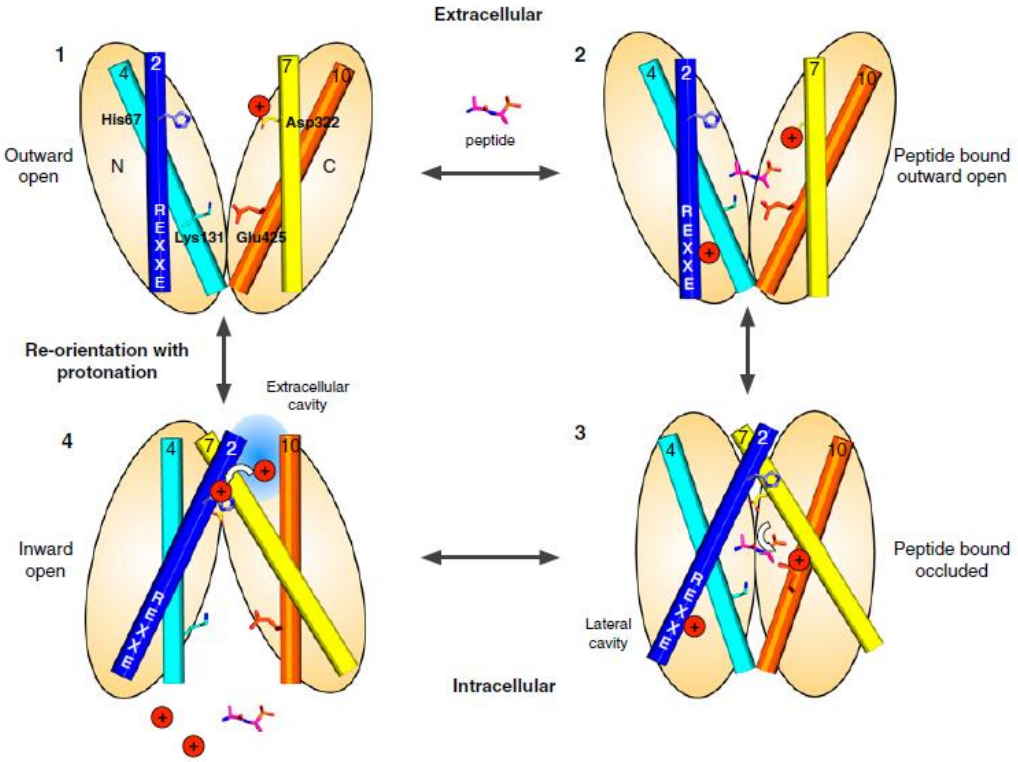

Figure 1.4 Alternating access model of proton coupled transport by the "mammalian-like" POT proteins. Transport is predominantly controlled through the opening and closing of two gates that sit on both side of a central binding site. The ExxER motif on TMD 1 is indicated. The extracellular cavity created in the inward-facing state allows protonation the TMD 2 histidine from the extracellular side resulting in the reorientation of the transporter to the outward facing state (Parker et al., 2017).

According to the proposed model, the extracellular cavity created in the inward-facing state (step 4 in **Figure 1.4**) allows to protonate the histidine on TMD 2 from the extracellular side. The protonation destabilizes the extracellular gate resulting in the reorientation of the transporter from the inward- to the outward-facing state (step 4→1 in **Figure 1.4**).

Data indicate that the mechanism for proton coupling within the POT family can be divided into two types: one that contains the conserved histidine in TMD 2, which includes PepTSo and others "mammalian-like" bacterial members, and

another without the histidine residue in TMD 2, which includes PepTSt and GkPOT.

Recently Batista and coworkers performed a series of adaptive biasing force (ABF) molecular dynamic simulations of PepTSt to map the conformational free energy profile of the transporter in the presence or absence of ligand and protonation (Batista et al., 2019). The results revealed that both proton and ligand significantly changed the conformational free-energy profile of PepTSt. In the absence of ligand and protonation, the transporter is able to shift between inward-open and occluded states only. The protonation of the conserved glutamate on TMD 7 acts on the link that determines extracellular gate, permitting to the transporter to change the conformation and to come back to the outward-open conformation. Ligand binding, on the other hand, stabilizes the transporter in the occluded conformation (Batista et al., 2019).

The occluded state structures of bacterial POT family members, crystallized in complex with several peptides, provided important insight into the transporter biochemical basis for peptide binding and substrate selectivity (Lyons et al., 2014; Guettou et al., 2014).

Physiological functions

In the intestine of vertebrates, the H^+-dependent oligopeptide transporter PepT1 is expressed in differentiated enterocytes and in L-enteroendocrine cells with distinct localization in the apical plasma membrane (**Figure 1.5**). PepT1 represents the major route of di- and tripeptides absorption in intestine. Beside its nutritional role, recent functional studies in mammalian enteroendocrine cells hypnotized an additional role of PepT1 as transceptor: a transporter/sensor of luminal peptides involved in gut hormones release.

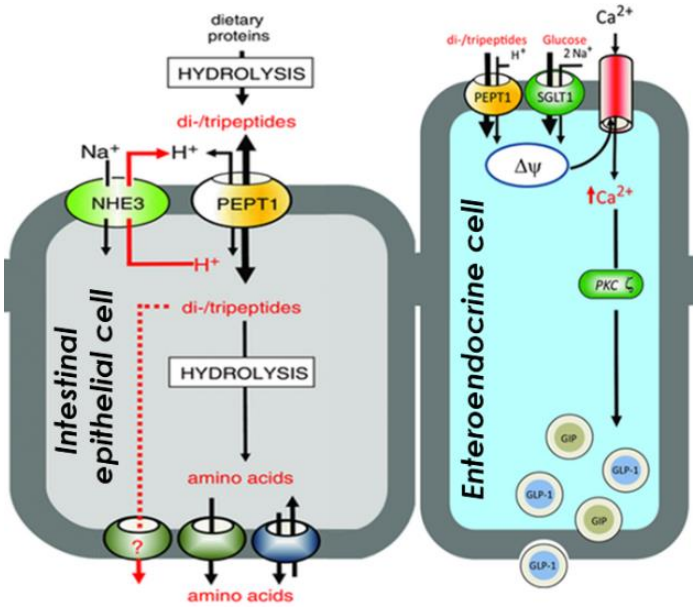

Figure 1.5 Schematic diagram displaying PepT1 transporter in its nutritional role in intestinal epithelial cells (left) and in its sensor function in enteroendocrine cells (right) (Daniel and Zietek, 2015).

PepT1 nutritional role

As primary means of absorption of small peptides, PepT1 has an important significance in nutritional physiology. Due to the direct correlation between dietary protein availability and accretion of body weight, fish are an outstanding model for studying the role of PepT1 on the peptide absorption and the effect of protein diets on the animal growth (Verri et al., 2011).

Following apical influx via PepT1, di- and tripeptides are sequentially hydrolyzed by cytosolic hydrolases in free amino acids that reach the systemic circulation via different basolateral transport systems. The efflux of not-hydrolized peptides can be mediated via basolateral peptide-transporting systems not yet identified on a molecular basis (Daniel, 2004).

PepT1 transporters operate as Na^+-independent and H^+-dependent system. Their function is dependent on the internally directed proton electrochemical

gradient, which is the driving force of the substrate translocation across membranes. The proton electrochemical gradient is granted by the apical sodium-proton exchanger NHE3. Sodium influx via NHE3 is compensated by export through the basolateral Na^+/K^+ ATPase and potassium ions taken up leave the cell by the potassium channels (Daniel and Kottra, 2004).

PepT1 mediates an enantioselective transport with a variable proton to substrate (H^+: S) stoichiometry for the uptake of neutral and charged peptides. Irrespectively to the substrates net charge, the uptake of di- and tripeptides is associated with proton translocation, thus the transport is always electrogenic (Daniel and Kottra, 2004). Given its rheogenic activity, the functional properties of this transport system can be examined using electrophysiological techniques.

Electrophysiological properties of PepT1

The Two Electrode Voltage Clamp technique (TEVC) applied in combination with a PepT1 over-expression in *X. laevis* oocytes, resulted in precise electrophysiological measurements, thus revealing detailed features in the transporter kinetic mechanism.

PepT1, as most cotransporters, displays two types of electrical activity: transport-associated currents recorded in the presence of substrate, and transient pre steady-state currents generated by charge relocation during voltage steps in the absence of organic substrate (Mager et al., 1993). The electrophysiological approach allowed functional data collection of both transport-associated and pre steady-state currents of many PepT1 orthologues (Mackenzie et al., 1996b; Nussberger et al., 1997; Sangaletti et al., 2009; Renna et al., 2011b). These data were collected under the same experimental conditions, e.g. substrate type or concentration, external condition of pH and temperature, membrane voltage condition, thus their comparison resulted easier. When data

on kinetic parameters, pre steady-state currents and substrate specificity were compared in response to the change of physiochemical parameters (pH, temperature and membrane potential), teleost fish PepT1 exhibited unexpected functional properties respect to the mammal counterpart (Verri et al., 2017; Renna et al., 2011b).

pH dependence- In many functional studies PepT1 was reported to be pH dependent, with an increase of the uptake of transported substrate reaching the optimum pH range from 5.0 to 6.0 in heterologous expression system. In general, in mammalian PepT1 the change of external proton concentration from alkaline to acidic pH increased the transporter apparent affinity without affecting the maximal transport rate (Kottra and Daniel, 2001). Notably, in the human transporter both apparent affinity and transport rate were increased by acidification of external pH (Mackenzie et al., 1996a). Interestingly, with the functional characterization of teleost PepT1, it was noticed that whereas the increase in apparent substrate affinity for decreasing pH was conserved between mammals and fish, the pH effect on the maximal transport rate in the tested orthologues was not always similar to mammalian transporters (Verri et al., 2017). No significant effect of pH was observed on the maximal transport rate in PepT1 of European sea bass (Sangaletti et al., 2009) and Antarctic icefish (Rizzello et al., 2013). Conversely, the functional characterization of the zebrafish transporter highlighted an unexpected increase of maximal transport rate at alkaline extracellular concentration (Verri et al., 2003), which was observed slightly in Atlantic salmon transporter too (Ronnestad et al., 2010). The authors postulated that the peculiar pH dependence shown by zebrafish PepT1 could be explained by two complementary anatomical-physiological scenarios: the agastric state of zebrafish and the most likely lack of the functional interaction between PepT1 and the sodium-proton exchanger in the apical side of zebrafish enterocytes (Verri et al., 2003).

In addition, external pH affected pre steady-state currents of PepT1 as emerged by electrophysiological and biophysical analysis of both mammalian (Nussberger et al., 1997) and fish transporters (Sangaletti et al., 2009; Renna et al., 2011b). In 2011, Renna and coworkers compared pre steady-state currents recorded from the rabbit transporter to those from two different teleost fish species (European sea bass and zebrafish), using the same experimental setup (Renna et al., 2011b). The data showed that the pre steady-state currents of the fish transporters were similar while rabbit transporter differed by having slower-decaying currents, this was ascribed to different operating temperature of the different orthologues (Bossi et al., 2012). Nonetheless, all PepT1 orthologues were similarly affected by external pH, showing acidity-induced slowing of pre steady-state currents. The analysis was extended to calculate the unidirectional rate constants of charge movement in the membrane electrical field and their dependence on external pH. The results suggested that an increase in external protons slowed down both inward and outward charge movements in all the PepT1 proteins of the examined species. All these data allowed the authors to propose a unified model that explained electrophysiological properties of each PepT1 orthologue and their different behaviors in term of pH dependence. This model included a transition state in which the transporter binds the H^+ in an allosteric site. The fixing of the transporter in this protonated state may explain then the decrease in inward rate of positive charge movement caused by acidic pH observed in all tested PepT1 orthologues (Renna et al., 2011b). Even if this putative allosteric site still remains unknown, it is believed that it could be the cause of the smaller transport current observed at acidic pH in the zebrafish PepT1 (Verri et al., 2003; Verri et al., 2017).

Transport of differently charged substrates- One of the unsolved question in the study of PepT1 transport mechanism, is how the transporter is able to translocate neutral and differently charged dipeptides using the same transport mode.

In 1997, Stell and colleagues proposed a model to explain the stoichiometry of neutral and charged dipeptides transported by rabbit PepT1 expressed in *X. laevis* oocytes (Steel et al., 1997). Based on the rate of intracellular acidification, the initial uptake rates of radiolabelled peptides and the associated charge fluxes, the resulting proton-substrate coupling ratios were: 1:1 for neutral dipeptides, 2:1 for anionic dipeptides and 1:1 for cationic dipeptides. After 5 years, Kottra and coworkers refined the previous model, demonstrating that the binding domain of PepT1 is asymmetric and selective for cationic dipeptides according to the location of the charged side chain within the substrate molecule (Kottra et al., 2002). Notably, when the charged residue was provided in an amino-terminal position the substrate was transported in both zwitterionic and positive charged form; conversely when the charged residue was provided in carboxyl-terminal position only the neutral form was transported. Anionic dipeptides were transported in their neutral form, but a minimal fraction of them could be transiently protonated in the close proximity of the cellular membrane and thus they were translocated virtually as charged species with proton-substrate coupling ratio of 2:1.

The proposed model, in **Figure 1.6**, explained the transport characteristics observed in rabbit PepT1 transporter when the positive charge substrate, lysine-glycine (Lys-Gly), was tested using TEVC technique and compared to the zwitterionic substrate, glycine-glutamine (Gly-Gln). At pH 7.5 when lysine-containing peptide was in neutral form for 17%, the maximal relative current of Lys-Gly was higher (168%) than that of Gly-Gln (100%) but it decreased to 107% when the percentage of neutral form increased at 67% at pH 8.5.

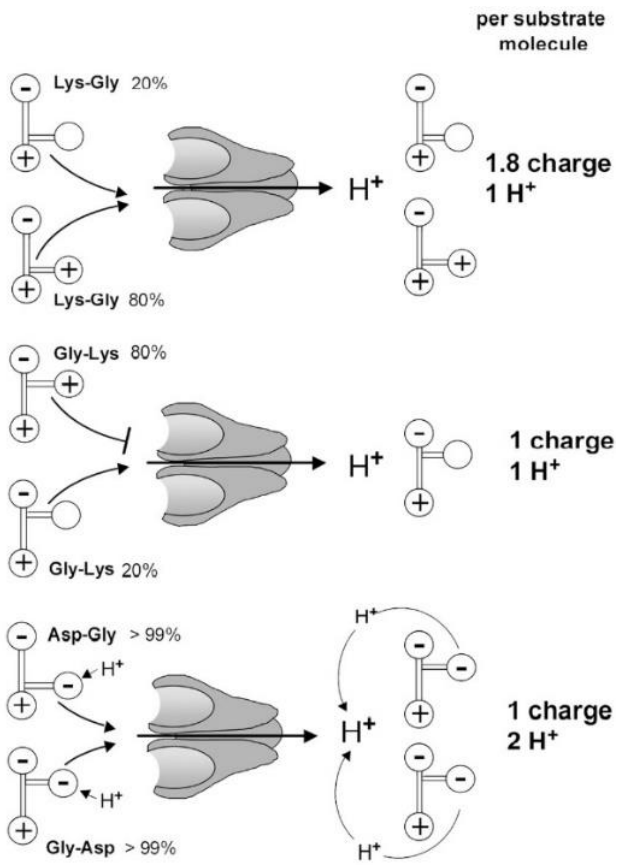

Figure 1.6 A scheme for the transport of charged dipeptides by PepT1 (Kottra et al., 2002).

These data were not confirmed for the reversed substrate, glycine-lysine (Gly-Lys), that at pH 7.5 showed an amount of 17% of molecules recognized by the transporter in contrast to 100% of the Lys-Gly molecules (Kottra et al., 2002). In teleost fish, differently charged dipeptides were tested for the first time with the zebrafish PepT1 (Verri et al., 2009). The data on the kinetic parameters in the presence of lysine-containing dipeptides, i.e. Lys-Gly and Gly-Lys, and of aspartic (Asp)-containing substrates, i.e. Asp-Gly and Gly-Asp, showed that also for the zebrafish PepT1 transporter the position of the charged side chain within the dipeptide affected the transport process (Verri et al., 2009).

Interestingly, with respect to the current generated by Gly-Gln (100%) in the zebrafish transporter the maximal relative current of Lys-Gly increased from 126% at pH 7.5 to 220% at pH 8.5. In presence of Gly-Lys the maximal relative current with respect to Gly-Gln was 94% at pH 7.5 and increased at 191% at pH 8.5.

Uptake of dipeptides containing essential amino acid (EAA)- Later studies on PepT1 of different teleost species focused on the transport kinetic of substrates composed by lysine (Lys) and/or methionine (Met) for the importance of these molecules in animal nutrition. These two EAAs are known to impact body metabolism in general and to be crucial in growth performances in vertebrate and particularly for teleost fish (Verri et al., 2017). To determine similarities and differences in the uptake of substrates containing methionine and/or only lysine, the kinetic properties of one mammalian transporter (rabbit PepT1) and two PepT1s from different teleost species (European sea bass and zebrafish) were collected and systematically compared (Margheritis et al., 2013).

In rabbit and sea bass transporter, the Lys- and Met- contained dipeptides (i.e. Lys-Gly and Lys-Met) showed higher currents than the reference current of the zwitterionic substrate, (Gly-Gln). In zebrafish PepT1, all tested dipeptides showed comparable currents which were in general smaller than that generated by the Gly-Gln, with the exception of Lys-Lys that at more negative potentials evoked a higher current. In rabbit and sea bass, the Lys-Lys dipeptide was instead only modestly transported. Interestingly, Atlantic salmon PepT1 conformed more to European sea bass transporter, and also to mammalian model, than to zebrafish transporter model. In fact, when tested in Atlantic salmon PepT1 arginine-lysine (Arg-Lys), which is structurally similar to Lys-Lys, was found having the lowest value of transport efficiency among the tested lysine-containing substrates (Ronnestad et al., 2010; Verri et al., 2017).

Taken together, the comparative functional analysis between mammal and fish proteins indicated that the molecular diversity among PepT1 proteins was the

basis of their differences in functional properties and thus could be the starting point of further investigation. Considering the results obtained from the molecular modeling (Pedretti et al., 2008), the sequence comparisons allowed to identify residues that may account for the different behavior of PepT1 orthologues. For instance, this approach led Margheritis and colleagues to the identification in the TMD 8 of the zebrafish transporter of an amino acid substitution, that was relevant for its particular behavior with respect to rabbit and seabass transporters (Margheritis et al., 2013). This amino acid substitution involved a threonine (Thr) that is substituted with an isoleucine (Ile) in PepT1 of zebrafish (Ile334Thr). Functional data highlighted the role of this residue in transporter substrate selectivity, affinity and consequently transport efficiency. The multiple alignment of the PepT1b and PepT1a amino acid sequences from some teleost fish allowed to find the Thr-to-Ile substitution in three sequences of PepT1a from five representative species throughout the East African haplo-tilapiine lineage (Verri et al., 2017). However, this substitution was not present in the PepT1b sequence of the same species. This evidence led the authors to the hypothesis that after gene duplication the retained duplicated gene may have diverged in function through sub- or neofunctionalization (Verri et al., 2017).

PepT1 enteroendocrine role

In the gastrointestinal tract, 1% of the total epithelial cell population is represented by enteroendocrine cells (EECs) that form the largest endocrine organ in the body. EECs are specialized cells capable of sensing luminal content and releasing signaling molecules that can modulate a variety of physiological and homeostatic functions (Latorre et al., 2016).

The secretory products can act as classic hormones reaching distant targets via the circulatory system, as paracrine signaling activating locally other ECCs and

other cytotypes of the intestinal mucosa, or directly on nerve endings close to the site of release. These signaling molecules, mainly peptides and hormones, play a key role in the control of gut secretion and mobility and in the regulation of food intake, postprandial glucose level and metabolism (Latorre et al., 2016).

Along the gastrointestinal tract distinct types of EECs have been identified, which produce and release more than 20 peptide/hormones. Typically, EECs subtypes have been classified based on the primary hormone product; many recent studies showed the high plasticity of EECs phenotypes depending on their location in the intestine (Habib et al., 2012; Egerod et al., 2012; Sykaras et al., 2014) and thus suggested that a review of the first classification is necessary. Based on classical nomenclature, EECs secreting GLP-1, GLP-2 and PYY are referred to as L cells, whereas GIP-producing cells are classified as K cells.

Among these gut hormones, GLP-1 and GIP have received the highest attention due to their insulinotropic action, and thus they gained relevance as therapeutic target for metabolic disorders (Zietek and Rath, 2016). EEC secretory products are released in response to many types of stimuli such as nutrients, degradation products, toxic chemicals, microorganisms and bacteria products (Latorre et al., 2016). In nutrient sensing, carbohydrates, lipids and proteins are detected via their digestion end products by a wide range of sensors expressed in the apical membrane of EECs (**Figure 1.7**). Most of the known EECs receptors involved in nutrient sensing are G protein-coupled receptors (GPCRs) (Zietek and Rath, 2016).

The GPCR group comprises amino acid- and oligopeptide-sensing receptors, metabotropic glutamate receptors and taste receptors (TRs). Furthermore, GPCR are responsible for detection of lipid-derived long-chain/medium-chain fatty acids (FA) and short-chain fatty acid (SCFAs), derived after fermentation of dietary fiber by the microbiota (Zietek and Rath, 2016).

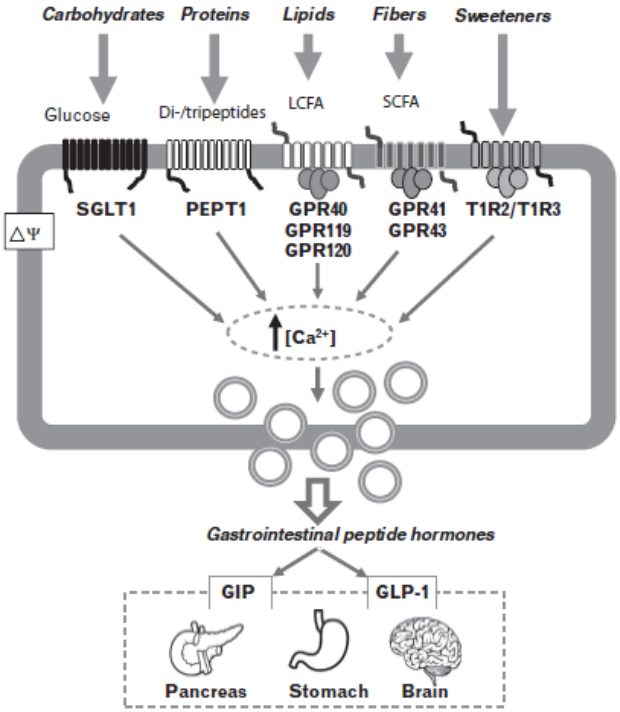

Figure 1.7 Nutrient sensing and stimulus-secretion coupling in intestinal endocrine cells (Zietek and Daniel, 2015).

Recently intestinal nutrient transporters like the Na^+ dependent glucose transporter (SGLT1), the Na^+ dependent amino acid transporter (SLC6A19) (Broer and Broer, 2017; Javed et al., 2018; Cheng et al., 2017) and the H^+ dependent di- and tripeptide transporter (PepT1) have been proposed as sensors in nutrient-signaling pathways suggesting a possible role as transceptors (Zietek and Daniel, 2015; Daniel and Zietek, 2015; Roder et al., 2014; Kuhre et al., 2015; Diakogiannaki et al., 2013). They are integral membrane proteins that are expressed at apical membrane of EECs where they recognize specific substrates in the intestinal lumen and transport them into cells. The transport activity operated by transceptors represents the intracellular trigger to activate the

gastrointestinal peptide hormones release that thus results linked to the sensing of the nutrients. Specifically, the role of transceptors in the enteroendocrine system seems to be due to their electrogenic transport mechanism. The intracellular cation flow, coupled with transport of the organic substrate, causes membrane depolarization in the EEC that leads the opening of the voltage-gated calcium channels. Finally, the increase of intracellular calcium level is followed by the exocytosis and hormone release from vesicles (Zietek and Daniel, 2015).

In the intestinal lumen, glucose is the most powerful stimulus that induces the release of incretin hormones *in vivo*. Recent experimental data showed the involvement of the SGLT1 in glucose-mediated hormone secretion. This transporter is expressed in the apical membrane of L and K cells and its role as a transceptor is confirmed by several experiments (Roder et al., 2014; Kuhre et al., 2015).

Several studies suggest that the neutral amino acid transporter SLC6A19 (B0AT1) is enriched in L cells where can act as nutrient sensor (Broer and Broer, 2017; Joshi et al., 2013; Norton and Murphy, 2017). Studies on mice lacking B0AT1 reported that the animals showed signs of protein restriction, protection from diet-induced obesity, improvement of glycemic control and increase of basal levels of GIP and GLP-1 (Javed et al., 2018; Jiang et al., 2015).

In 2013, Diakogiannaki and colleagues reported that the intestinal transporter PepT1 together with Ca^{2+} sensitive receptor (CaSR) acts as a sensing system for small peptides, activating the opening of the L-type Ca^{2+}channels with subsequent GLP-1 release from primary murine L-cell culture. The experiments showed that the secretion of GLP-1 in response to dipeptide glycine-sarcosine (Gly-Sar) presented the following characteristics: it was pH-dependent, with an increase of relative hormone release at more acidic pH; it increased with increments of Gly-Sar concentration; it was blocked in presence of the competitive antagonist, 4-aminomethylbenzoic acid (4-AMBA) and it was

markedly reduced in primary L-cell cultures from *Pept1* knockout mice (Diakogiannaki et al., 2013). The association between GLP-1 release and PepT1-dependent uptake of small peptides was confirmed by studies in intestinal organoids prepared from mouse small intestine (Zietek et al., 2015).

The dual role of SGLT-1, B0AT1 and PepT1 in nutrient uptake and sensing is thus a remarkable feature of intestinal transporters expressed in enterocytes and enteroendocrine cells. The role in sensing seems to be linked to the electrogenic nature of the transport mechanism. Non-metabolizable substrates, e.g. Gly-Sar for PepT1 and α-MDG (α-methyl-glucopiranoside) for SGLT-1, induce the GPL-1 release that thus is not dependent on the substrate *per se,* but on the cation influx generated by transporter activity (Zietek and Daniel, 2015).

Given the insulinotropic action of some enteroendocrine hormones, the transceptors assume importance as a therapeutic target for metabolic disorders, such as diabetes and obesity (Norton and Murphy, 2017). Although the inhibitors of B0AT1 have the potential to be used as drugs to treat metabolic disorders, B0AT1 human mutations result in Hartnup disorder, suggesting that this transporter is not optimal as therapy target (Cheng et al., 2017; Norton and Murphy, 2017).

PepT1 pathological implications

Several studies have demonstrated PepT1 involvement in pathological states that alter the expression level and the function of the transporter.

Intestinal epithelial cells, constituting an interface between the gut microbiota and the immune system, are crucial for maintaining intestinal homeostasis. A failure in controlling inflammatory processes affecting intestinal epithelia cells level may critically contribute to intestinal inflammation. Moreover, during intestinal inflammation are reported also alterations in the EECs number,

secretion of gut hormones and thus changes in feeding patterns that often accompanying these conditions (Zietek and Rath, 2016).

The Inflammatory Bowel disease (IBD) is classified as a group of inflammatory intestinal disorders, i.e. ulcerative colitis (UC) and Crohn's disease (CD), that are associated with alteration of both innate and adaptative immune system, an increase of luminal and mucosa-associated microbiota and an impairment of intestinal epithelia cells functions (Sartor, 2006). Despite the controversial results obtained regarding steady-state expression of PepT1 in colon (Wuensch et al., 2013), PepT1 expression was documented in colonic mucosa of CD and UD patients, at both mRNA and protein level (Merlin et al., 2001; Ziegler et al., 2002). This evidence suggested an induction of aberrant expression of the transporter in the state of chronic inflammation. Although the exact molecular mechanism by which PepT1 expression was induced remained uncertain, the collective findings suggested that changes in inflammatory cytokines and hormone levels during disease (Chouliaras et al., 2013; Valentini et al., 2009) affected the transporter expression and function. For example, in Caco-2 BBE cells, an epithelial cell line derived from human colon adenocarcinoma, the administration of proinflammatory cytokines TNF-α and IFN-γ was associated with an increase of PepT1 expression at protein level and resulting in an increase in transport activity (Buyse et al., 2003; Foster et al., 2009; Vavricka et al., 2006). Among the adipocyte-secreted hormones, leptin was detected in colonic epithelial cells from inflamed tissues (Sitaraman et al., 2004) and was shown also to increase PepT1 expression in Caco-2 BBE cells (Nduati et al., 2007).

Concomitantly with the expression of colonic PepT1, many studies reported the ability of PepT1 to transport a wide range of small peptides produced by bacterial intestinal flora, suggesting an involvement of the transporter in pathogenesis of intestinal inflammation.

For instance, PepT1 mediated transport of formyl-methionyl-leucyl-phenylalanine (fMLP) a bacterial chemiotactic oligopeptides (Merlin et al., 2001), muramyl dipeptide (MDP) a constituent of bacterial cell wall (Vavricka et al., 2004) and L-Ala-γ-D-Glu-meso-DAP (Tri-DAP) a peptide-glycan degradation product from bacteria (Dalmasso et al., 2010). Moreover, PepT1-mediated uptake of bacterial peptides could trigger the activation of inflammatory signaling pathways in colonic epithelial cells that exacerbated the disease state initiating a proinflammatory response. PepT1-mediated transport of fMLP potentially stimulated expression of MHC-1 (Merlin et al., 2001); MDP activated nuclear factor kappa B (NF-kB) and chemokine production (Vavricka et al., 2004). Additionally, Tri-DAP mediated the activation of the mitogen activated protein kinase (MAPK) pathway and upregulation of IL-8 (Dalmasso et al., 2010).

PepT1 was expressed also in macrophages, which might be recruited during intestinal inflammation (Ayyadurai et al., 2013). In macrophages, the PepT1-mediated uptake of bacterial products might modulate the secretion of proinflammatory cytokines that, together with the increased cytokine level in enterocytes, contribute to the pathogenesis of the intestinal inflammation (Spanier and Rohm, 2018).

Interestingly, the first study on the relationship between IL-16 and PepT1 in the pathogenesis of IBD was conducted on pufferfish (*Tetraodon nigroviridis*), a teleost fish model (Wang et al., 2013). The results provided both *in vivo* and *in vitro* evidence that IL-16 was able to trigger PepT1 expression, increasing the transporter-mediated uptake of fMLF, that thereby led to severe colon inflammation. The use of a fish model of IBD, as complementary to mammalian models, showed to produce great benefits providing new insights into the molecular mechanism underlying IBD development. Better understanding of the IL-16 biology from fish to mammals should aid the development of IL-16 based therapies for IBD (Wang et al., 2013).

To date there is no known pathology associated with the malfunction of the PepT1 oligopeptide transporter. Despite this, two single nucleotide polymorphisms (SNPs) found in ethnically diverse cohorts, were associated with altered PepT1 activity. Specifically, the exchange of phenylalanine to tyrosine in position 28 (Phe28Tyr) reduced transporter-to-substrate affinity but did not influence transporter expression (Anderle et al., 2006); the exchange of proline to leucine in 586 position (Pro586Leu) impaired transport capacity and decreased PepT1 protein expression (Zhang et al., 2004b). In the context of identifying human PepT1 polymorphisms for associations with IBD, Zucchelli and colleagues analyzed two cohorts of Swedish and Finnish IBD patients. They discovered one functional PepT1 SNP, namely rs2297322, that was associated with CD in both cohorts. Interestingly, the SNP showed an opposite effect: in Swedish cohorts it was associated with increased risk of CD, while in Finnish cohorts it was shown to be protective against the disease state (Zucchelli et al., 2009). Notably, a recent study failed to identify an association between the rs2297322 and IBD susceptibility in a German cohort, suggesting that the role of this SNP in disease still remains unclear (Wuensch et al., 2014).

PepT1 expression was shown to be altered in some carcinomas such as pancreatic carcinoma, prostate cancer, hepatocellular carcinoma, gastric cancer and colorectal cancer (Landowski et al., 2005; Tai et al., 2013; Gong et al., 2017; Viennois et al., 2016). In patients with IBD, the long-term exposure to chronic inflammation was the primary risk factor for colorectal cancer, also referred to as colitis-associated cancer (CAC). In a recent study, Viennois and coworkers reported a role of PepT1 in promoting CAC. Compared to wild-type animals, a significantly increase in tumor growth and size was reported in mice overexpressing human PepT1; the opposite effect was observed in *Pept1* knockout mice (Viennois et al., 2016).

Moreover, several studies suggested an alteration of PepT1 expression and function during metabolic disease such as obesity and diabetes. The leptin

resistance is one of the patophysiological factors in the development of obesity, which is mainly due to impaired leptin receptor signaling. Hindlet and coworkers reported that, although the acute leptin treatment enhanced the absorption of di- and tripeptides via PepT1 transporter (Hindlet et al., 2007), PepT1 levels and activity were downregulated in hyperleptinemic states of leptin resistance (Hindlet et al., 2009). Thus, the intestinal PepT1 activity may be impaired by leptin resistance in obesity, possibly affecting the PepT1 mediated uptake of peptides known to induce satiety (Spanier and Rohm, 2018).

PepT1 expression and activity was also affected by insulin level and diabetes. Studies in Caco-2 cells treated with insulin, showed an increase of PepT1 protein in apical membrane (Thamotharan et al., 1999). The PepT1 activity was investigated in kinetic analysis in BBMVs prepared from jejunum of diabetic rats. Transport data showed unaltered transporter affinity but an increase of transporter maximal rate, which was probably due to an increase of number of transporters expressed on cellular membrane (Gangopadhyay et al., 2002). Interestingly, some antidiabetic drugs were known to inhibit the transporter in noncompetitive manner, such as Glibenclamide and Nateglinide (Sawada et al., 1999; Terada et al., 2000).

PepT1 therapeutic applications

The wide range of substrate specificity is a remarkable feature of the SLC15 family. This suggests the possibility to develop peptide-based prodrugs that target intestinal transport to improve oral drug delivery. Although structural basis of PepT1 substrate promiscuity remains largely unknown, the crystal structures from several PepT1 homologues reveals conserved features and provide a template for prodrug development.

Recently, Minhas and colleagues used previous dipeptide-bound crystal structures of PepT to find the commonalities in the binding position in a new

prodrug-bound crystal structure of PepT1 from the bacterium *Staphylococcus hominis*, PepTSh. Based on the experimental results, the authors proposed a structure-based pharmacophore model for valacyclovir binding to peptide transporters, suggesting a novel route for prodrug scaffold design (Minhas and Newstead, 2019). Interestingly, three different template structures of bacterial POT transporters were used to construct multiple structural models of human PepT1 that represent different conformational states of the transporter during transport and inhibition phases. Based on the features of binding site of human PepT1 models, computational methods allowed to identify also several compounds that bind to them. Finally, the selected substrates were tested with uptake kinetics measurements and electrophysiological assays revealing one new substrate and four novel inhibitors of human PepT1 (Colas et al., 2017).

Studies performed in 1970s and 1980s reported that intestinal peptide transporters can also recognize and even transport compounds bearing sterical resemblance to the backbone of di- and tripeptides (Brandsch et al., 2008).

Classical and well-characterized drug substrates of PepT1 are the numerous amino β-lactam antibiotics such as many belonging to the penicillin and cephalosporin classes (Ganapathy et al., 1995; Bretschneider et al., 1999); selected angiotensin-converting enzyme (ACE) inhibitors such as captopril and ACE inhibitor ester prodrugs such as enalapril and fosinopril (Zhu et al., 2000; Shu et al., 2001). Others well-known PepT1-compatible drugs include bestatin (Inui et al., 1992), alafosfalin (Brandsch et al., 2008) and amino acid-conjugated antiviral drugs such as valacyclovir, an ester prodrug used as oral treatment of viral infection (Balimane et al., 1998). PepT1 is able to recognize also substrates that do not present a classical peptide bond, such as 4-aminophenylacetic acid, ω-amino fatty acids (Doring et al., 1998) and δ-amino levulinic acid (ALA) a precursor of cellular porphyrin synthesis which is used as a photodynamic agent in treatment of gastrointestinal tumor (Anderson et al., 2010).

The broad substrate specificity, the high transport rate and the intestinal expression make PepT1 a good target for efficient oral delivery of poorly bioavailable drugs. It is worth to mention that one of the leading causes of compound failure in preclinical and clinical drug development resides in its poor oral bioavailability. So, a possible approach is to increase drug oral availability developing prodrugs that target intestinal transporters. For example, the interactions in gut epithelium between ACE inhibitor prodrugs and PepT1 provide an oral availability of the drugs in a dose generally between 40% and 90% (Zhu et al., 2000; Shu et al., 2001).

Moreover, PepT1 has been shown to increase the bioavailability of molecules attached to amino acids or di- and tripeptides becoming an attractive target for potential therapeutic models for developing and enhancing drug-delivery systems.

Recently, target therapy has become a potent therapeutic strategy for tumor. Particularly, the delivering of antitumor drugs into specific locations of a tumor provides the advantage of limiting toxicity in healthy tissues. In this context, the attention on some antitumor target such as nanoparticle, tumor specific antigen, tumor specific receptor has increased even more. For example, Gong and coworkers explored the feasibility of targeting PepT1 to improve the antitumor efficacy of Doxorubicin in human hepatocellular carcinoma therapy using a Doxorubicin-tripeptide conjugate (Gong et al., 2017). Indeed, *in vivo* and *in vitro* experiments proved that Doxorubicin-tripeptide conjugates can be transported into liver cancer cells by PepT1 playing an anti-tumor action. Moreover, the anti-cancer treatment by Doxorubicin-tripeptide conjugates showed a greater efficacy and a lower toxicity than that of Doxorubicin (Gong et al., 2017).

Moreover, with the rapid nanotechnology advances, nanoparticulate drug delivery systems (nano-DDS) show great progress in drug delivery and represent a promising nanoplatform to facilitate oral delivery of drugs with low

bioavailability. Among the various delivery strategies in the field of nano-DDS, transporter-targeted prodrug strategies have been widely investigated.
PepT1 transporter has been investigated to assess the ability to uptake dipeptide modified nanoparticles. Although few studies have been conducted up to now, the results are promising and show that PepT1 could work as a desirable mediator of oral nanoparticulate drug delivery (Du et al., 2018; Gourdon et al., 2017; Gourdon et al., 2018; Kou et al., 2018).

In this thesis work it is reported the functional characterization of the newly cloned PepT1a-type proteins from intestine of zebrafish and Atlantic salmon, which completes the functional picture of the PepT type transporters expressed by these teleost fish species, adding important information regarding structure-function relationship.

Chapter 2. Materials and Methods

Molecular biology

PepT1 cDNAs

The full-length cDNA encoding zebrafish PepT1a (submission: BankIt2285160 zfPepT1a GenBank MN723161; date release: June 21, 2020) and the open reading frame (from start ATG to stop codon) encoding Atlantic salmon PepT1a (GenBank Acc. No. XM_014172951.1) and PepT1b (GenBank Acc. No. NM_0011466882.1) were subcloned in pSPORT1 for expression in *X. laevis* oocyte. All constructs were verified by sequencing.

To improve the expression of Atlantic salmon PepT1a and PepT1b in the membrane of *X. laevis* oocytes, a 3'UTR sequence from rat Divalent metal transporter 1 (rDmt1, *alias* rat *slc11a2*; GenBank Acc. No. NM_013173.2) was added to the end of the Atlantic salmon PepT1a and PepT1b coding sequences (CDS), as previously reported for *Dictyostelium discoideum* natural resistance-associated macrophage protein 1 (Nramp1) and 2 (Nramp2) (Buracco et al., 2015). The 1725 bp sequence added contains two poly-adenylation signals and a poly(A) tail at the 3'end.

Plasmid amplification, extraction and purification

The recombinant plasmids (pSPORT1-zfPepT1a, pSPORT1-asPepT1a and pSPORT1-asPepT1b) were introduced into JM109 strain of *E. Coli* after heat-shock procedure. First, cells were incubated with DNA on ice for 20 minutes; subsequently the cells were exposed to heat-shock at 42°C for 2 minutes, then

they were put back on ice for 2 minutes. Transformed bacteria were then left to grow in agitation at 37°C for about 1 hour in Luria-Bertani medium (LB), centrifuged (4000 g for 10 minutes) and plated on Petri plates containing selective medium (LB-Agar added with ampicillin 50 mg/mL) and incubated at 37°C. After 24 hours, single colonies were picked up and inoculated in liquid selective medium (LB added with ampicillin 50 mg/mL) and incubated at 37°C over night with shaking. The plasmid DNAs were extracted using Wizard® Plus SV Miniprep (Promega Italia, Milan, Italy) following supplier instructions and eluted in 50 µl of nuclease free water.

In vitro transcription

In order to achieve an efficient *in vitro* transcription, the recombinant plasmid (pSPORT1-zfPepT1a, pSPORT1-asPepT1a and pSPORT1-asPepT1b) was linearized in 3' direction with respect to the coding region with NotI (Promega Italia), purified with Wizard SV Gel and PCR clean-up system (Promega Italia) and eluted in 40 µl of nuclease free water.

The linearized DNA was incubated at 37°C for 3 hours in presence of 200 units of T7 RNA polymerase (Promega Italia). The *in vitro* transcription reaction was composed as follow: 18 µl of Transcription Buffer 5X, 8 µl of DTT 100 mmol/L, 2 µL of RNasin® Ribonuclease Inhibitors 40 U/µL, 13 µL rNTPs mix (rATP, rCTP, rUTP 5 mmol/L and rGTP 0.5 mmol/L), 6.5 µL of Cap Analog 10 mmol/L, 10 µl T7 RNA polymerase 20 U/µL (final volume 90 µL). After 10, 20, and 40 minutes from the beginning of the incubation, 1 µL of rGTP 25 mmol/L was added to the reaction. After 1 hour from the start of the transcription, a mix of 4 µl of Trascription Buffer 5X, 1 µl of DTT 100 mmol/L, 1 µL of RNasin® Ribonuclease Inhibitors 40 U/µL, 5 µL of rNTPs mix, 1 µL of T7 RNA polymerase 20 U/µL, 1 µL of GTP 25 mmol/L, 4 µL of

nuclease-free water, was added to the sample. At the end of 3 hours, the reaction was stopped by adding 101 µL of nuclease-free and 150 µL of LiCl 8 mol/L and stored at -80 °C over night. All reagents and enzymes were supplied by Promega Italia. The transcribed cRNA was precipitated and washed with EtOH 70%. The purified cRNA was then resuspended in a small volume of nuclease-free water, visualized by denaturing formaldehyde-agarose gel electrophoresis and quantified by NanoDrop™ 2000 Spectrophotometer (Thermo Fisher Scientific).

Heterologous expression in *Xenopus laevis* oocytes

X. laevis oocytes result to be very useful expression systems for carrying out experimentations. They grant a high expression rate of exogenous proteins (even after only 18 hours) with high density of proteins produced after cytoplasmic injection of mRNA. Their efficient biosynthetic apparatus allows to reproduce the post-translational modifications needed for the correct targeting and the functionality of the proteins. Moreover, *X. laevis* oocytes allow the co-expression of many proteins just requiring co-injections of the corresponding mRNAs. In *X. laevis* oocytes the endogenous membrane proteins have low expression levels, furthermore the endogenous channels have been studied extensively, thus it is an easy task to distinguish between exogenous and endogenous proteins. *X. laevis* oocytes can survive in culture for long periods of about ten days, without requiring particular sterile conditions. Their dimensions suit well for microinjections and for applying the voltage clamp technique. Despite the above-mentioned advantages, *X. laevis* oocytes, have also some disadvantages. Unfortunately, the expression of exogenous proteins is just transient in *X. laevis* oocytes and even if their cells are in quiescent state, the oocytes genetic pool might affect the expression of exogenous proteins. Lastly,

it is worth to mention that the ideal temperature for maintain *X. laevis* oocytes is about 18°C and it is significantly lower than the one needed for many exogenous proteins, so the folding process can suffer from this difference.

All the employed oocytes were prepared following the procedures described (Bossi et al., 2007) and they were collected from adult females of *X. laevis* (Envigo, San Pietro al Natisone, Italy). The frogs were anaesthetised by immersion in a solution of 0.10% (w/v) of tricaine methansulfonate (MS222) in tap water adjusted at final pH 7.5 with sodium bicarbonate. After the treatment with an antiseptic agent (Providone-iodine 10%), the frog abdomen was incised, and the portions of the ovary were removed. Then, the oocytes were treated with 1 mg/mL of collagenase (Sigma collagenase Type IA from *Clostridium histolyticum*) in Ca^{+} free solution, ND96 (NaCl 96 mmol/L, KCl 2 mmol/L, $MgCl_2$ 1 mmol/L, $CaCl_2$ 1.8 mmol/L, HEPES 5 mmol/L, pH 7.6), for a period of at least 1 hour at 18°C. The healthy and full-grown oocytes were selected and separated manually in NDE solution (ND96 plus pyruvate 2.5 mmol/L and gentamycin sulphate 0.05 mg/mL). After 24 hours at 18 °C, the oocytes were injected with 25 ng (in 50 nL of water) of *in vitro* synthesised PepT1 cRNA using a manual microinjection system (Drummond Scientific Company, Broomall, PA, USA). Before electrophysiological studies the oocytes were then incubated at 18 °C for 3-4 days in NDE. All the experiments and the surgical operations were conducted using experimental protocol approved locally by the Committee of the *"Organismo Preposto al Benessere degli Animali"* of the University of Insubria (OPBA-permit no. 02_15) and by the Italian Ministry of Health (permit no. 1011/2015).

Electrophysiology and data analysis

The use of electrophysiology results very helpful in studies on membrane transporters. By recurring to this technique, it is possible to control the cell membrane voltage and to hold it during the experiments. Moreover, the results may be obtained immediately, so the data can be analysed and interpreted almost in real-time. This feature allows to modify or to adjust the protocols employed if needed, while the experimental session is ongoing. Therefore, it results clear that this technique greatly reduces the downtime and increases the efficiency of each experiment. During the transport cycle, electrogenic transporters translocate the electric charges and they are affected greatly by the transmembrane potential. As a consequence, when the membrane voltage as well as the electrical gradient are uncertain, the experimental results on the transporter activity are not very accurate. Using the so called voltage-clamp technique, it is possible to hold the membrane potential to a desired value, thus the measured currents can be considered caused only by the transporter activity.

Two Electrode Voltage Clamp (TEVC)

During the first '40s, Marmont and Cole presented the voltage-clamp technique (Cole and Curtis, 1941). Shortly after, Hodgkin, Huxley and Katz used it for investigating the ionic currents underlying the action potential in nerve axons (Hodgkin et al., 1952). As soon as the first transporter was cloned and expressed in *X. laevis* oocytes, the voltage-clamp technique, particularly the Two Electrode Voltage Clamp (TEVC) technique has started to be employed extensively for studying membrane transporters (Hediger et al., 1987; Ikeda et al., 1989; Parent et al., 1992; Mager et al., 1993).

In TEVC, two microelectrodes are used, one is responsible for recording the transmembrane voltage, while the other for passing the required current. Like in

a feedback system, the measured voltage is compared to the holding potential; if needed a feedback current is injected into the cell so the desired voltage is held. Therefore, the membrane voltage is the independent variable and it is controlled, the dependent variable is the membrane current and it is measured.

When the ion-coupled transporters are located in the membrane, the transmembrane current take place due to the transport activity causing membrane voltage changes, thus the current injected to compensate this variation can be recorded and it is an indication of the activity of transporters.

The TEVC circuit (**Figure 2.1**) consists of two operational amplifiers, one to stabilize the measured membrane potential via the voltage follower and one to perform voltage clamp by negative feedback amplifier; an ammeter to measure the current flow (I_M); two resistances, one of the potential measuring (R_{PE}) and the other of the current supplying electrode (R_{CE}); a model membrane is represented as a parallel circuit of a resistor (R_M) and a capacitor (C_M) (Bierwirtz and Schwarz, 2014).

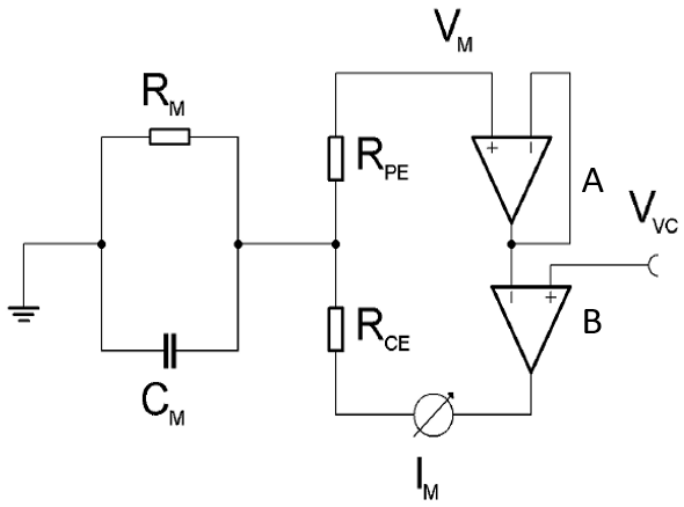

Figure 2.1 Two electrode voltage-clamp circuit. The schematic drawing of a voltage follower (operational amplifier with unity gain) in A, and an operational amplifier that acts as a negative feedback amplifier in B. V_{VC} is the voltage command that is to be clamped to the membrane. I_M represents ampere meter. R_{PE} and R_{CE} represent the potential electrode resistance and the

current electrode resistance, respectively. C_M is the membrane capacitance and R_M is the membrane resistance (Bierwirtz and Schwarz, 2014).

TEVC experimental setup, protocols and data analysis

The membrane currents under voltage clamp conditions, controlled by Clampex 10.2 (Molecular Devices, Sunnyvale, CA, USA), were recorded by TEVC (Oocyte Clamp OC-725C, Warner Instruments, Hamden, CT, USA) that was connected to a computer through an AD/DA (analog-digital, digital-analog) converter (DIgiData 1440A, Axon Instr.). A stereoscope (Wild M3B, Leica Microsystems AG, Wetzlar, Germany) was used to visualize and to place the oocytes in the recording chamber connected to perfusion system. The solution in the chamber was aspired by a vacuum pump through a suction reservoir connected to the oocyte well. In the recording chamber, the oocytes were impaled with two Ag/AgCl electrodes positioned on the electrode holders that were moved using micromanipulators (MM-33, Märtzhäuser Wetzlar GmbH & Co. KG, Wetzlar-Steindorf, Germany). The intracellular glass microelectrodes, with a tip resistance of 0.5-4 MΩ, were filled with KCl 3 mol/L. Bath electrodes were connected to the experimental oocyte chamber via agar bridges (3% agar in KCl3 mol/L). All the equipments needed for the recording are placed inside a Faraday cage. The cage and all the instruments inside of it were grounded.

The holding potential was kept at -60 mV; the voltage pulse protocol consisted of 10 square pulses from -140 to +20 mV (20 mV increment) of 700 ms each. Signals were filtered at 0.1 kHz or 0.5 kHz before sampling at 2 kHz or 1 kHz, respectively. Transport-associated currents were calculated by subtracting the traces in the absence of substrate from those in its presence.

To study the pre steady-state (*PSS*) currents elicited by voltage jumps in absence of organic substrate, the isolation method consisted of a double-exponential fitting (Sala-Rabanal et al., 2006; Mertl et al., 2008; Sangaletti et al., 2009). This

method allows to separate the transporter mediated transients (or *PSS* currents) from the total current across the oocyte membrane by subtraction of the fast capacitive and steady state components. The total current to the time course of the "on" response was fitted with double-exponential function **[2.1]**:

$$I_t = I_m\, e^{\left(-\frac{t}{\tau m}\right)} + I_{PSS}\, e^{\left(-\frac{t}{\tau_{PSS}}\right)} + I_{SS} \qquad \textbf{[2.1]}$$

where I_t is the total current across the oocyte membrane; t is the time; I_m is the initial value of the membrane capacitive current, which has a time constant of decay τ_m; I_{PSS} is the initial transporter *PSS* current, which has a time constant of decay τ_{PSS}; and I_{SS} is the steady state current (Sala-Rabanal et al., 2006).

The fast component of transient currents has time constant (τ_m) of about 1 ms that is potential-independent and it represents the charging of membrane capacitance, whereas the slow one has a time constant (τ_{PSS}) on average of tens of milliseconds and that is potential-dependent, strictly related to the presence of transporters on the plasma membrane.

To determine the time constant value at the holding potential of -60 mV, the currents at the "off" response at all tested potentials, were fitted with double exponential and the obtained values of $\tau_{PSS_{off}}$ were averaged. At each voltage, the amount of displaced charge (*Q*) was calculated by integrating the isolated traces after zeroing any residual steady-state transport current. Data was analyzed using Clampfit 10.7 (Molecular Devices).

For statistical analysis, descriptive statistic, fitting and figure preparation, Origin 8.0 (OriginLab, Northampton, MA, USA) was used. Number of samples and batch were reported in each figure. The analysis of the statistical significance between transport-associated currents under different experimental conditions

was done using one-way ANOVA followed by Bonferroni's *post-hoc* multiple comparison test (differences were considered significant with at least $p<0.05$).

Solutions

The external control solution had the following composition: NaCl (or TMA) 98 mmol/L, $MgCl_2$ 1 mmol/L, $CaCl_2$ 1.8 mmol/L. For pH 6.5 the buffer solution Pipes 5 mmol/L was used; Hepes 5 mmol/L was used to obtain a pH 7.6 and pH 8.5. The final pH values were adjusted with HCl or NaOH. The substrate oligopeptides tested were: glycine-glutamine (Gly-Gln), alanine-alanine (Ala-Ala), glycine-glycine-glycine (Gly-Gly-Gly), glycine-sarcosine (Gly-Sar), glycine-aspartate (Gly-Asp), aspartate-glycine (Asp-Gly) (Sigma-Aldrich, Milan, Italy); lysine-glycine (Lys-Gly) (Bachem, Bubendorf, Switzerland); glycine-lysine (Gly-Lys), methionine-lysine (Met-Lys), lysine-methionine (Lys-Met) (Genicbio, Shangai, China, www.genicbio.com). Every oligopeptide was added at the indicated concentrations (from 0.01 to 30 mmol/L) in the NaCl or TMA buffer solutions with appropriate pH.

Chapter 3. Results

With the increase in availability of genome sequences of several teleosts in databanks, it progressively became evident that teleost PepT1-type proteins were the result of a gene duplication, and the presence of PepT1a form of SLC15A1 (SLC15A1a) protein was confirmed in many fish species (Verri et al., 2017), but to date it is still not known if PepT1a-type proteins are functional. To the best of the author knowledge, in this work the data about PepT1a function are investigated and described for the first time.

Sequence analysis

Zebrafish *pept1a* (*slc15a1a*) cDNA is 2478 bp long, with a coding sequence (CDS) of 2154 bp encoding a protein of 717 amino acids. The complete CDS of Atlantic salmon *pept1a (slc15a1a)* of 2157 bp encodes for a protein of 718 amino acids. PepT1a (Slc15a1a) *vs.* PepT1b (Slc15a1b) amino acid sequences share 78% similarity and 62% identity in zebrafish and shared 77% similarity and 64% identity in Atlantic salmon (see supplementary material, **Figure S.1** for zebrafish proteins and **Figure S.2** for Atlantic salmon proteins). Hydropathy analysis predict 12 potential transmembrane domains for both PepT1a proteins with a large extracellular loop between transmembrane domains IX and X. Important motifs such as the PTR2 family proton/oligopeptide symporter signatures are present in zebrafish PepT1a sequence as well as in Atlantic salmon PepT1a. The predicted membrane topology of zebrafish PepT1a and Atlantic salmon PepT1a are reported in **Figure 3.1** and **Figure 3.2**, respectively.

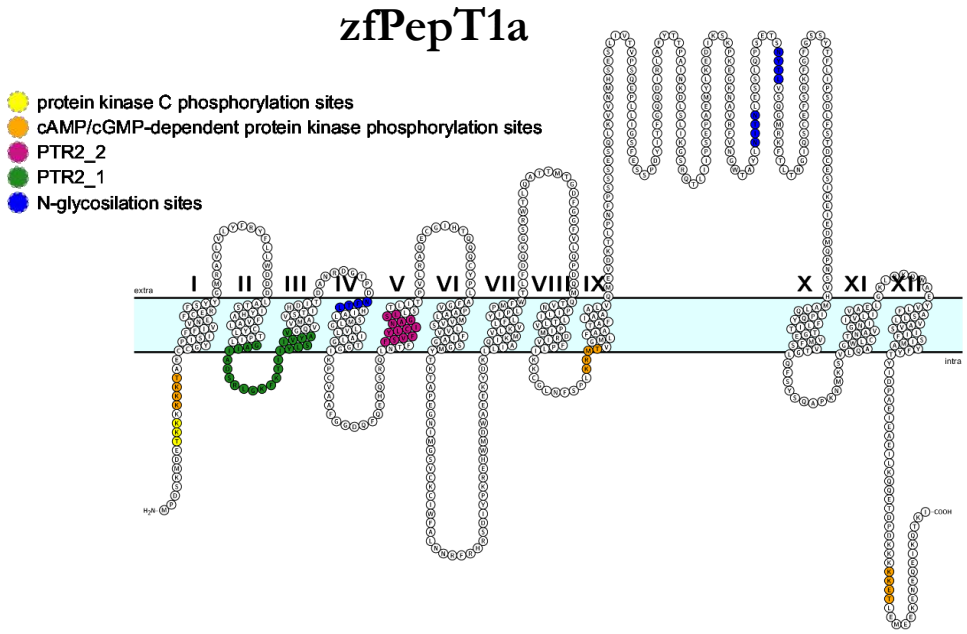

Figure 3.1 Predicted membrane topology of zebrafish PepT1a (zfPepT1a). In the amino acid sequence, putative transmembrane domains, obtained using the TMHMM v. 2.0 (http://www.cbs.dtu.dk/services/TMHMM/) program as implemented in SMART (Letunic et al., 2015), are indicated and named I to XII. Predicted conserved PTR2 family proton/oligopeptide symporters signatures were obtained using the ScanProsite tool (https://prosite.expasy.org/scanprosite/) (Hulo et al., 2006): PTR2_1 motif 1 - PROSITE pattern PS01022 - amino acid residues 80-104 (in green); and PTR_2 motif 2 - PROSITE pattern PS01023 - amino acid residues 173-185 (in purple). Potential extracellular N-glycosylation sites (blue), potential cAMP/cGMP-dependent protein kinase phosphorylation sites at the cytoplasmic surface (in orange) and potential protein kinase C phosphorylation sites at the cytoplasmic surface (in yellow) were obtained using the ScanProsite tool. The picture was obtained using Protter - visualize proteoforms (http://wlab.ethz.ch/protter/) (Omasits et al., 2014).

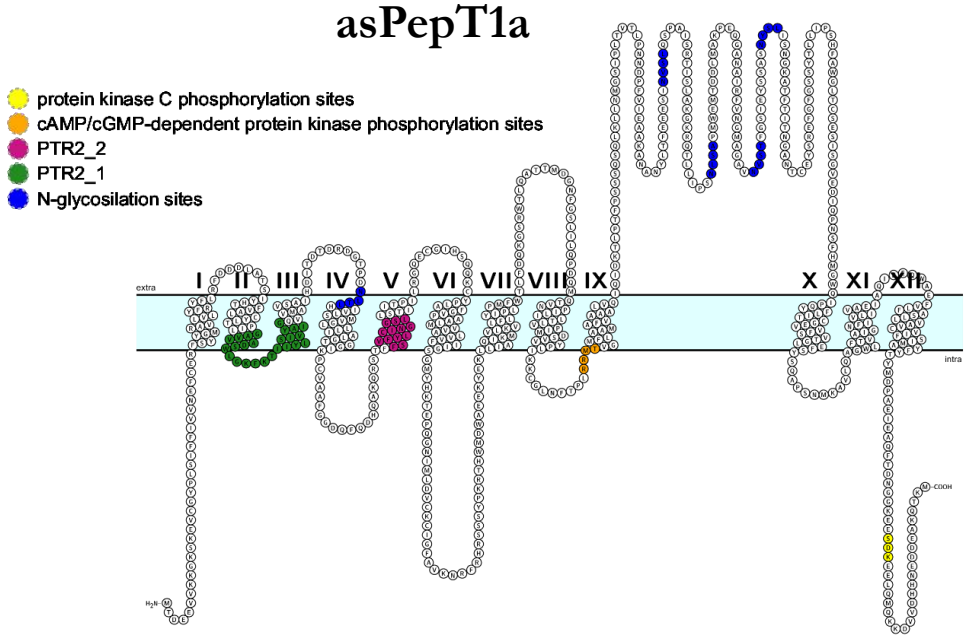

Figure 3.2 Predicted membrane topology of Atlantic salmon PepT1a (asPepT1a). In the amino acid sequence, putative transmembrane domains, obtained using the TMHMM server v. 2.0 (http://www.cbs.dtu.dk/services/TMHMM/), are indicated and named I to XII. The predicted conserved PTR2 family proton/oligopeptide symporters signatures were obtained using the ScanProsite tool (https://prosite.expasy.org/scanprosite/)(Hulo et al., 2006): PTR2_1 motif 1 - PROSITE pattern PS01022 - amino acid residues 76-100 (in green); and PTR2_2 motif 2 - PROSITE pattern PS01023 - amino acid residues 169-181 (in purple). Potential extracellular N-glycosylation sites (blue) were obtained using NetNGlyc 1.0 server (http://www.cbs.dtu.dk/services/NetNGlyc/).Potential cAMP/cGMP-dependent protein kinase phosphorylation sites at the cytoplasmic surface (in orange) and potential protein kinase C phosphorylation sites at the cytoplasmic surface (in yellow), were obtained using the ScanProsite tool (Hulo et al., 2006). The picture was obtained using Protter - visualize proteoforms (http://wlab.ethz.ch/protter/) (Omasits et al., 2014).

Functional data

Several ion-coupled transporters show distinctive kinds of current, which are believed to represent the operating modes of these proteins. The transport associated currents are steady state currents elicited in the presence of the substrates. These currents are due to the translocation through the cell membrane of substrates together with the co-transported ions. The transient currents, or pre steady-state currents, are typically caused by voltage or ion concentration changes. These are capacitive currents arising from the confined movement of charges within the membrane electrical field. The moved charges can be either the driving ions that interact with protein residues and/or the intrinsic charged amino acids of the transporter. Transport currents and transient currents are mutually exclusive; while the former are visible in the presence of substrate and increase till reaching saturating concentration, the latter are clearly observable in absence of substrate and disappear completely when saturating amount of substrate is present. Both the above-mentioned currents are present in *X. laevis* oocytes overexpressing of PepT1 and they can be measured by Two Electrode Voltage Clamp (TEVC) technique. The biophysical analysis of the transport currents and of the pre steady-state currents shows different properties when PepT1 orthologues are compared.

Transport currents

Seventy-two hours after injection of 25 ng of cRNA encoding zebrafish and Atlantic salmon PepT1a and PepT1b, oocytes were tested through TEVC technique for evaluating the transporter function. Inward transport currents were recorded in voltage clamp at the holding potential of -60 mV in the presence of 1 mmol/L of Gly-Gln, Ala-Ala and Gly-Gly-Gly in sodium solution at increasing pH (6.5, 7.6 and, for the zebrafish only, pH 8.5 due to its peculiar

gut condition). The representative current traces, reported in **Figure 3.3**, show that the newly cloned zebrafish and Atlantic salmon PepT1a are electrogenic transporters, as well as their PepT1b counterparts. The inward currents elicited by the indicated substrates result differently affected by external pH (**Figure 3.3**).

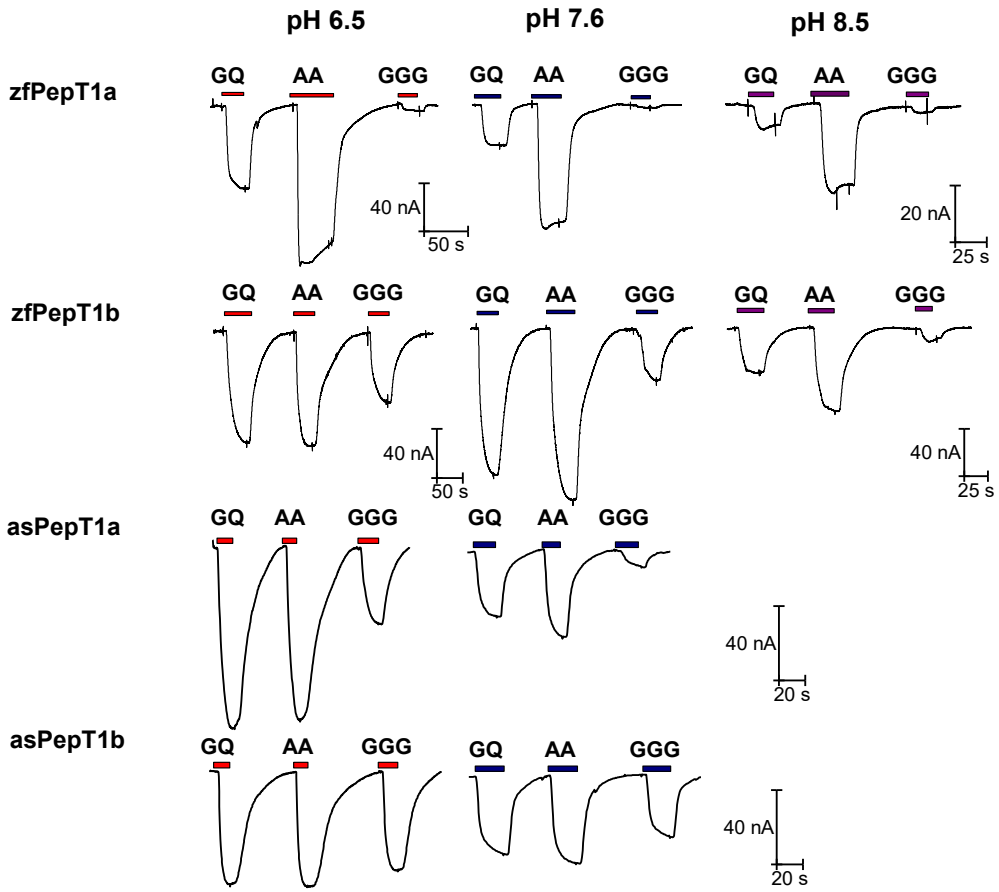

Figure 3.3 The representative traces of transport currents in zebrafish (zfPepT1a and zfPepT1b) and Atlantic salmon (asPepT1a and asPepT1b) transporters heterologously expressed in *Xenopus laevis* oocytes. For all cases, the currents were recorded at the holding potential (V_h) of -60 mV and for pH values of 6.5 and 7.6, in the presence of (1 mmol/L) Gly-Gln (GQ), Ala-Ala (AA) and Gly-Gly-Gly (GGG) substrates indicated by the bars above. For zebrafish transporters only, the currents were measured also at pH 8.5.

To evaluate the effect of sodium on the transport activity of both PepT1a transporters, the currents elicited by 3 mmol/L of Gly-Gln were compared in two different buffer solutions. The first contained sodium, whereas in the second the sodium was substituted by tetramethylammonium (TEA). During these experiments, the currents were evaluated in a membrane potential range from -140 mV to + 20 mV at pH 7.6.

No differences in current amplitudes and in the shape of I/V relationship are highlighted confirming that zebrafish PepT1a and Atlantic salmon PepT1a are both sodium-independent, (**Figure 3.4**).

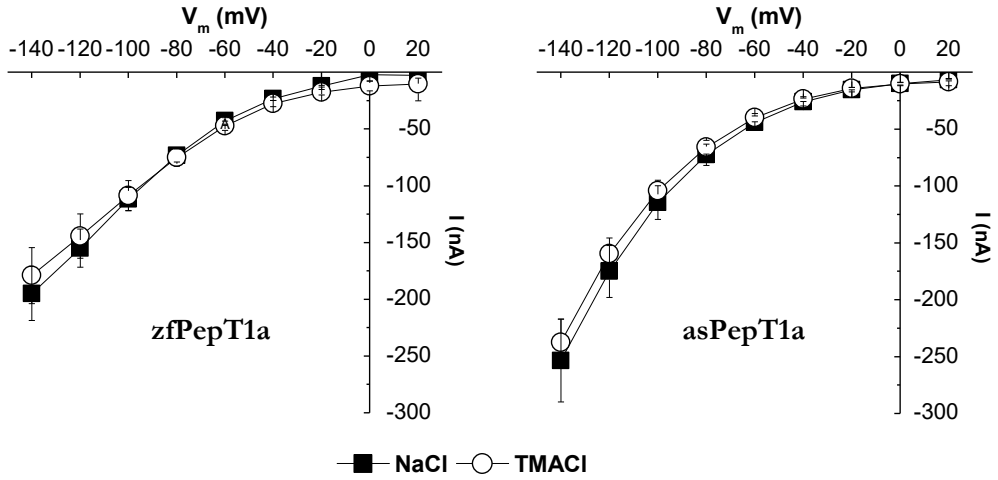

Figure 3.4 Current-voltage relationships of transport-associated currents in zebrafish PepT1a (zfPepT1a, right) and Atlantic salmon PepT1a (asPepT1a, left), in the presence of 3 mmol/L Gly-Gln in sodium (Na) saline buffer (square) and tetramethylammonium (TMA) saline buffer (empty circle) at pH 7.6. The values are the mean ± SEM of 5 up to 12 oocytes belonging to one or two batches, in each case. The transport-associated currents were obtained by subtracting the currents recorded in absence of the substrate to those in its presence.

The pH dependence of the transport activity of zebrafish and Atlantic salmon PepT1a and PepT1b transporters was investigated and statistically compared. The transport associated currents were recorded under the same experimental

conditions previously described and shown in **Figure 3.3**, the currents reported in the histogram were obtained by subtracting the currents recorded in absence of the substrate to those in its presence. These currents were collected from 4 to 7 oocytes belonging to at least 2 different batches and their amplitudes were averaged. In the same experiment the mammalian PepT1 transporter of rabbit (GenBank Acc. No. U13707.1) (Boll et al., 1994) was tested as well. The results are shown in the histograms in **Figure 3.5**.

The transport current amplitudes, elicited in oocytes expressing the tested proteins, show different profiles and pH dependences.

In zebrafish PepT1a the transport associated currents, in the presence of Gly-Gln and Ala-Ala dipeptides, decrease with the increase of the pH from 6.5 to 8.5, with significant differences in current amplitudes between these two pH conditions ($p<0.01$ for Gly-Gln and $p<0.05$ for Ala-Ala).

Under the same experimental conditions, zebrafish PepT1b shows higher currents at pH 7.6 with respect to the ones obtained for the other two pH conditions (pH 6.5, pH 8.5). In zebrafish PepT1b, the differences in current amplitudes in the presence of dipeptides are statistically different between pH 7.6 and pH 8.5 ($p<0.001$ for Gly-Gln and $p<0.01$ for Ala-Ala) and between pH 6.5 and pH 8.5 ($p<0.01$ for Gly-Gln).

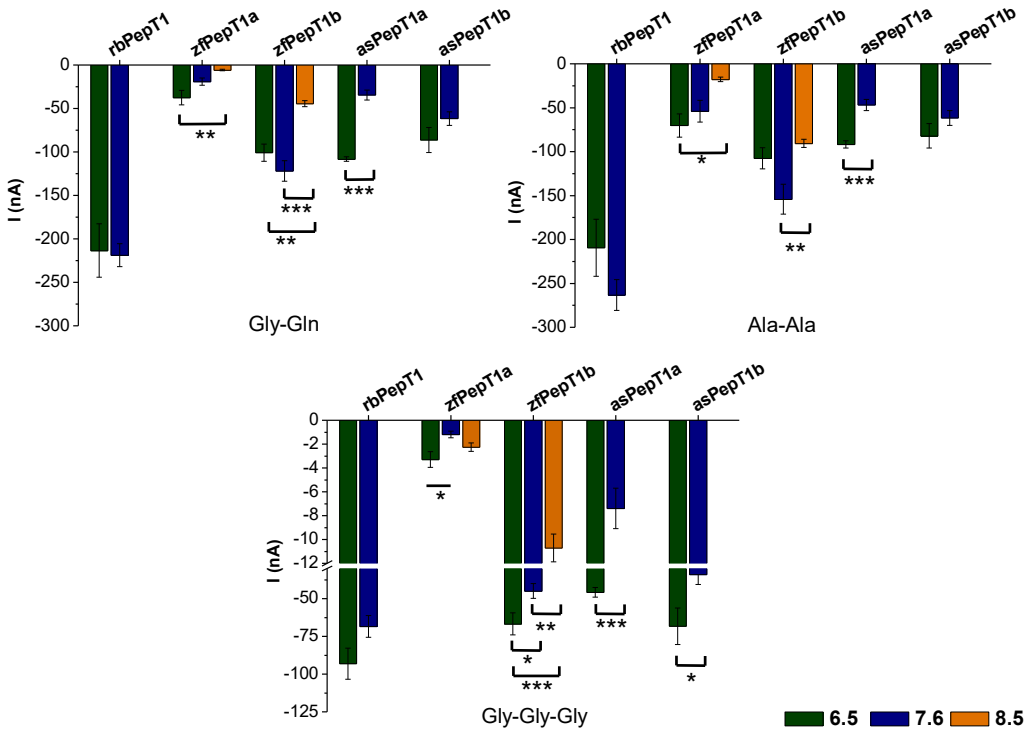

Figure 3.5 The means of the transport-associated currents at different pH conditions, at pH 6.5, 7.6 and 8.5 for zebrafish transporters (zfPepT1a and zf PepT1b); at pH 6.5 and 7.6 for rabbit (rbPepT1) and Atlantic salmon (asPepT1a and asPepT1b) transporters. The transport currents elicited by Gly-Gln (top left), Ala-Ala (top right) and Gly-Gly-Gly (bottom) (1 mmol/L) at -60 mV at pH 6.5 (green), 7.6 (blue) and 8.5 (orange) are reported as mean ± SEM of 4 up to 7 oocytes from 1 to 2 batches (*Anova, Bonferroni*; * *p<0.05*, ** *p<0.01* and *** *p<0.001*).

For zebrafish PepT1a and PepT1b the current amplitudes elicited by Gly-Gln and Ala-Ala did not differ statistically between pH 7.6 and 6.5. Although zebrafish transporters work well with neutral substrates, PepT1a shows higher currents of the presence of Ala-Ala, while PepT1b exhibits similar current amplitudes for both dipeptides at the three pH conditions tested.

In Atlantic salmon PepT1b, only a slight increase in the currents is observed in the presence of Gly-Gln and Ala-Ala when decreasing the pH from 7.6 to 6.5; in PepT1a the currents show large increase at pH 6.5, with significant differences

in amplitudes if compared to the values at pH 7.6 ($p<0.001$) for all the tested substrates.

When the substrate is the tripeptide Gly-Gly-Gly, the transport associated currents are drastically reduced to few nanoamperes regardless of the pH conditions in zebrafish PepT1a. At pH 6.5, the same tripeptide elicits currents of few tens of nA in Atlantic salmon PepT1a that significantly decrease at pH 7.6 ($p<0.01$). In contrast to the peculiar alkaline pH preference of zebrafish PepT1b, reducing the external pH from 7.6 to 6.5 significantly increases ($p<0.05$) the current amplitudes in the presence of Gly-Gly-Gly. The same effect is observed in Atlantic salmon PepT1b but not for rabbit PepT1 confirming that also in the presence of the tripeptide, the pH effect on transport associated currents is not statistically detectable for the mammalian transporter.

To define the voltage dependence and apparent substrate affinity of zebrafish and Atlantic salmon PepT1a, the transport currents for Gly-Gln from 0.01 to 30 mmol/L, were recorded at two pH values (7.6 and 6.5), in the range of voltage from -140 mV to +20 mV (**Figure 3.6**).

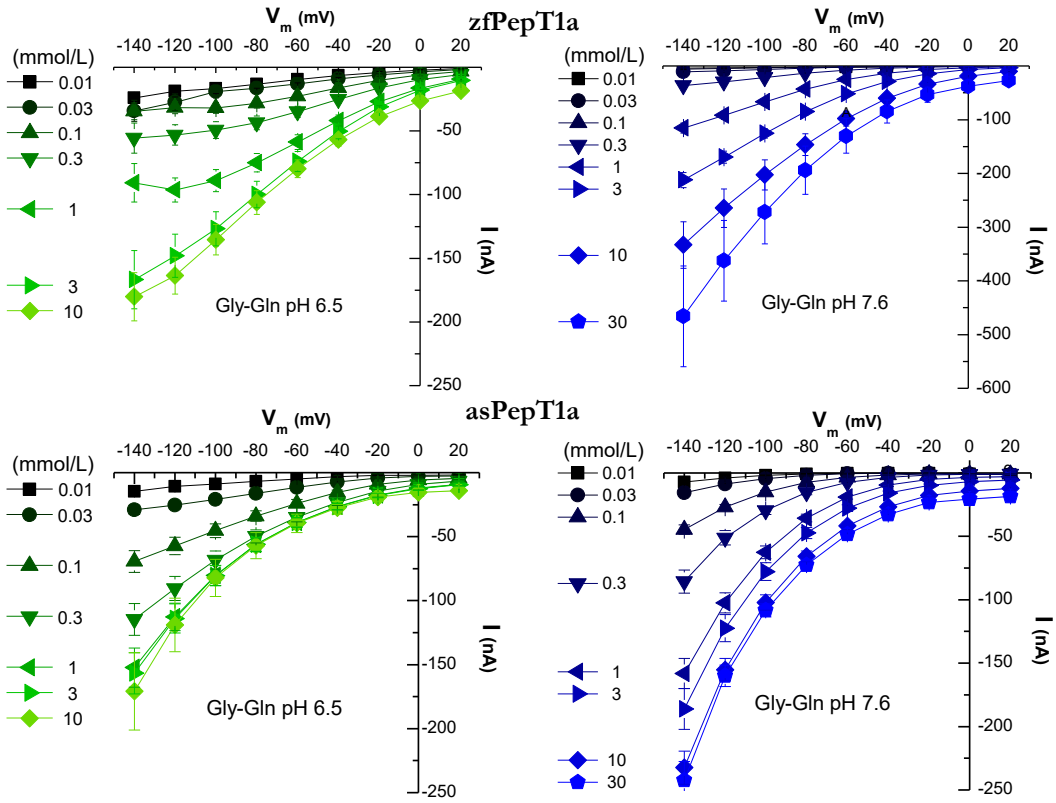

Figure 3.6 Current *vs.* Voltage (I/V) relationships for zebrafish PepT1a (top) and Atlantic salmon PepT1a (bottom) were obtained by subtracting the current traces in the absence of the substrate to that in the presence of Gly-Gln from 0.01 to 10 mmol/L at pH 6.5 and to 30 mmol/L at 7.6. Data are reported as mean ± SEM of 9 up to 14 oocytes from 3 batches. The transport-associated currents were obtained by subtracting the current recorded in absence of the substrate to those in its presence.

The data of the transport associated currents, collected at pH 6.5, show that for zfPepT1a the Gly-Gln 3 mmol/L is the saturating value; in fact, a further increment of the concentration to 10 mmol/L in fact does not increase the current amplitude, independently from the tested voltages. For Atlantic salmon PepT1a transporter the I/V curves recorded in the presence of Gly-Gln concentrations from 1 to 10 mmol/L largely overlap suggesting that at pH 6.5 the saturating values is reached at 1 mmol/L of Gly-Gln. The I/V plot at pH

7.6 shows that the transport associated currents in the zebrafish transporter constantly increase with the substrate concentration and do not reach the maximal value even in the presence of 30 mmol/L of Gly-Gln. At pH 7.6 in the Atlantic salmon transporter the saturating concentration is reached around 10 mmol/L of the substrate. The I/V relationship at the two pH values for both transporters was fitted with the Michaelis-Menten equation to determine the kinetic parameters: the maximal relative current (I_{max}), the apparent substrate affinity (i.e. the apparent concentration of peptide that yields one-half of Imax; $K_{0.5}$) and the transport efficiency ($I_{max}/K_{0.5}$) (**Figure 3.7**).

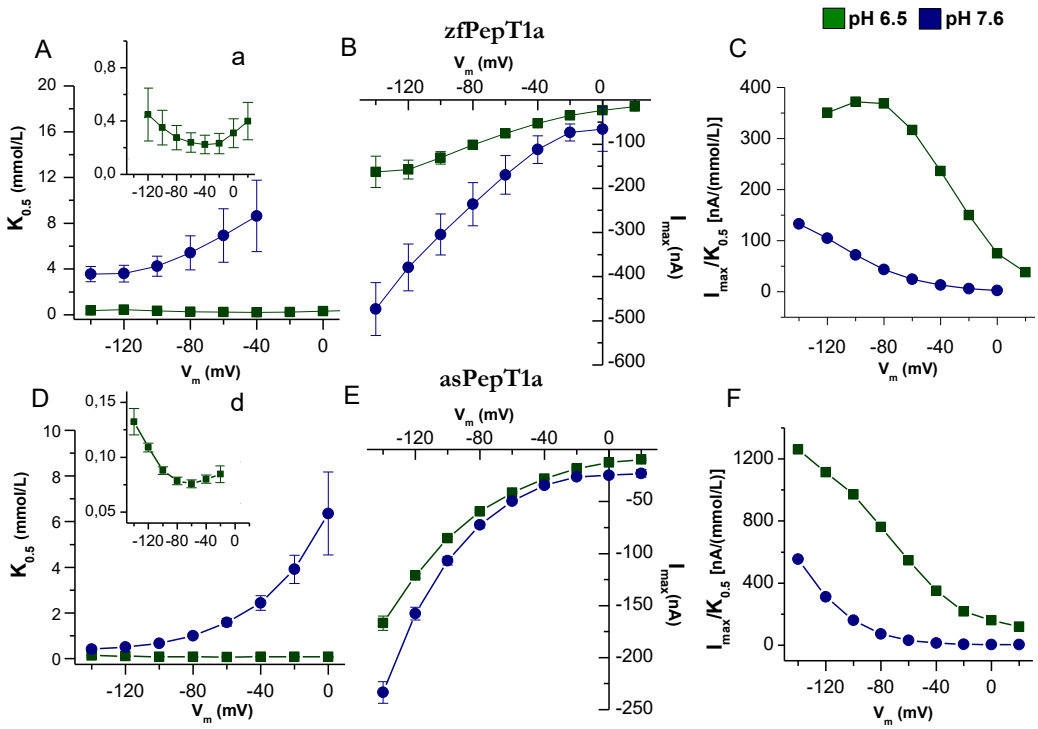

Figure 3.7. Dose response analysis: $K_{0.5}$, I_{max} and transport efficiency of zebrafish (**A, B**, **C**) and Atlantic salmon (**D**, **E**, **F**) PepT1a (Slc15a1a) evaluated in the presence of Gly-Gln. The current values (**Figure 3.6**) were subsequently fitted with the Michaelis-Menten equation $\left[I_0 = \frac{-I_{max}}{1+([S]/K_{0.5})} + I_{max}\right]$ to obtain $K_{0.5}$, i.e. the substrate concentration that elicits half of the maximal current (I_{max}), at each indicated voltage and at pH 6.5 (green square) and 7.6 (blue

circle): **A** and **D**, the inserts (**Aa** and **Dd**) are enlargements of $K_{0.5}$ at pH 6.5. The relative maximal current (I_{max}) at each voltage and pH is plotted in **B** and **E**. In **C** and **F,** the transport efficiency is reported, evaluated as the ratio of $I_{max}/K_{0.5}$ values at each membrane potential and pH condition.

As **Figure 3.7** shows in **A** and **D**, zebrafish and Atlantic salmon PepT1a affinity ($1/K_{0.5}$) for Gly-Gln increases with the decrease of pH, and at pH 6.5 affinity is only slightly influenced by voltage. At pH 6.5, the $K_{0.5}$ is in the micromolar range for both PepT1a transporters. Zebrafish PepT1a shows $K_{0.5}$ minimal value of 0.22 ± 0.06 mmol/L at -40 mV and maximal value of 0.44 ± 0.19 mmol/L at -120 mV. Atlantic salmon PepT1a shows higher apparent affinity for Gly-Gln than the zebrafish transporter with minimal value of $K_{0.5}$ of 0.075 ± 0.003 mmol/L at -60 mV and maximal value of 0.13 ± 0.01 mmol/L at -140 mV. At pH 7.6, the values of $K_{0.5}$ increased to millimolar range and became voltage dependent for both transporters. By changing the cellular membrane potential from -140 mV to -40 mV, the $K_{0.5}$ values increase about three times for zebrafish (from 3.55 ± 0.67 mmol/L at -140 mV to 8.63 ± 3.12 mmol/L at -40 mV), and about six times for Atlantic salmon (from 0.42 ± 0.04 mmol/L at -140 to 2.44 ± 0.31 at -40 mV). The PepT1a relative maximal currents elicited by Gly-Gln are reported in **Figure 3.7B** for zebrafish and in **Figure 3.7E** for Atlantic salmon. As expected from electrogenic transporters, the maximal relative currents I_{max}, of both PepT1a exhibit a clear dependence on membrane potential with current amplitudes that decrease passing from -140 mV to less negative potentials for both external pH (**Figure 3.7B** and **3.7E**). For zebrafish PepT1a the rise of extracellular pH from 6.5 to 7.6 results in a pronounced increase in the maximal transport currents of about three-fold at -140 mV (from -162.78 ± 35.35 nA at pH 6.5 to -473.09 ± 59.88 nA at pH 7.6) (**Figure 3.7B**). The rise in the maximal transport rate with the increase of extracellular pH represents a unique feature of the zebrafish transporter as observed for the PepT1b (Verri et al., 2003). Atlantic salmon PepT1a, in a range from 0 mV to -

80mV, shows very slight differences in Gly-Gln relative maximal current values at two pH conditions. While, for more negative voltage values than -100 mV, the relative maximal current results affected by the pH showing higher amplitude at 7.6 than at 6.5 (**Figure 3.7E**). Accordingly, also the transport efficiency, evaluated as the ratio $I_{max}/K_{0.5}$, is influenced largely by the pH in zebrafish and Atlantic salmon PepT1a (**Figure 3.7C** and **Figure 3.7F**). It shows higher values at pH 6.5, with a maximum at about -90 mV for zebrafish transporter. For Atlantic salmon transporter, the transport efficiency reaches higher values at more negative potentials, presumably around -160 mV. For both transporters, the efficiency values are smaller at pH 7.6, and the maximum might be reached at even more negative potentials.

Highlighting the effect of pH on kinetic parameters, a deepest analysis was necessary to refine the results summarized in **Figure 3.5**. The dose response curves of Gly-Gln generated by oocytes expressing PepT1a and PepT1b of zebrafish and Atlantic salmon were compared at different pH conditions (**Figure 3.8**). In particular, the pH was varied from 6.5 to 7.6 in both fish, reaching the value of pH 8.5 for the zebrafish transporters only. The transport associated currents elicited by increasing the concentration of substrate from 0.01 to 10 mmol/L at membrane potential of -60 mV were plotted as current-concentration relationships. Then, they were fitted with a Michaelis-Menten equation showing a hyperbolic behavior, with large differences between different pH conditions for zebrafish transporters and slighter differences for Atlantic salmon transporters.

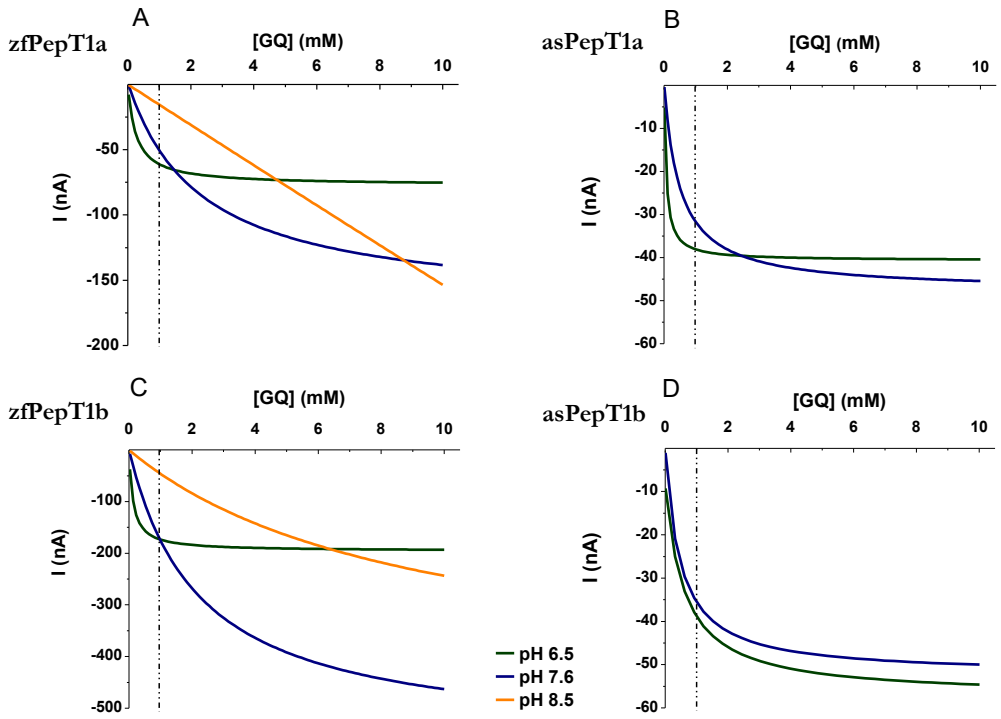

Figure 3.8 Fitting curves of the Gly-Gln transport associated inward currents as function of substrate concentration (from 0.01mol/L to 10 mol/L) and pH (pH 6.5 in green, pH 7.6 in blue and pH 8.5 in orange) at the membrane potential of -60mV. In **Figure A** and **C**, zebrafish PepT1a and PepT1b transporters (zfPepT1a and zfPepT1b). In **Figure B** and **D** Atlantic salmon PepT1a and PepT1b transporters (asPepT1a and asPepT1b).

The fit is shown in **Figure 3.8A** and **3.8C** where the dose response curves are represented for zebrafish PepT1a and PepT1b, respectively. In **Figure 3.8B** and **3.8D**, the corresponding graphs are reported for Atlantic salmon PepT1a and PepT1b transporters. The data show that the acidic pH affects similarly the function of the zebrafish proteins. Due to the high affinity to Gly-Gln of both zebrafish transporters at pH 6.5, the transport-associated current reaches the I_{max} value (see **Figure 3.7B** for PepT1a and Verri et al., 2003 for PepT1b) for Gly-Gln concentration lower than 10 mmol/L. At pH 7.6, the current generated by the concentration of 1 mmol/L (indicated by the dashed line in **Figure 3.8**),

results far from the maximum in both transporters. At this pH, the proteins bind the substrate with lower affinity and the current rises when the concentration is increased, without showing saturation in the tested range. When the experiments are conducted at pH 8.5, the fitted curves suggest a pronounced increase in the $K_{0.5}$ values; consequently, a larger amount of substrate is needed to reach the maximal current value, particularly for PepT1a. Interestingly, the transport currents elicited by concentrations of Gly-Gln up to 1 mmol/L differ only of few nanoamperes between pH 6.5 and 7.6 for both transporters at membrane potential of -60 mV. Atlantic salmon transporters show slight differences in maximal current values at the two pH conditions. The fitting curves show a parallel trend for PepT1b, at pH 6.5 the current is slightly higher than at pH 7.6 (**Figure 3.8D**). For PepT1a, the fitting curves cross each other at concentrations higher than 1 mmol/L of Gly-Gln. According to the data shown in **Figure 3.5** and to the data about the substrate apparent affinity in **Figure 3.7D**, the maximal current value is higher at pH 6.5 than at pH 7.6, for lower substrate concentrations (**Figure 3.8B**). Although there are only small differences in the current amplitude recorded at two pH conditions of about tens of nanoamperes, for Atlantic salmon PepT1a the highest values of maximal relative current are reached increasing the external concentration of Gly-Gln at pH 7.6, as it can be seen in **Figure 3.8B**.

The detailed biophysical and kinetic analysis of transport associated currents highlights some characteristics that distinguish the two proteins (PepT1a *vs.* PepT1b) in each of the two fish species investigated. Further data were collected about the I_{max}, $K_{0.5}$ and their ratio in the presence of Gly-Gln for zebrafish transporters and of Gly-Sar for Atlantic salmon PepT1a and PepT1b. During the experiment, two pH conditions were tested (6.5 and 7.6) at two membrane potentials (-60 mV and -120 mV). The results are summarized in **Table 3.1**.

	pH	% neutral	-60 mV			-120 mV			n/N
		Gly-Gln	$K_{0.5}$ mmol/L	I_{max} nA	$I_{max}/K_{0.5}$ nA/(mmol/L)	$K_{0.5}$ mmol/L	I_{max} nA	$I_{max}/K_{0.5}$ nA/(mmol/L)	
zfPepT1a	6.5	98.4	0.24 ± 0.07	-75.76 ± 6.04	316.37	0.449 ± 0.199	-157.38 ± 21.48	350.81	9/3
	7.6	83	6.92 ± 2.34	-169.57 ± 43.75	24.51	3.607 ± 0.73	-378.82 ± 53.07	105.02	14/3
zfPepT1b	6.5	98.4	0.127 ± 0.02	-195.7 ± 8.89	1535.32	0.13 ± 0,02	-396.24 ± 22.2	3032.16	7/1
	7.6	83	2.2 ± 1.03	-566.2 ± 212.4	254.54	1.01 ± 0.35	-1142.3 ±285.4	1129.7	7/1

			-60 mV			-120 mV			n/N
		Gly-Sar	$K_{0.5}$ mmol/L	I_{max} nA	$I_{max}/K_{0.5}$ nA/(mmol/L)	$K_{0.5}$ mmol/L	I_{max} nA	$I_{max}/K_{0.5}$ nA/(mmol/L)	
asPepT1a	6.5	98.9	0.53 ± 0.10	-39.23 ± 4.49	75.06	0.69 ± 0.14	-109.34 ± 12.49	159.14	9/3
	7.6	87.6	9.21 ± 0.34	-48.84 ± 10.42	5.30	2.70 ± 0.41	-124.79 ± 3.19	46.37	10/3
asPepT1b	6.5	98,9	0.50 ± 0.08	-61.90 ± 3.33	123.8	0.41 ± 0.04	-148.54 ± 7.55	362.29	*
	7.5	89,9	1.44 ± 0.12	-80.6 ± 10.4	55.9	0.52 ± 0.04	-238.8 ± 30.2	459.23	*

Table 3.1 The kinetic parameters: $K_{0.5}$, I_{max} and the transport efficiency ($I_{max}/K_{0.5}$). Data are obtained from *Xenopus laevis* oocytes for clamped voltages of -60 mV and at -120 mV, when perfused with Gly-Gln in sodium chloride buffer solutions at pH 6.5 and 7.6/7.5. The values are expressed as the averages ± SEM of *n* oocytes reported (each oocyte represents an independent observation). The kinetic parameters were calculated using the least-square fit of the Michaelis-Menten equation, **Figure 3.7**. The percentage of substrate present in its neutral (zwitterionic) form at a given pH is calculated using the Henderson-Hasselbach equation and the following pKa values: pKa1 = 2.88, pKa2 = 8.29 for Gly-Gln and pKa1 = 2.83, pKa2 = 8.45 for Gly-Sar. (*) For comparison, the kinetic parameters of Atlantic salmon PepT1b are reported, as extracted from Ronnestad et al., (2010).

Notably, all the changes in both I_{max} and $K_{0.5}$ result in a consistent reduction of zebrafish and Atlantic salmon PepT1a transport efficiency ($I_{max}/K_{0.5}$). In all the tested conditions, the transport efficiency is systematically lower that that recorded for the corresponding PepT1b transporters.

Data about the I_{max}, $K_{0.5}$ and their ratio for Atlantic salmon PepT1a were collected also in the presence of Ala-Ala, Gly-Asn, and Gly-Pro at pH 6.5 and are summarized (compared to Gly-Gln and Gly-Sar) in **Table 3.2**.

Substrate	$K_{0.5}$ mmol/L	I_{max} nA	$I_{max}/K_{0.5}$ nA/(mmol/L)	Oocytes/Batches n/N
Gly-Gln	0.076 ± 0.004	-41.317 ± 0.835	546	9-12/2
Gly-Sar	0.523 ± 0.102	-39.228 ± 4.490	75	9/3
Ala-Ala	0.024 ± 0.005	-18.404 ± 0.759	736	8/2
Gly-Asn	0.237 ± 0.106	-39.486 ± 7.099	167	9/2
Gly-Pro	0.317 ± 0.118	-26.479 ± 5.219	84	7/2

Table 3.2 The kinetic parameters of the inwardly directed transport of the selected di/tripeptides *via* the Atlantic salmon PepT1a (Slc15a1a). They were measured in Two-Electrode Voltage Clamp (TEVC) experiments. All values are expressed as the average ± SEM of n oocytes reported (each oocyte represents an independent observation). *Xenopus laevis* oocytes were voltage clamped at -60 mV and perfused with solutions at pH 6.5. The kinetic parameters ($K_{0.5}$ and I_{max}) were calculated by least-square fit to the Michaelis-Menten equation (**Figure 3.7**).

Pre steady-state (PSS) currents

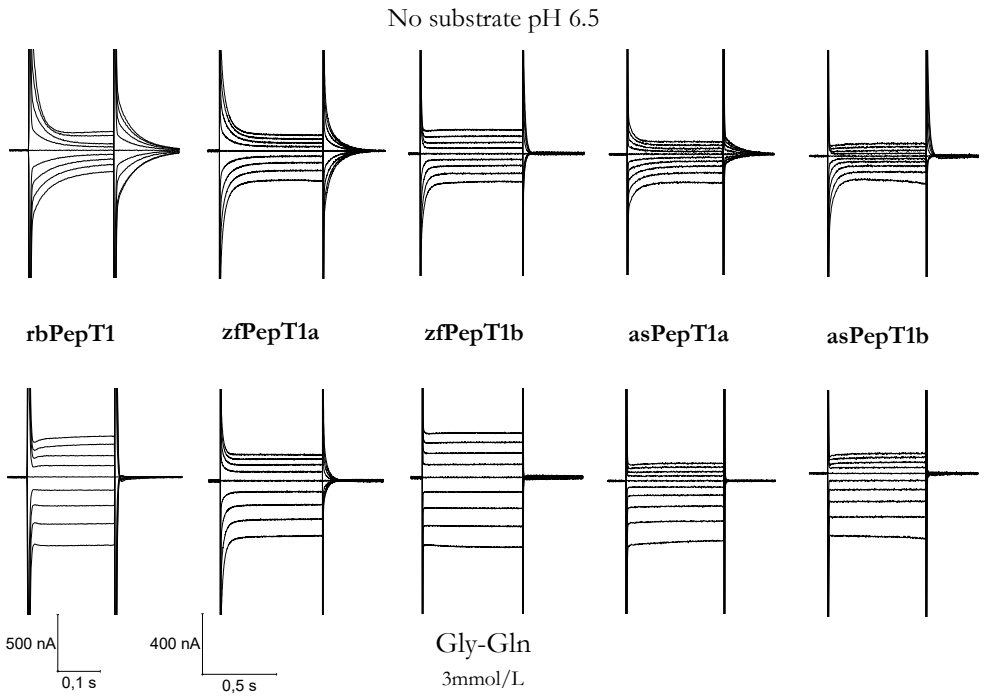

Figure 3.9 Comparison of PepT1 pre steady-state currents from mammalian (rabbit, rbPepT1) and two teleost fish species (zebrafish, zfPepT1a and zfPepT1b; Atlantic salmon, asPepT1a and asPepT1b). Voltage pulses, in the range from -140mV to +20mV, were applied starting from voltage holding of -60mV at pH 6.5. In absence of organic substrate (top), all tested transporters display transient currents in "on" and "off" of rectangular voltage jumps. In the presence of 3 mmol/L of reference substrate (Gly-Gln) (bottom), the mammalian and fish transporters show steady-state currents.

The pre steady-state (*PSS*) currents of rabbit PepT1, and zebrafish PepT1b have been already described and analyzed (Nussberger et al., 1997; Renna et al., 2011b), while those of Atlantic salmon PepT1b have not been investigated yet. The parameters that can be derived from these currents are crucial to understand the kinetics of the transport cycle steps.

The *PSS* of the newly cloned PepT1a transporters and PepT1b of Atlantic salmon were recorded and compared to the transient currents of well-known transporters: zebrafish PepT1b and rabbit PepT1. The experiments were performed on *X. laevis* oocytes expressing the proteins, under voltage pulses of 20 mV from -140 to +20 mV both in absence and in the presence of Gly-Gln (3 mmol/L), at pH 6.5. As shown in **Figure 3.9**, PepT1b of Atlantic salmon, similarly to what was previously reported for the zebrafish PepT1b and also for the seabass PepT1 transporter (GenBank Acc. No. FJ237043; Sangaletti et al., 2009), exhibit slow decaying, better visible for the "on" and "off" hyperpolarization voltage steps (from -140 mV to -80 mV) than in depolarization condition (from -40mV to +20 mV). Surprisingly, the transient currents of PepT1a transporters, similarly to the rabbit transporter, show symmetric behavior around the holding potential of -60 mV. The transient currents in response to the "on" and "off" voltage steps are well defined and particularly slow. This behavior is more emphasized in the zebrafish transporter. The traces in **Figure 3.9** (bottom) show the switch of the *PSS* to steady state transport currents in the presence of 3 mmol/L of Gly-Gln substrate at saturating concentration. Under this experimental condition, the *PSS* are almost completely abolished in all proteins, except for zebrafish PepT1a.

The *PSS* currents in PepT1 transporters, analyzed so far, shows a marked dependence on extracellular pH, in fact in rabbit and seabass PepT1 and in zebrafish PepT1b, increasing pH values of external medium has been shown to accelerate the decay of the *PSS* currents. This happens also in PepT1a transporters, as shown by the representative traces of **Figure 3.10**. At pH 7.6, both *PSS* of PepT1a transporters lost the symmetry around the holding potential. The transients become more observable in hyperpolarization than in depolarization. Even in Atlantic salmon PepT1b, the changes in external pH from 6.5 to 7.6 greatly accelerate the decay of transient currents. These observations are confirmed when comparing the time constant *vs.* potential

(τ/V) and the charge *vs.* potential (*Q*/V) curves at the two different pH conditions, in the right side of **Figure 3.10**

.

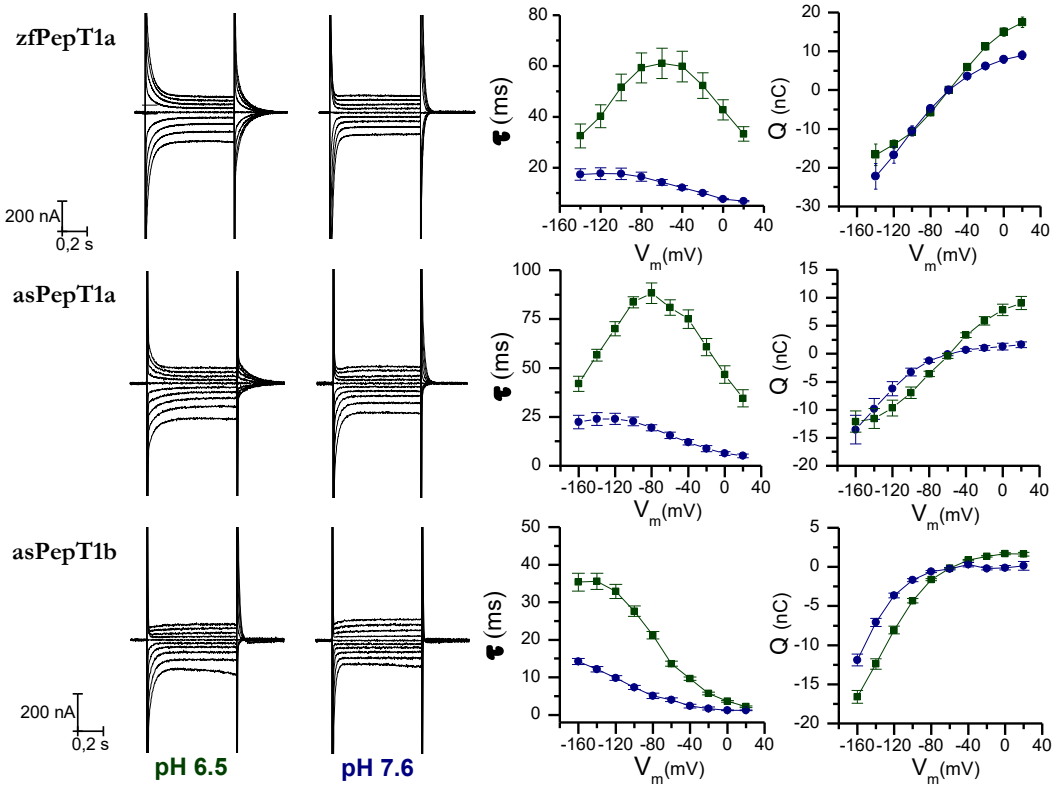

Figure 3.10 Current traces and pre steady-state currents analysis for zebrafish PepT1a (zfPepT1a), Atlantic salmon PepT1a (asPepT1a) and PepT1b (asPepT1b). In the left side, there are the representative traces of currents elicited by voltage pulses in the range -160 to +20 mV (20 mV steps from V_h of -60 mV) in absence of substrate at pH 6.5 and pH 7.6. In the right side, there are the analysis of pre steady-state currents reported as τ/V and Q/V. The time constants (τ) were obtained from the slow component of a double exponential fitting of the traces in absence of the substrate (the values were estimated from the "on" transients, except for the value at -60 mV (V_h), which was estimated from the "off" transients). The charge *vs.* voltage curves were obtained by integration of the transient isolated at the two pH values ("on" and "off" integrals were averaged for each individual oocyte before calculating the cumulative mean). The data are the mean ± SE from 10 to 15 oocytes.

The voltage dependences of the time decay constant τ and the intramembrane moved charge *Q* are obtained from the isolated *PSS* currents, using double exponential function fitting the currents recorded in the absence of substrate (Sangaletti et al., 2009). This method allows to separate transporter-*PSS* currents from the fast peaks due to the endogenous oocyte capacity. As for the mammalian transporter rabbit PepT1, the τ/V curves of both fish PepT1a are bell-shaped with a maximum at about -60 mV, at pH 6.5. This confirms the symmetrical behavior of transient current around the holding potential. For Atlantic salmon PepT1b, the analyses of the time decay constant as function of voltage show only a right half of bell-shaped curve at pH 6.5 and it appears to have a maximum at about -140 mV, as observed for the already characterized transporters in other teleost fish species (Renna et al., 2011b). For all transporters, the change of external pH to 7.6 produces negative shifts in the τ/V. The maximum is reached at about -120 mV for PepT1a transporters, whereas the maximal value of τ for Atlantic salmon PepT1b might be found at even more negative voltages. Furthermore, the levelling of τ/V curves at pH 7.6 is a consequence of an acceleration in the decaying of the *PSS* currents that are faster for Atlantic salmon PepT1b than for PepT1a transporters.

The moved charge *Q* is computed as the integral of the transient currents over time. The values reported are the average of the values obtained for the "on" and the "off" responses.

When plotted, the charge *vs.* voltage (*Q*/V) curves show a clear sigmoidal shape at pH 6.5 for both PepT1a transporters, whereas in the Atlantic salmon PepT1b only the rightmost part of sigmoid is visible. This evidence confirms once again the similarity of the PepT1a transporters to the mammalian orthologue as well as the similar behavior of the PepT1b transporter with the seabass PepT1 and PepT1b of zebrafish. Moreover, the alkalization of the external medium produces negative shift for both PepT1a and PepT1b transporters in charge *vs.* voltage curves, as expected.

To analyze the transient currents of transporters and to better understand their significance, it can be assumed that the transporter charge (intrinsic or extrinsic) can be in two-states ("In" and "Out") within the electrical membrane field. The charge *vs.* voltage curves represent the probability of the distribution of transporters between these two possible conformations/positions. The probability to be in one or in the other state is related to the differences in the voltage across the membrane. The charge movement process can be described with the simple reaction **[3.1]** where the outrate and the inrate are the unidirectional rate constants. Q_{in} is the amount of charge located near the inner side of the membrane electrical field and Q_{out} is the amount of charge displaced toward the outer membrane margin (Renna et al., 2011b).

$$Q_{in} \underset{inrate}{\overset{outrate}{\rightleftharpoons}} Q_{out} \qquad \textbf{[3.1]}$$

In order to facilitate the subsequent analysis and for taking into account the correction due to the different levels of transport proteins functionally expressed in plasma membranes of oocytes, the data of charge *vs.* voltage in **Figure 3.10** were normalized against the maximal moveable charge Q_{max}. The Q_{max} of different transporters were obtained by fitting using the Boltzmann function **[3.2]**, and the unitary charge level (Q =1) was set to the saturation value at positive potential (Q_{in}).

$$Q = \frac{Q_{max}}{1 + \exp\left[\frac{-(V - V_{0.5})}{\sigma}\right]} \qquad \textbf{[3.2]}$$

The Boltzmann equation describes the equilibrium distribution of the moved charge during the *PSS* currents. Q_{max} is the maximal moveable charge obtained

from saturating values of Q/V sigmoidal curve. For the experiments in which it was not possible to reach the saturation values of Q/V curves at hyperpolarized potentials, the Q_{max} was predicted by fitting the available data of the Q/V curve with the sigmoidal equation. $V_{0.5}$ is the voltage at which half of the maximal charge is moved (the midpoint of the Q/V sigmoidal). $\sigma = kT/q\delta$ represents a slope factor, in which q is the elementary electronic charge, k is the Boltzmann constant, T is the absolute temperature, and δ is the fraction of electrical field over which the charge movement occurs (Renna et al., 2011b).

The parameters obtained by fitting of charge *vs.* voltage curves (Q/V) with the Boltzmann function (Q_{in} and Q_{max}) and the time decay constant *vs.* voltage curves (τ/V) can be used to determine the unidirectional inward, and outward rate constants of the charge movement, through the equations **[3.3]** (Renna et al., 2011b).

$$inrate = \frac{1}{\tau}\frac{Q_{in}}{Q_{\max}}$$

$$outrate = \frac{1}{\tau}\left(1 - \frac{Q_{in}}{Q_{\max}}\right) \qquad \textbf{[3.3]}$$

In **Figure 3.11**, The voltage- and pH-dependence of the unidirectional rate constants for zebrafish PepT1a and Atlantic salmon PepT1 transporters are reported. Assuming a positive mobile charge, the outward rates increase when the inner side of cellular membrane presents a positive voltage and decrease to zero for membrane voltage values lower than -100/-140 mV. Conversely, the inward rates increase and decrease respectively with hyperpolarization and depolarization of the membrane potential. At pH 6.5, the outward and the inward rates of both zebrafish and Atlantic salmon PepT1a are slightly voltage dependent. Their trends are described by symmetrical curves that intersect in

the range from -80 mV to -40 mV in agreement with τ maximal value at this pH. At the same pH condition, Atlantic salmon PepT1b shows an asymmetric behavior of the outward and inward voltage curves.

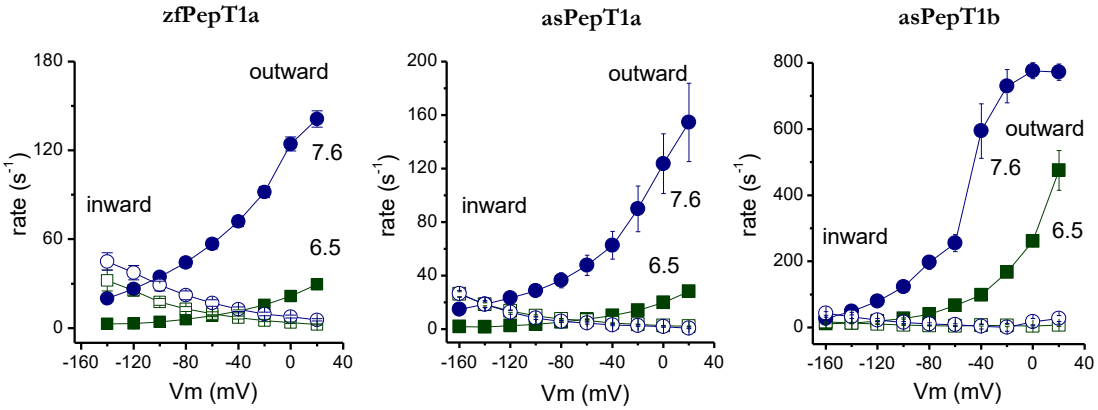

Figure 3.11 The unidirectional rate constants, inward (open symbols) and outward (solid symbols), of the intramembrane charge movement of zebrafish PepT1a (zfPepT1a) and Atlantic salmon PepT1 transporters (asPepT1a and asPepT1b). The decay rates were derived from the time constant and the charge at the two pH conditions (pH 6.5 green square and pH 7.6 blue circle) and were plotted as function of membrane potentials, in the range from −160 mV to +20 mV. Data are the mean ± SE from 5 to 15 oocytes.

The inward rate is affected slightly by voltage, while the outward rate is strongly voltage dependent with great acceleration recorded at positive membrane potentials. Changing external pH from 6.5 to 7.6, the outward rates become highly voltage dependent and faster when the membrane potential is made more positive in both PepT1a transporters.

For zebrafish PepT1a the inward rate *vs.* voltage curve slightly increases at pH 7.6 with respect to pH 6.5. Independently from the voltage tested, no differences between the two pH conditions are observed on the inward rate *vs.* voltage curves for Atlantic Salmon PepT1a.

The increase of external pH from 6.5 to 7.6 increase similarly the inward and outward rates in Atlantic salmon PepT1b (for the inward rate at -140 mV the ratio is 0.4, while for the outward rate at +20 mV the ratio is 0.6).

Furthermore, the decay rates of both fish PepT1a transient currents are like those of rabbit PepT1 and are much slower than those previously described for both zebrafish and the Atlantic salmon PepT1b as well as for the seabass PepT1 (Renna et al., 2011b). To summarize and to compare the data obtained by the analysis of the *PSS* currents of the mammalian PepT1 and the fish PepT1a and PepT1b transporters, the parameters obtained by fitting with the Boltzmann equation **[3.2]** and the Q/V curves are reported in **Table 3.3**.

	Q_{max} (nC)		$V_{0.5}$ (mV)		σ (mV)	
	6.5	**7.5 - 7.6**	**6.5**	**7.5 - 7.6**	**6.5**	**7.5 - 7.6**
rbPepT1	33.2 ± 1.9	31.5 ± 1.2	-41.4 ± 2.5	-100 ± 2.3	42.9 ± 3.1	39.5 ± 1.7
zfPepT1a	41 .0 ± 0.7	53.0 ± 0.6	-57.6 ± 0.6	-110 ± 0.7	33.6 ± 0.8	39.3 ± 0.4
zfPepT1b	11.0 ± 0.3	9.9 ± 1.1	-108 ± 1.6	-119 ± 7.2	31.1 ± 0.9	33.5 ± 3.3
asPepT1a	24.6 ± 0.8	24.9 ± 1.3	-67.6 ± 1.4	-145 ± 3.3	33.6 ± 1.8	32.5 ± 1.2
asPepT1b	27 ± 1.6	22.6 ± 4.1	-136 ± 3.6	-157 ± 8.0	30.4 ± 1.6	22.8 ± 2.3

Table 3.3 The Boltzmann equation parameters of rabbit PepT1 (rbPepT1), zebrafish PepT1 transporters (zfPepT1a and zfPepT1b) and Atlantic salmon PepT1(s) (asPepT1a and asPepT1b). Q_{max} is the maximal moveable charge, $V_{0.5}$ is the voltage at which half of the charge is moved, σ represents a slope factor of sigmoidal curve. The parameters are calculated at two pH conditions: at pH 6.5 and pH 7.5 for rabbit PepT1 and zebrafish PepT1b (Renna et al., 2011b); at pH 6.5 and pH 7.6 for zebrafish PepT1a and Atlantic salmon transporters.

It is worth to mention that the slope factor σ in the Boltzmann model relates to the apparent charge moved and gives information about the "position" of the proton binding site based on the two states model **[3.1]**.

Transport of charged substrates and dipeptides containing essential amino acid (EAA)

PepT1 transporters are known to bind several di- and tripeptide substrates possessing several different charges. The human PepT1 mediates the active transport of neutral, cationic and anionic dipeptides in a H^+ dependent manner (Amasheh et al., 1997). The interaction of differently charged dipeptides with the transporter's substrate binding site is strongly dependent on the position of the charged amino acid (Vig et al., 2006) and it is strongly dependent on external pH (Amasheh et al., 1997). In rabbit (Kottra et al., 2002) and seabass PepT1 (Margheritis et al., 2013) the amplitude of the transport current increases for lysine containing dipeptides with the charged residue in the amino-terminus position. These transport currents at fixed substrate concentration of 1 mmol/L for both rabbit and seabass PepT1 have been found to be slightly dependent on the alkalinity or acidity of the external solution. In zebrafish PepT1b, the transport associated currents for lysine containing dipeptides are regulated by the pH of external solution (Margheritis et al., 2013). In the context of the comparative analysis on substrate selectivity between PepT1a and PepT1b transporters, the transport associated current in the presence of different charged peptides were recorded. To investigate the importance of the position of the charged residue in the interaction with the PepT1 protein, the experiments were conducted in the presence of specific charged dipeptides, with the charged amino acid residue in either the amino- or in the carboxy-terminal position. These experiments were performed at pH 7.6. The data collected are summarize in **Figure 3.12A** for negative charged dipeptides Gly-Asp/Asp-Gly,

and in **Figure 3.12B** and **3.12C** for two couples of cationic substrates Gly-Lys/Lys-Gly and Met-Lys/Lys-Met, respectively. The recordings at -60 mV were normalized to the current elicited by 1 mmol/L of neutral reference substrate, Gly-Gln, for each tested transporter allowing to rapidly compare similarities and differences among PepT1a and PepT1b.

Anionic dipeptides- In the representative traces and in the histogram reported in **Figure 3.12A**, the Asp-Gly evokes larger currents in PepT1a expressing oocytes if comparted to the current in the presence of reference substrate Gly-Gln. Conversely the same substrate elicited only very small current in zebrafish PepT1b transporter and a current smaller than Gly-Gln in Atlantic salmon PepT1b transporter. For both PepT1a transporters, changing the position of negative charge residue, i.e. in dipeptide Gly-Asp, the amplitude of the transport-associated current is reduced, becoming equal to the reference current generated by Gly-Gln. The currents evoked by the two anionic substrates show comparable values in PepT1b transporters suggesting in this case that the position of the charge residue in the dipeptide it is not a discriminating factor for the transport activity. Even if in zebrafish PepT1b the currents elicited by the two anionic substrates have a reduced amplitude.

Cationic dipeptides- Currents recorded in the presence of dipeptides containing lysine and glycine show that the position of the charged residue establishes the amplitude of the transport current for both PepT1b; in fact, when the current evoked by Gly-Lys and Lys-Gln are compared, the transport current are always larger in the presence of Lys-Gly (**Figure 3.12B**). When the neutral amino acid is methionine, the importance of the charge position is confirmed in Atlantic salmon PepT1b (**Figure 3.12C**). Notably, the current evoked by Lys-Met is higher than the current in the presence of Met-Lys. Instead, the charge position is not essential in zebrafish PepT1b in which the Lys-Met and Met-Lys show comparable currents (**Figure 3.12C**). Moreover, except for the Gly-Lys, in Atlantic salmon PepT1b, the lysine containing peptides elicit larger currents than

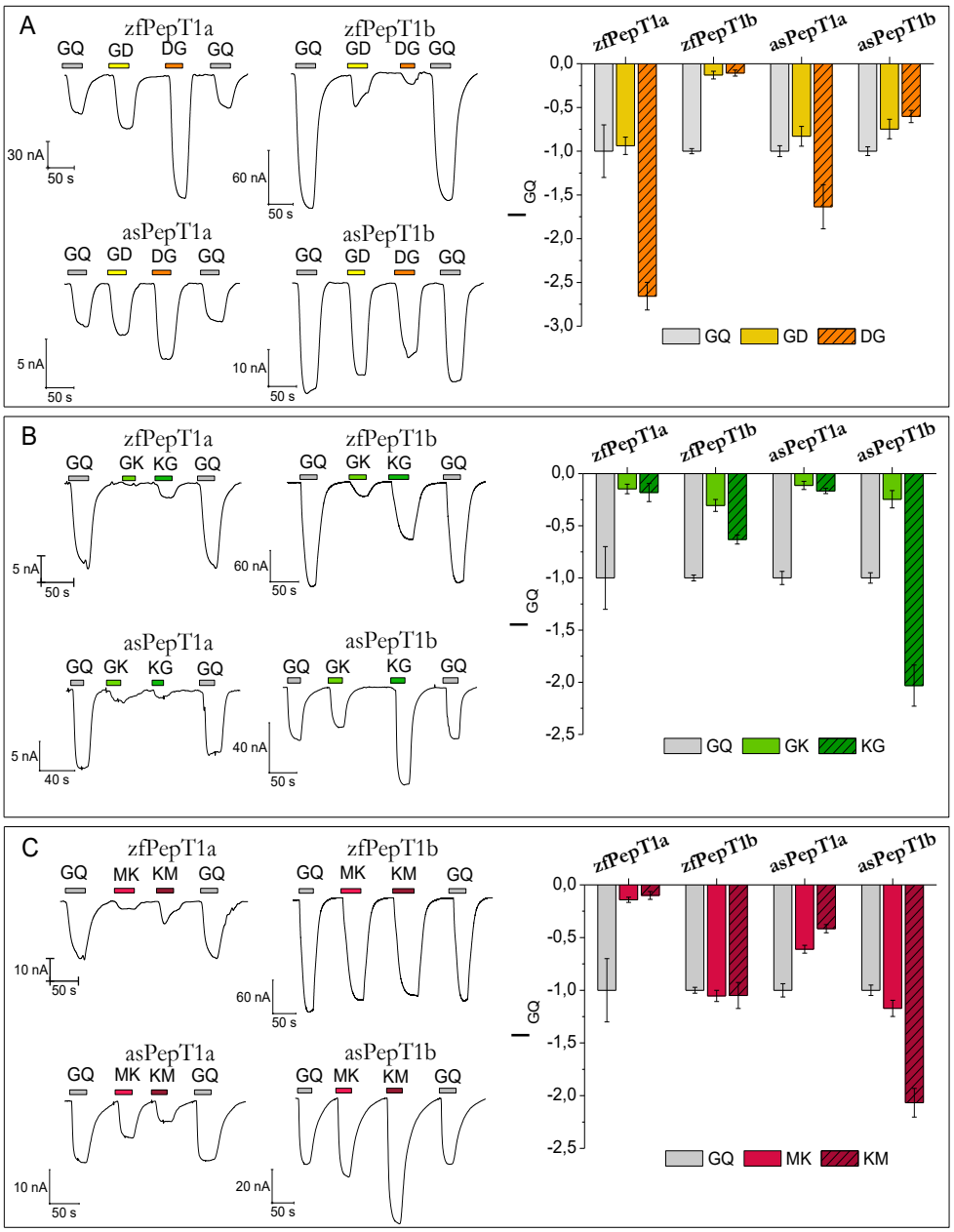

Figure 3.12 Transport current elicited by differently charged dipeptides compared with Gly-Gln (GQ) (all at 1 mmol/L) for the indicated PepT1 transporters: zebrafish PepT1a and PepT1b (zfPepT1a, zfPepT1b), Atlantic salmon PepT1a and 1b (asPepT1a and asPepT1b). The transport current elicited by Gly-Asp and Asp-Gly (GD, DG) in **A**, by Gly-Lys and Lys-Gly (GK, KG) in **B**, by Met-Lys and Lys-Met (MK, KM) in **C** were recorded at the holding potential of -60 mV and at pH 7.6. In the left part of all figures representative traces of transport current induced by the presence of each substrates indicated by the differently colored bars. In the right part of **A**, **B** and **C** the mean of the transport associated current were normalized respect Gly-Gln current. Values are mean ± SE from 7 to 15 oocytes from different batches.

the reference substrate (Gly-Gln). The same substrates in zebrafish PepT1b generate small (for Lys-Gly) or similar (as for both Met-Lys and Lys-Met) currents to those generated by Gly-Gln. For both PepT1a, the transport currents in the presence of all the tested cationic peptides are always smaller than Gly-Gln currents and are not influenced by the position of the positive charge residue in dipeptide (Gly-Lys and Lys-Gly in **Figure 3.12B**; Met-Lys and Lys-Met in **Figure 3.12C**).

To verify how the membrane voltage affects the transport of differently charged dipeptides, zebrafish and Atlantic salmon transporters were tested in the presence of 1 mmol/L of anionic dipeptides (Asp-Gly and Gly-Asp), and cationic dipeptides (Lys-Gly and Gly-Lys) applying the pulse protocol (step of 20 mV from -140 to +20 mV). The currents in the presence of the tested substrates were normalized to the Gly-Gln current value at the membrane potential of -140 mV. According to the Henderson-Hasselbalch equation, the percentage of each substrate species as function of pH was calculated to have about 98% of the molecules in the charged form. The transport currents of anionic substrates and cationic substrates were recorded at pH 7.6 and pH 6.5, respectively.

I/V relationships of anionic dipeptides- Except for zebrafish PepT1b, all the tested transporters show voltage dependent currents in the presence of both Asp-Gly and Gly-Asp with an increment of the inward currents recorded from +20 mV to -140 mV (**Figure 3.13A**).

According to the values of the current at -60 mV, Asp-Gly evokes higher current than Gly-Gln at all the tested potentials in zebrafish PepT1a, but not in Atlantic salmon PepT1a, where the I/V relationships are similar between Asp-Gly and Gly-Gln with a slight decrease of Asp-Gly current at the negative voltage condition of -140 mV. For both PepT1a transporters, the comparison of the I/V curve of Gly-Asp with the reference curve shows a similar behavior from -20 mV to -80 mV. A decrease of Gly-Asp current amplitude is noted at

the hyperpolarization conditions from -100 mV to -140 mV. In PepT1b transporters, the I/V relationships are similar between the anionic dipeptides, with the currents always smaller than that elicited by Gly-Gln. In Atlantic salmon PepT1b an increase of Asp-Gly and Gly-Asp currents is observed at the most hyperpolarizing membrane potentials. At the same conditions only a slight increase of the transport currents is observed in zebrafish transporter.

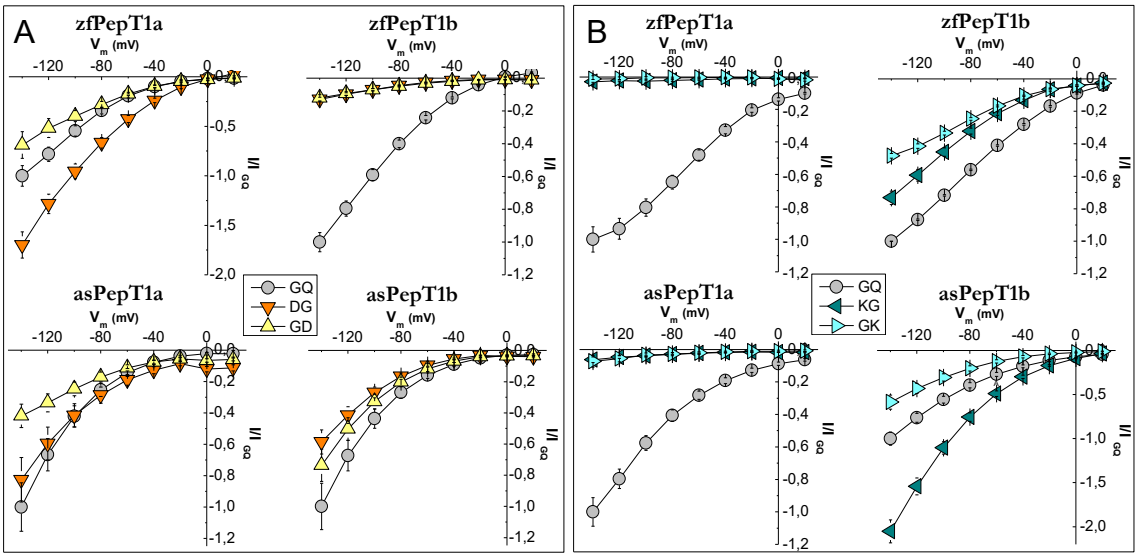

Figure 3.13 Current-voltage (I/V) relationships of transport-associated currents in the presence of 1 mmol/L of aspartate- and lysine- containing dipeptides in zebrafish (zfPepT1a and zfPepT1b, top) and in Atlantic salmon (asPepT1a and asPepT1b, bottom) transporters. In **A** I/V in the presence of Asp-Gly (DG, orange-down triangles), Gly-Asp (GD, yellow-up triangles) and Gly-Gln (GQ, gray circle) at pH 7.6. In **B** I/V in the presence of Lys-Gly (KG, dark cyan-left triangles), Gly-Lys (GK, light cyan-right triangles) and Gly-Gln (GQ, gray-circle) at pH 6.5. The currents elicited by voltage pulses in the range from -140 to +20 mV (20 mV steps from V_h of -60 mV) are obtained by subtracting from the current in the presence of substrate, the current in its absence and are presented as mean ± SE from 7 to 15 oocytes from different batches normalized respect to the current value of Gly-Gln at -140mV.

I/V relationships of canionic dipeptides- The cationic dipeptides do not give rise to any currents at all tested potentials for both PepT1a transporters, whereas

species-specific differences are observed comparing I/V curves in the presence of cationic dipeptides between PepT1b transporters particularly in the presence of Lys-Gly (**Figure 3.13B**). With respect to the reference substrate, Lys-Gly is the best substrate at all tested potentials in Atlantic salmon transporter, while in zebrafish PepT1b it shows always smaller current than those of Gly-Gln. For both PepT1b transporters at all tested potentials, Gly-Lys elicits small current with respect to the current of Gly-Gln. Moreover, in zebrafish PepT1b the position of charged residue in dipeptide influences the voltage-dependence of the current amplitude in the range from -80 mV to -140 mV with larger current recorded in the presence of Lys-Gly than in the presence of Gly-Lys.

To completely characterize the PepT1a protein and their role in transporting important nutritional peptides such as lysine and methionine containing dipeptides, they were tested under the same experimental conditions reported in (Margheritis et al., 2013). The same was done for Atlantic salmon PepT1b.

The membrane voltage and the external pH dependence of the transport currents were investigated using the pulse protocol at two different pH conditions. The current voltage relationships at pH 6.5 and 7.5 for zebrafish PepT1a and Atlantic salmon transporters are illustrated in **Figure 3.14**.

In Atlantic salmon PepT1b, the current generated by Gly-Lys at two pH values are significantly different ($p<0.001$) in the potential range from -20 mV to -140 mV, with higher current values at pH 6.5 (**Figure 3.14A**). The current evoked by Lys-Gly, Met-Lys and Lys-Met are affected by external pH in function of the membrane potential. In fact, the current values in the range of -20 mV to -60 mV are higher at pH 6.5 than those at pH 7.6, with significant differences in amplitude of currents at -20 mV ($p<0.001$ for Lys-Gly and Met-Lys and $p<0.05$ for Lys-Met). At the most negative voltages tested (-120 mV and -140 mV), the currents increase in the presence of the same substrates from pH 6.5 to 7.6, with significantly different values at -140 mV ($p<0.001$ for Lys-Gly and $p<0.05$ for Met-Lys and Lys-Met), (**Figure 3.14B**, **3.14C** and **3.14D**). In PepT1a

transporters no effect of pH is observable in Gly-Lys and Lys-Gly induced currents, (see **Figure 3.14I** and **3.14L** for zebrafish transporter, **3.14E** and **3.14F** for Atlantic salmon PepT1a). The only exception is the Lys-Gly, in fact this dipeptide gives rise to a current significantly higher at pH 7.6 at -140mV ($p<0.01$) in Atlantic salmon PepT1a (**Figure 3.14F**). When the substrate is the Met-Lys, the pH effect on the current voltage relationship is similar in both PepT1a transporters. In fact, the transport currents are significantly higher at pH 6.5 in the range from -20 mV to -100mV (with $p<0.001$ at -20 mV and $p<0.01$ at -100 mV) for Atlantic salmon (**Figure 3.14G**). For zebrafish, the transport currents are significantly high at pH 6.5 in the range from -20 mV to -120mV (with $p<0.001$ at -20 mV and $p<0.05$ at -120 mV), (**Figure 3.14M**). For both PepT1a, once set the membrane voltage at -140 mV and external pH at 7.6, the current evoked by Lys-Met apparently increases without statistically significant difference respect to the current recorded at pH 6.5 (**Figure 3.14N**). The same substrate in the voltage range from -20 mV to -60mV shows currents higher at pH 6.5 than those at pH 7.6 with significant differences for Atlantic salmon PepT1a ($p<0.001$ at -20 mV and $p<0.05$ at -60 mV); no statistically significant differences emerge for the zebrafish transporter.

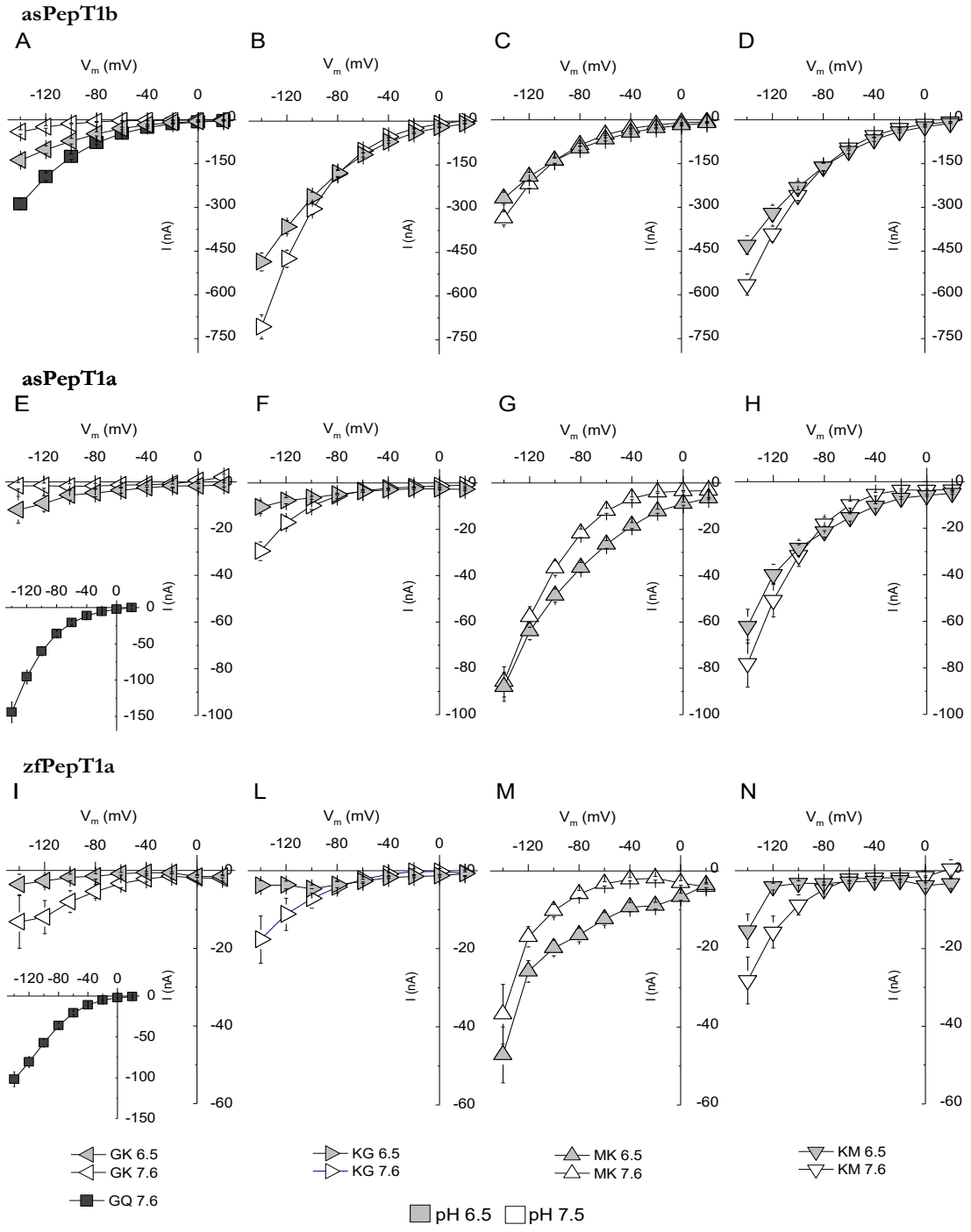

Figure 3.14 Current-voltage (I/V) relationships of transport-associated currents in the presence of lysine containing peptides in Atlantic salmon PepT1b (asPepT1b) in **A-D** and in Atlantic salmon PepT1a (asPepT1a) in **E-H** and in zebrafish PepT1a in **I-N** (zfPepT1a). The currents elicited by voltage pulses in the range -140 to +20 mV (20 mV steps from V_h of -60 mV) were

recorded in the presence of 1 mmol/L of different substrates (Gly-Lys (GK) in **A**, **E** and **I**; Lys-Gly (KG) in **B**, **F** and **L**; Met-Lys (MK) in **C**, **G** and **M**; Lys-Met (KM) in **D**, **H** and **N**) at pH 6.5 (light gray symbols) and pH 7.6 (empty symbols). Gly-Gln (GQ) values at pH 7.6 are reported as reference (dark gray symbols). The current value reported in I/V relationship were the obtained by subtracting from the current in the presence of substrate, the current in its absence. Data are reported as mean ± SE from 8 to 11 oocytes from different batches.

To better understand the behavior of the two Atlantic salmon PepT1 transporters in the presence of lysine containing peptides, the transport currents for Lys-Gly were collected perfusing the oocytes expressing PepT1a and PepT1b with increasing concentration of substrate from 0.1 to 30 mmol/L at pH values of 7.6 at the holding potential of -60 mV.

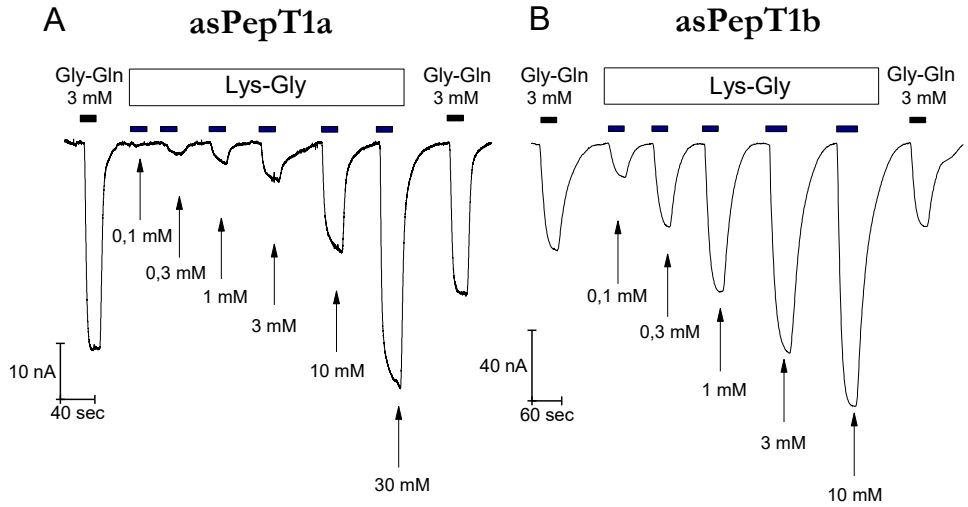

Figure 3.15 Inward currents in *Xenopus laevis* oocytes expressing Atlantic salmon PepT1a (asPepT1a) in **A**, and Atlantic salmon PepT1b (asPepT1b) in **B**. The currents were recorded at the holding potential (V_h) of -60 mV at pH 7.6. The oocytes were perfused consecutively with increasing concentrations of the Lys-Gly from 0.1 mmol/L to 10 mmol/L for PepT1b and to 30 mmol/L for PepT1a. The top bars indicate the substrate administration and the bottom arrows indicate the different concentration of substrate. The current of reference substrate Gly-Gln at 3 mmol/L was recorded at the start and at the end of each traces as indicated by the top black bars.

In oocytes expressing the Atlantic salmon PepT1b, the currents elicited by 1 mmol/L Lys-Gly are larger than the currents in the presence of Gly-Gln 3 mmol/L. The increasing Lys-Gly concentrations further enhanced the transport current (**Figure 3.15B**). The same concentration of 1 mmol/L Lys-Gly on PepT1a expressing oocytes gave rise only to small currents and in the presence of 30 mmol/L the current was similar to that in the presence of Gly-Gln 3 mmol/L (**Figure 3.15A**). If the same concentrations of Lys-Gly were tested from -140 to 0 mV, the current *vs.* concentration relationships showed that for PepT1a the maximal current was never reached at the tested voltages (**Figure 3.16A**). Moreover, in the presence of the Lys-Gly 30 mmol/L, the Atlantic salmon PepT1a showed residual *PSS* currents (**Figure 3.16C**). Conversely, Atlantic salmon PepT1b currents in the presence of 1 mmol/L of Lys-Gly were similar to those recorded at higher substrate concentrations at all tested potentials (**Figure 3.16B**). Moreover, the absence of *PSS* currents in the presence of 1 mmol/L of Lys-Gly confirms the saturation of the transport system (**Figure 3.16D**).

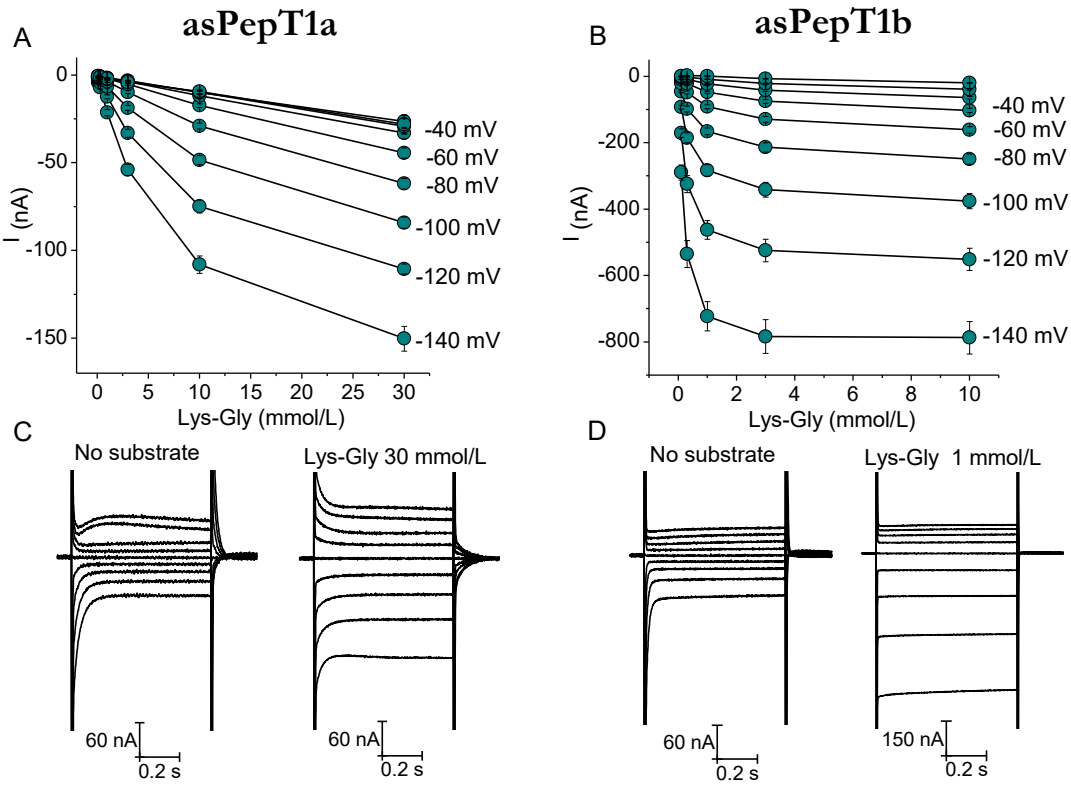

Figure 3.16 Current-substrate concentration relationships at different voltage conditions in Atlantic salmon PepT1a in **A** and PepT1b in **B**. The current values at each tested concentration of Lys-Gly (from 0.1 mmol/L to 10 mmol/L for PepT1b and to 30 mmol/L for PepT1a) were obtained by subtracting the current traces in absence of the substrate to those occurring in its presence. Data are reported as mean ± SEM of 10 or 12 oocytes from 3 batches. In **C** and **D** respectively: the representative traces of Atlantic salmon PepT1a and PepT1b in the absence of substrate (in the left part of figure **C** and **D**) and in the presence of 30 mmol/L of Lys-Gly for PepT1a (in the right part of figure **C**) and in the presence of 1 mmol/L of Lys-Gly for PepT1b (in the right part of figure **D**).

The current-substrate concentration relationships were used to determine the kinetic parameters by the fitting with the Michaelis-Menten equation. The relative apparent affinity ($1/K_{0.5}$) values for Atlantic salmon PepT1b transporter are reported as function of potential (**Figure 3.17A**). Changing the cellular membrane potential from -140 mV to 0 mV, the $K_{0.5}$ values increase progressively from the minimal value of 0.18 ± 0.01 mmol/L recorded at -140

mV to the maximal value 7.463 ± 2.16 mmol/L recorded at 0 mV. As expected, the maximal relative current is influenced by membrane potentials with the maximal value reported of -827.24 ± 17.33 nA at -140 mV (**Figure 3.17B**).

The lack in transport saturation for PepT1a impeded to determine the kinetic parameters for this transporter; only values at -140 and -120 mV have been estimated, as reported in the insert in **Figure 3.17**.

In **Figure 3.17A(a)**, there are the estimated values of relative apparent affinity (10.36 ± 1.19 mmol/L at -120 mV and 6.33 ± 0.78 mmol/L at -140 mV) and in **Figure 3.17B(b)**, there are the values of the maximal relative current (-149.07 ± 8.26 nA at -120 mV and -173.34 ± 9.54 nA at -140 mV). The transport efficiency was calculated only for PepT1b and reported in **Figure 3.17C**.

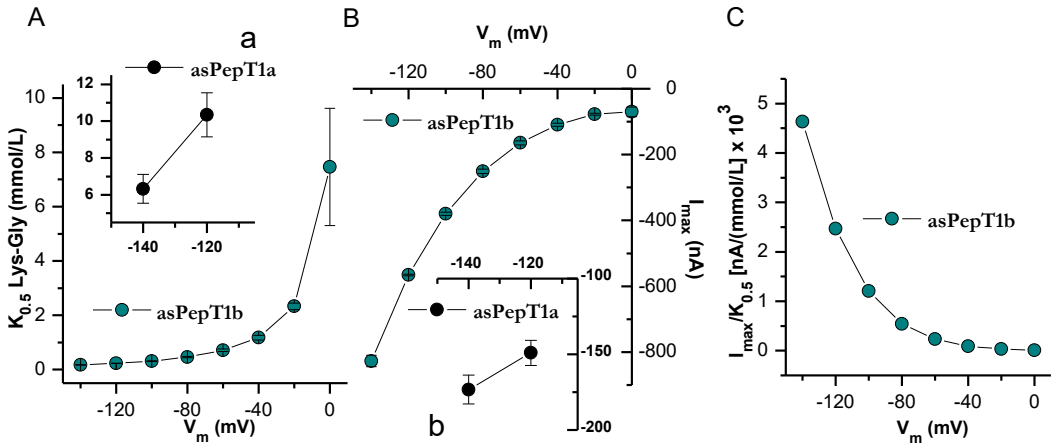

Figure 3.17 Dose response analysis of Atlantic salmon PepT1b: $K_{0.5}$, I_{max} and transport efficiency, respectively in **A**, **B** and **C** evaluated in the presence of Lys-Gly. The current values (**Figure 3.16**) were subsequently fitted with the Michaelis-Menten equation $\left[I_0 = \frac{-I_{max}}{1+([S]/K_{0.5})} + I_{max}\right]$ to obtain the apparent relative affinity ($1/K_{0.5}$) and the maximal relative current (I_{max}) and transport efficiency ($I_{max}/K_{0.5}$) at each indicated voltage and at pH 7.6. In **A** and **B**, the inserts (**Aa** and **Bb**) there are the estimations of kinetic parameters at -120 mV and -140 mV for Atlantic salmon PepT1a transporter.

For the zebrafish PepT1a transporter, the dose response experiments were performed in the presence of the cationic dipeptide Lys-Gly and the anionic dipeptide Gly-Asp. The experimental substrate and pH condition were the same reported for PepT1b (Verri et al., 2003) to permit the comparison. The kinetic parameters for zebrafish PepT1a were obtained from a few numbers of oocytes of batch, therefore these data are to be considered as preliminary and they are summarized in the **Table 3.4**.

zfPepT1a			***-60 mV***		***-120 mV***		
		%	I_{max}	$K_{0.5}$	I_{max}	$K_{0.5}$	*Oocytes*
	pH	*neutral*	nA	mmol/L	nA	mmol/L	(n)
Lys-Gln	8.5	67%	-70.51 ± 15.05	11.24 ± 2.88	-135.58 ± 16.15	7.93 ± 1.13	4
	7.6	17%	-80.55 ± 11.09	18.35 ± 3.51	-123.29 ± 13.65	10.78 ± 1.92	4
Gly-Asp	7.6	<1%	-397.70 ± 92.21	5.89 ± 2.14	-695.23 ± 227.53	5.17 ± 2.04	4
	5.5	8%	-173.23 ± 5.47	0.27 ± 0.03	-260.31 ± 26.04	0.66 ± 0.16	4

*zfPepT1b			***-60 mV***	
		%	I_{max}	$K_{0.5}$
	pH	*neutral*	nA	mmol/L
Lys-Gln	8.5	67%	-252 ± 14	3.5 ± 1.26
	7.6	17%	-440 ± 20	16 ± 1.26
Gly-Asp	7.6	<1%	-128 ± 28	21 ± 5
	5.5	8%	-94 ± 8	0.21 ± 0.03

Table 3.4 The kinetic parameters of the inwardly directed transport of cationic and anionic dipeptides *via* the zebrafish PepT1a measured in Two-Electrode Voltage Clamp (TEVC) experiments. All values are expressed as mean ± SEM of n oocytes (each oocyte represents an independent observation). *Xenopus laevis* oocytes were voltage clamped at -60 mV and at -120 mV and perfused with solutions at the indicated pH conditions. The kinetic parameters ($K_{0.5}$ and I_{max}) were calculated by least-square fit to the Michaelis-Menten equation. All amino acids were L-type. The percentage of the zwitterionic form at a given pH was taken from Kottra et al. (2002). To facilitate the comparison, kinetic parameters of zebrafish PepT1b are reported in the bottom table (*) (Verri et al., 2009).

Chapter 4. Discussion

PepT1 transport proteins have been studied from functional and structural points of view and a huge amount of data are available about their expression and regulation in different species. The electrophysiological results on the transport activity of several PepT1 orthologues show many functional differences in the various species. Particularly, the functional characterization of PepT1 from teleost fish exhibited transport peculiar transport properties that are species-specific in fish and differ with respect to the mammalian counterparts. The functional plasticity found in fish orthologues reflects the molecular adaptation of the PepT1 transporter to the astonishing range of habitats and/or of anatomical peculiarities which characterize each species (Romano et al., 2014). Moreover, the specific whole duplication event occurred during Actinopterygian lineage evolution have led to a more complex gene repertoire in teleost fish than in higher vertebrates. This aspect represents a great and important value for studies in fish model organisms. The identification of the PepT1-type paralogues named PepT1a and PepT1b suggests that in teleost fish more than one PepT1-type protein might be expressed and might function as transport system. Functional data available in literature on teleosts are referred to PepT1b-type only, such as for zebrafish (Verri et al., 2003), seabass (Sangaletti et al., 2009), ice fish (Rizzello et al., 2013) and Atlantic salmon PepT1b transporters (Ronnestad et al., 2010).

Recently, the complementary DNAs coding for PepT1a-type transporters have been cloned from the gut of zebrafish and Atlantic salmon. By sequence analysis, the two predicted PepT1a proteins share about 80% similarity and about 60-65% identity with their species paralogue PepT1b. The functional characterization of the newly cloned PepT1a-type transporters performed by using TEVC methods is one of the main topics reported in this work.

Overexpression of PepT1a-type and PepT1b-type transporters in *X. laevis* oocytes allows precise electrophysiological transport measurement and the comparison between PepT1 transporters, emphasizing similarities and differences in the kinetic mechanism of the new PepT1a transporters with respect to the well-characterized PepT1b(s) and mammalian PepT1.

These studies are important not only for relating the physiological role of each transporter to its kinetic parameters but also to functionally identify regions and residues that confer specific macroscopic features. In this respect, the kinetic differences between transporters that show high similarities, such as paralogue or orthologue products, are invaluable tools. These evidences, together with structural data collected mainly from bacterial orthologues, deepen the description of the steps of translocation of substrates and drugs (Newstead, 2017b). Despite the oocyte internal pH and external temperature are important factors in determining the transport kinetics of PepT1 (Nussberger et al., 1997; Bossi et al., 2012), in this work the oocyte internal pH is assumed to be constant (assuming a fixed value of 7.5 pH). All experiments were conducted at the external temperature range from 18°C to 20°C according to the experimental procedures of oocytes.

Recording the transport currents at fixed voltage, it has been demonstrated that the zebrafish and Atlantic salmon PepT1a transporters are electrogenic and capable of transporting di and tripeptides in a proton dependent manner. Moreover, in **Figure 3.4**, the overlapping of I/V relationship obtained with 3 mmol/L Gly-Gln in sodium and sodium-free solutions shows that PepT1a transporters mediate translocation of substrate independently of the presence of sodium in the external environment. Considering that in the first experiments the currents were recorded: i) at fixed membrane potentials of -60 mV, ii) at different pH conditions (6.5, 7.6 and 8.5), and iii) with perfusion of 1 mmol/L Gly-Gln, Ala-Ala and Gly-Gly-Gly, the representative traces (**Figure 3.3**) and the statistically analysis of the transport associated currents

(**Figure 3.5**) clearly indicate that the differences in amino acid sequence, between PepT1a and PepT1b transporters, have functional implication(s) both in pH dependence and in substrate preferences. In fact, if compared to the well-characterized PepT1b transporter of zebrafish, the protein PepT1a: i) prefers Ala-Ala to Gly-Gln; ii) works well at acidic pH; iii) gives rise to relatively smaller currents in all conditions tested; iii) produces currents of few nanoamperes for Gly-Gly-Gly regardless of the pH conditions.

When transport currents are compared between transporters of Atlantic salmon, PepT1a shows a more marked pH dependence than PepT1b. In fact, Atlantic salmon PepT1a works well at acidic pH with transport currents that differ statistically between pH 6.5 and 7.6, for all tested substrates.

However, while eliciting transport currents, the 1 mmol/L substrate condition is not the most adequate for testing the transporter pH dependence, because of the considerable effect of protons on the substrate affinity. When the transport associated currents are recorded in the presence of increasing concentrations of Gly-Gln using the standard step protocol, the rising of pH increases the amount of substrate necessary to reach the maximal current amplitudes greatly increasing the current value (**Figure 3.6**). The Gly-Gln transport follows the Michaelis Menten saturation kinetics for both zebrafish and Atlantic salmon PepT1a transporters. Moreover, the maximal relative current (I_{max}) and the apparent affinity ($1/K_{0.5}$) values are affected differently by membrane potential and external pH (**Figure 3.7**). Regarding I_{max}, the Atlantic salmon PepT1a is affected only slightly by pH (**Figure 3.7E**), with an increase in I_{max} at pH 7.6 observed when the membrane potential is clamped at hyperpolarization values, from -100 mV to -140 mV.

Conversely, I_{max} of zebrafish PepT1a is affected largely by external pH, with the maximal transport activity always higher at pH 7.6 than pH 6.5 regardless of membrane potential, (**Figure 3.7B**). For both PepT1a transporters, the

$K_{0.5}$ values are in the hundreds of the micromolar range and result only slightly voltage-dependent at pH 6.5 (**Figure 3.7Aa** and **3.7Dd**). At pH 7.6, the $K_{0.5}$ values increase to millimolar range and are strongly voltage dependent (**Figure 3.7A** and **3.7D**).

The data on kinetic parameters of zebrafish and Atlantic salmon PepT1a transporters show that PepT1a-type represents a classical low-affinity/high-capacity system. When the extracellular pH is raised from 6.5 to 7.6, the increase in the maximal transport activity is confirmed to be a peculiar feature of the zebrafish transporters (Verri et al., 2003; Nalbant et al., 1999). Interestingly, Atlantic salmon PepT1a exhibits only a slight increase of maximal transport current changing the pH from 6.5 to 7.6, almost similar to Atlantic salmon PepT1b (Ronnestad et al., 2010).

The observed pH dependencies on maximal transport rates may be related to the actual pH values found in the intestinal lumen, which is alkaline under normal physiological conditions in both zebrafish and Atlantic salmon. Both these teleost species are carnivorous fish, with a short intestinal tract. Like other cyprinids and salmonids respectively, zebrafish and Atlantic salmon possibly have no or only very low levels of mRNA of NHE3 in enterocytes (Ronnestad et al., 2010; Verri et al., 2003). This lack contributes to create the alkaline microenvironment at apical membrane level where PepT1 operates. Moreover, the emphasized response to extracellular alkalinisation of the zebrafish PepT1 transporters could be explained by the occurrence of the agastric state of this species (Verri et al., 2003).

When the kinetic parameters are compared between paralogues transporters, PepT1a shows some common features with PepT1b (**Table 3.1**).

Interestingly, the membrane voltage affects the $K_{0.5}$ in different ways, according to external pH. When the voltage became more negative at pH 6.5, the kinetic values reported for -60 mV and for -120 mV suggest that PepT1a transporters show a slight increase while PepT1b transporters are

not affected or slightly decrease, in zebrafish and in Atlantic salmon respectively. At pH 7.6 the $K_{0.5}$ decreases in all PepT1 at -120 mV, with the greatest differences in Atlantic salmon transporters. The effects of membrane potential on the I_{max} are similar in all the proteins tested at both pH conditions. The ratios between I_{max} at -60 mV and I_{max} at -120 mV show similar values for the tested proteins (from ~0.33 to ~0.49) suggesting that the maximal relative current for zwitterionic substrates increases proportional to the increase in favorable electrochemical gradient.

Analyzing the pH effect on substrate affinity, the PepT1a $K_{0.5}$ is influenced mostly by the pH. In PepT1a transporters, the substrate amount required to reach one-half of the maximal currents ($K_{0.5}$) increases from 6.5 to pH 7.6. For example, at -60 mV, the $K_{0.5}$ at pH 7.6 *vs.* the $K_{0.5}$ at pH 6.5 shows a ratio of ~ 28.83 for zebrafish and a ratio of ~ 17.37 for Atlantic salmon. For PepT1b, at -60 mV, the $K_{0.5}$ at pH 7.6 *vs.* the $K_{0.5}$ at pH 6.5 shows a ratio of ~ 17.07 for zebrafish and a ratio of ~2.88 for Atlantic salmon. These analytical data overall suggest that both PepT1a transporters have a strong pH dependence with respect to PepT1b (this is confirmed also by the data reported in **Figure 3.8**).

It is generally reported that in mammalian PepT1 the decrease in external pH enhances the transporter apparent affinity but does not affect the maximal transport rate.

E.g. in rabbit PepT1, the kinetic parameters of Gly-Gln dose response experiments showed that the I_{max} was dependent on the potential, but it was only modestly dependent on external pH. In contrast, the apparent $K_{0.5}$ values were dependent on both membrane potential and pH. Notably, the value of $K_{0.5}$ at -60 mV decreased from 7.5 to 6.5 with a ratio of ~ 3.88 (Kottra and Daniel, 2001). In the human PepT1, the I_{max} elicited by Gly-Sar reduced with the increase in extracellular pH and the affinity was dependent upon membrane voltage with the maximal value recorded at pH 6.0

(Mackenzie et al., 1996b). In another study on the human transporter, it was shown that I_{max} elicited by Gly-Gln was solely dependent on membrane potential and essentially unaffected by pH, whereas the apparent affinity was modestly affected by alteration in membrane potentials and remained unaffected by pH. At -60mV the $K_{0.5}$ at pH 7.6 *vs.* the $K_{0.5}$ at pH 6.5 showed a ratio of ~0.9 (Amasheh et al., 1997).

Comparing the effect of external pH on the kinetic parameters of fish and mammalian PepT1 orthologues, it is evident that in the most of the cases the effect on the apparent affinity are similar with an increase of the values at pH 6-6.5, conversely a large heterogeneity is shown on the maximal relative currents.

In absence of organic substrates, the *PSS* currents of many ion-coupled transporters arise from the ion-transporter interaction and are related qualitatively and quantitatively to the transport activity. The properties of *PSS* currents of rabbit PepT1 and zebrafish and seabass PepT1b were previously investigated and related to the pH dependency (Renna et al., 2011b). In this work, the *PSS* currents of PepT1a transporters and of Atlantic salmon PepT1b were analyzed with the aim of collecting this kind of additional information on their transport activity.

Overall, the transient currents of Atlantic salmon PepT1b are similar to the ones of zebrafish PepT1b and in general show a coherent behavior with the fish models currently known (Renna et al., 2011b). On the contrary, PepT1a transporters clearly differ from fish model while they share many characteristics of the transient currents with the mammalian PepT1 (**Figure 3.9**). Moreover, in zebrafish PepT1a the transient currents are particularly slow and do not disappear (even with the concentration of 3 mmol/L of Gly-Gln at pH 6.5). The presence of residual *PSS* currents may have two different explanations. The first is that the substrate was not enough to saturate the transport system (Renna et al., 2011a), but this is in contrast with

the data highlighted by I/V relationship and its analysis in the presence of increasing substrate concentration (**Figure 3.6**). The second explanation is that the persistency of *PSS* even in the presence of the substrate is due to one of the two components responsible for the existence of this kind of currents in PepT1 transporters. In fact, the PepT1 *PSS* currents are originated both by the rearrangement of intrinsic charges of the transporter (**Figure 4.1A**), and by the movement of external protons in the electrical membrane field (**Figure 4.1B**). Recently it has emerged that in the transport cycle, the reorientation of transporter from the inward to the outward facing states is mediated by the protonation of a histidine located in an extracellular cavity, which is created when the transporter is in the inward open conformation (Parker et al., 2017).

Through multiscale molecular dynamics (MD) simulations Parker and colleagues (2017) revealed that proton transport between key intracellular and extracellular residues can occur. Data indicate that different members of the POT family have developed specific mechanisms to couple transport to the proton gradient (Parker et al., 2017).

The transporter structural features that guarantee the transfer of protons from the extracellular side of the membrane onto the histidine could be different in zebrafish PepT1a if compared to other PepT1 transporters. Therefore, the intrinsic and extrinsic components of *PSS* in the membrane electrical field of the extracellular cavity could explain the differences found in zebrafish PepT1a transients currents (**Figure 4.1D**).

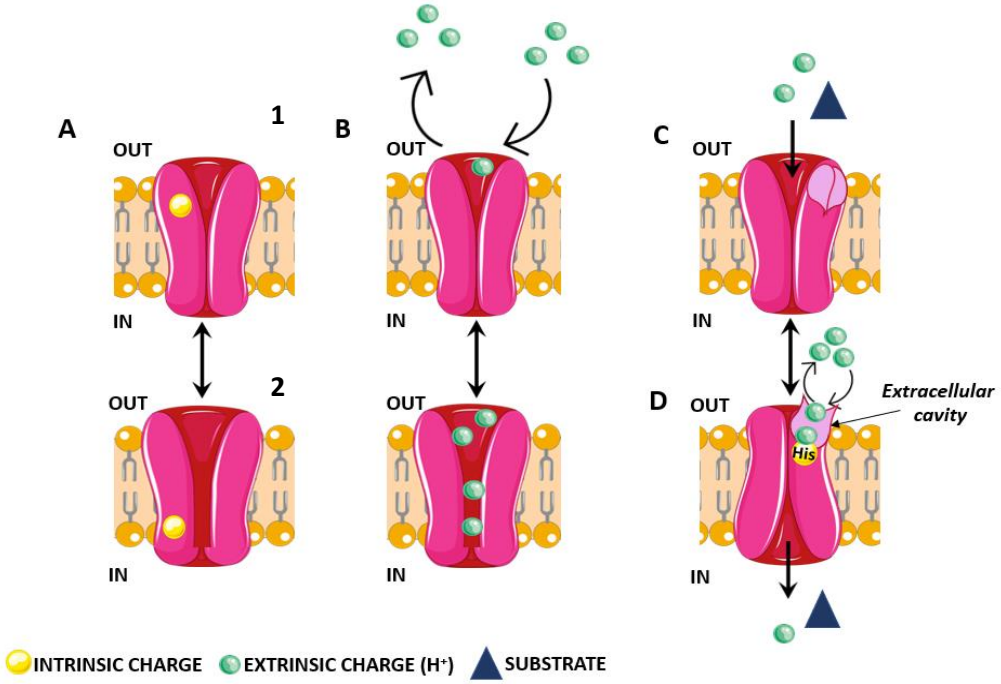

Figure 4.1 The model of PepT1 pre steady-state currents. **A** the rearrangement of the empty transporter between two states (**1** and **2**), involving the displacement of an intrinsic charge (yellow circles). **B** the extrinsic charge movement, (green circles), between the extracellular environment and the outside-opened transporter vestibule. In the presence of substrate (blue triangle), the reorientation of transporter from outward **C** to inward **D** facing states is mediated by the protonation of a histidine (His), located in the extracellular cavity. In **D** is reported the interaction between His and extrinsic charges in the membrane field of extracellular cavity.

The analysis of *PSS* currents shows that at the same external pH, the charge *vs.* voltage (Q/V) and time constant *vs.* voltage (τ/V) curves are positioned on the voltage axis accordingly with their similarity to mammalian or to fish model (Renna et al., 2011b). If compared to the "fish" model, the PepT1a(s) curves are positively shifted, like the mammalian model, while the Atlantic salmon PepT1b curves are coherent with the fish model.

In all transporters, the change of external pH from 6.5 to 7.6 speed up the transient decay, shifting to more negative potential the Q/V and τ/V curves (**Figure 3.10**). The unidirectional rate constants analysis of charge movement in

the membrane electrical field indicate that external protons affect the inward and outward rates of Atlantic salmon PepT1b. Notably, the outward rate at pH 7.6 reaches the maximal value of about 780 s^{-1} , as it can be seen by the flattening of the curve from 0 mV to +20 mV (**Figure 3.11**).

In PepT1a transporters, the acidification of the external solution does not affect the inward rate but strongly reduces the outward rate. The analysis on inward and outward rates provides an explanation for the pH and the voltage dependencies of the transporters apparent affinity for the Gly-Gln.

In PepT1a transporters, the inward and outward rate at pH 6.5 cross each other in a range from -80 mV to -40 mV, where the maximal apparent affinity for Gly-Gln is observed (**Figure 3.7Aa** and **3.7Dd**). The explanation may be that the major part of protonated transport proteins is in a steady-state equilibrium between the two different transport conformations, in this voltage range. Therefore, many proteins are available for the interaction with the external substrate and the binding equilibrium between protons and substrate will be reached. In such condition, the transport rate ($1/\tau$) is the lowest; consequently, the transporters apparent affinity will be high, because the substrate has more time to bind the PepT1 proteins. At extreme voltage conditions such as in hyperpolarization and depolarization, the outward and inward rates are higher and the number of transporters in the right protonated conformation for substrate interaction is reduced. Therefore, higher concentrations of substrate are needed to produce the half maximal current. This hypothesis is supported also by the data at pH 7.6. In this condition, the inward and outward rates cross between -140 mV and -100 mV, where the maximal value of Gly-Gln affinity of PepT1a transporters is reached. Moreover, the strong increase of the outward rate from -140 mV to +20 mV causes probably the voltage dependent decrease in the apparent affinity ($1/K_{0.5}$) (**Figure 3.7Aa** and **3.7Dd**).

To confirm the observations, the charge equilibration rate ($1/\tau$) and Gly-Gln $K_{0.5}$ values, collected i) at the same voltage range (from -140mV to +20 mV) and ii) at the same pH conditions (pH 7.6 and 6.5), are fitted with linear equation (**Figure 4.2**).

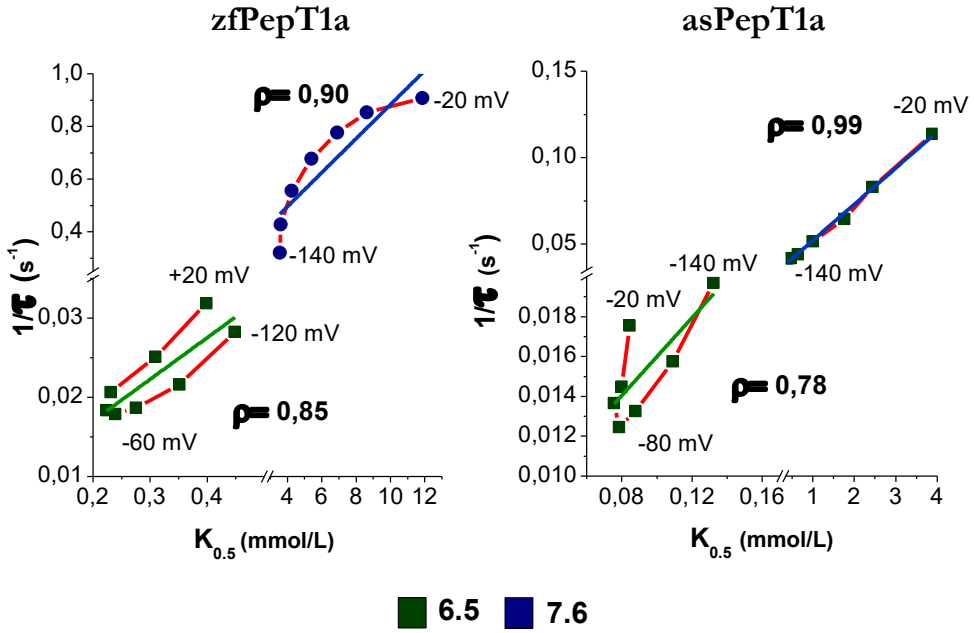

Figure 4.2 Plots of rate ($1/\tau$) versus the Michaelis Menten constant ($K_{0.5}$) obtained by Gly-Gln dose-response experiments for zebrafish PepT1a transporter (zfPepT1a) and Atlantic salmon PepT1a (asPepT1a). The data points are computed using the decay rate/voltage relationship and the $K_{0.5}$/voltage relationship at two pH conditions (pH 6.5 green square and pH 7.6 blue circle) and are correlated in function of membrane potentials. Straight lines are linear regression to the points, with the Pearson correlation coefficient (ϱ) indicated.

The Pearson correlation coefficient suggests a strongly positive correlation between these two parameters (the voltage dependency of $1/\tau$ and of $K_{0.5}$ is shown by red lines in **Figure 4.2**).

Although the Gly-Gln dose response experiments for the Atlantic salmon PepT1b are not reported in this work because the data have already been

published (Ronnestad et al., 2010), it is important to note that at both pH conditions 6.5 and 7.6, the $K_{0.5}$ values increase from -140 mV to +20mV (**Figure 4.3A** and **4.3Aa**).

In Atlantic salmon PepT1b, the behavior of both unidirectional rate constants shows that they have the slowest value at hyperpolarized voltage and that they accelerate moving toward the more positive voltage, at both pH conditions. The linear plot reports a perfectly positive correlation between $1/\tau$ and $K_{0.5}$ values (**Figure 4.3B**).

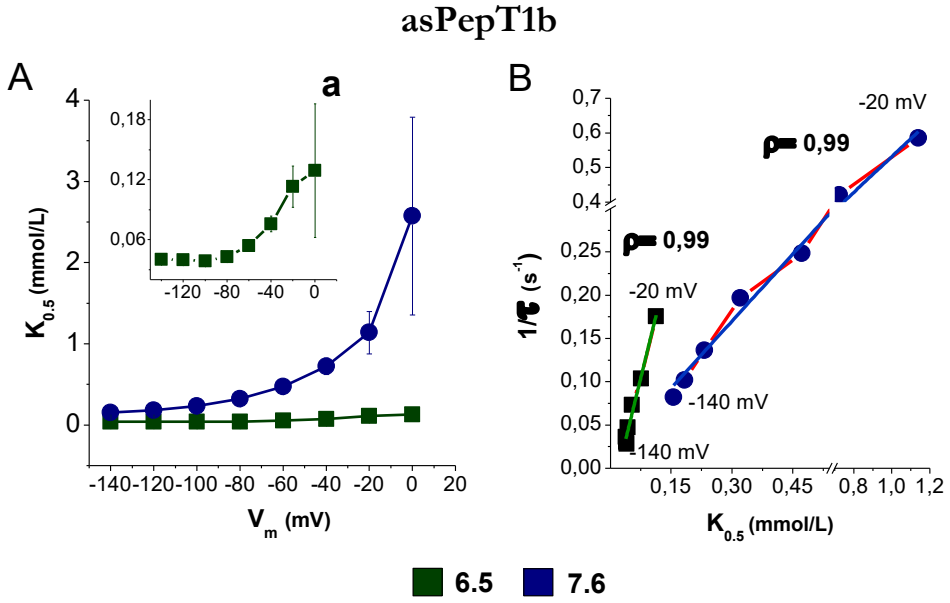

Figure 4.3 In **A** Atlantic salmon PepT1b $K_{0.5}$ values at each indicated voltage and at pH 6.5 (green square) and 7.6 (blue circle). The data are obtained by Gly-Gln dose-response experiment. The inserts (**Aa**) is enlargements of $K_{0.5}$ at pH 6.5**.** In **B** Plots of rate ($1/\tau$) versus the Michaelis Menten constant ($K_{0.5}$) for Atlantic salmon PepT1b. The data points are computing using the decay rate/voltage relationship and the $K_{0.5}$/voltage relationship at two pH conditions (pH 6.5 green square and pH 7.6 blue circle) and are correlated in function of membrane potentials. Straight lines are linear regression to the points, with the Pearson correlation coefficient (ϱ) indicated.

Comparing the parameters of the Boltzmann equation (see **Table 3.3**), the maximal moveable charge Q_{max} values measured for zebrafish PepT1a are the highest at all pH conditions and, differently from the others, zebrafish Q_{max} increase with the increase of external pH. Conversely, the lowest Q_{max} values are obtained by the analyses on the *PSS* currents of zebrafish PepT1b. The Atlantic salmon transporters show similar values of the maximal moveable charge. For all transporters, the alkalization of external medium causes a shift to more negative values of the voltage needed to move half of the charge ($V_{0.5}$). This effect is more evident in rabbit PepT1 with a ratio of ~2.42 and in zebrafish and Atlantic salmon PepT1a transporters with ratios of ~ 1.91 and ~ 2.14, respectively. The same effect is very faintly detectable in PepT1b with very small differences between the two pH.

Several studies documented that not only neutral dipeptides but also dipeptides carrying net positive or negative charge are able to induce inward currents via PepT1 (Amasheh et al., 1997; Kottra et al., 2002; Verri et al., 2010).

Although it is still controversial how PepT1 handles differently charged substrates together with H^+ and with which stoichiometry, the transport of positive and negative charged dipeptides is an electrogenic process that follows the Michaelis-Menten kinetics. Moreover, electrophysiological studies on rabbit and zebrafish transporters reported that the position of the charged amino acid chain in a substrate significantly affects the transport process.

To investigate whether similar differences may be observed in zebrafish PepT1a and in Atlantic salmon transporters, the transport current of 1 mmol/L of negatively charged dipeptides (Asp-Gly and Gly-Asp) and two pairs of positively charged dipeptides (Lys-Gly and Gly-Lys; Lys-Met and Met-Lys) were recorded and compared each other (**Figure 3.12**).

Transport currents recorded i) at fixed membrane potential of -60 mV and ii) at pH 7.6 and normalized to the current of the reference substrate (Gly-Gln), show differences between PepT1a and PepT1b transporters. The transport currents of

negative charged dipeptides depend on the position the charged amino acid in PepT1a(s) but not in PepT1b transporters. Conversely, the position of the charge residue in positive substrates defines the current amplitudes in Atlantic salmon PepT1b. This effect was observed also in rabbit PepT1, in seabass PepT1 and zebrafish PepT1b, even if in this latter only for the pair Lys-Gly and Gly-Lys (Margheritis et al., 2013).

In PepT1a, the currents elicited by dipeptides with a positive residue are definitely smaller for both orthologues (less than 20% in zebrafish for all dipeptides and in Atlantic salmon for Lys-Gly and Gly-Lys). In this last case, the transport currents of Lys-Met and Met-Lys are reduced to around 50% of Gly-Gln current. The position of the positive residue in the dipeptide marginally influences the transport activities of PepT1a transporters.

In zebrafish PepT1a, when the negative charge is in the amino-terminal position (Asp-Gly) the transport current increases (**Figure 3.12A**) and is greatly influenced by the voltage (**Figure 3.13A**). In Atlantic salmon PepT1a, Asp-Gly elicits larger current than the reference peptide Gly-Gln in a limited voltage range around to -60 mV. At -140 mV a slight decrease of current is recorded with respect to the current due to Gly-Gln. For both PepT1a transporters, when the negative charge is in carboxyl-terminal position (Gly-Asp) the transport currents are similar to the reference Gly-Gln current (**Figure 3.12A** and **Figure 3.13A**). In PepT1b, the negatively charged substrates elicit current that are always smaller than the reference Gly-Gln current at all tested voltages, particularly in zebrafish, where the relative currents are very small (**Figure 3.12A** and **3.13A**).

The different transport current amplitudes between PepT1a and PepT1b in the presence of negatively charged substrate are probably due to differences in the amino acid residues involved in substrate and/or in proton binding. It is reported that negatively charged dipeptides are transported in uncharged form, but a small fraction of them can be transiently protonated in the very proximity

of the membrane and thus translocated virtually as charged species together with two protons (Kottra et al., 2002). At pH 7.6 less than 1% of Asp-Gly and of Gly-Asp are present in the electrical neutral form. Thus, the largest inward current recorded for Asp-Gly but not for Gly-Asp in PepT1a(s) could be ascribed to the easy protonation of the negatively charged form in the proximity of the binding site as function of the charge position in the dipeptide.

This last hypothesis could explain the different current amplitudes of Asp-Gly between zebrafish PepT1a and PepT1b, when the values of Q_{max} are considered. Although it is thought that the PepT1 transporter *PSS* are mostly due to the rearrangement of intrinsic transporter charges (Renna et al., 2011b), the involvement of the external proton movements in the electrical membrane field is considered partly responsible of the *PSS* genesis. Thus, at pH 7.6 for zebrafish PepT1a, the highest value of Q_{max} (53.0 ± 0.6 nC) could be due to an increase in protons entering the open vestibule of the transporter that might increase the Asp-Gly protonation and thus its transport as charged substrate. Conversely, for zebrafish PepT1b, the smallest value of Q_{max} (9.9 ± 1.1 nC) could explain the negligible transport current in the presence of Asp-Gly together with the low relative affinity for this dipeptide ($K_{0.5}$ at pH 7.5 is 13 ± 1 mmol/L for Asp-Gly *vs.* 1.44 ± 1.18 mmol/L for Gly-Gln) (Verri et al., 2009).

Preliminary data on kinetic transport parameters of Gly-Asp in zebrafish PepT1a are reported in **Table 3.4**. The percentage of the negative charged dipeptide Gly-Asp in neutral form increase from <0.1 to 8% upon a pH reduction from 7.5 to 5.5. In rabbit PepT1 and in zebrafish PepT1b, it was reported that the reduction of pH led to a marked increase in binding affinity (ratio: ~ 39 in rabbit and ~ 100 in zebrafish PepT1b), whereas the simultaneous changes in I_{max} were only moderate in both transporters (ratio: ~ 0.7). Notably, changing the external pH from 7.5 to 5.5 an increase in I_{max} occurred in rabbit PepT1 while a decrease in I_{max} is observed in zebrafish PepT1b, according with its peculiar pH dependency. In zebrafish PepT1a upon a reduction of pH from

7.6 to 5.5, the apparent affinity increases (ratio: ~22), whereas a marked decrease in I_{max} is reported (ratio: ~2.3). Data on Gly-Asp kinetic parameters of zebrafish PepT1a suggest that at pH 5.5 the substrate apparent affinity is similar between PepT1a ($K_{0.5}$ 0.27 ± 0.03 mmol/L) and PepT1b ($K_{0.5}$ 0.21 ± 0.03 mmol/L, see Verri et al., 2010). When the external pH is increased at 7.5/7.6, the apparent affinity decreases in both transporters: in PepT1a with $K_{0.5}$ 5.89 ± 2.14 mmol/L and in PepT1b, more strongly, to a $K_{0.5}$ 21 ± 5 mmol/L, (Verri et al., 2009).

The results on the transport currents of positive charged substrates reveal that in Atlantic salmon PepT1b the substrates carrying the charged residue in amino terminal position (Lys-Gly and Lys-Met) elicits larger currents than Gly-Gln and the reversed dipeptides (Gly-Lys and Met-Lys) (**Figure 3.12B** and **3.12C**). The I/V relationship for Atlantic salmon PepT1b shows a larger Lys-Gly transport current and a smaller current in the presence of Gly-Lys if compared to the Gly-Gln current (**Figure 3.13B**).

Although in zebrafish PepT1b the Lys-Gly current is larger than Gly-Lys, both substrates elicit currents that are smaller than the reference current (**Figure 3.12B**) at all the tested voltages (**Figure 3.13B**). Data obtained by the transport activity of zebrafish PepT1b show comparable currents between Met-Lys, Lys-Met and Gly-Gln (**Figure 3.13C**).

For both PepT1a transporters, the currents in the presence of the four positively charged substrates are smaller than the reference current (**Figure 3.12B** and **3.12C**). Moreover, the I/V relationships for Lys-Gly and Gly-Lys clearly show that these substrates are almost unable to elicit significative currents in the range of tested voltage (**Figure 3.13B**).

In rabbit PepT1, the electrophysiological recordings combined with simultaneous intracellular pH measurement under voltage clamp condition showed that the Lys-Gly can be transported both in charged and neutral form (Kottra et al., 2002), whereas the Gly-Lys is transported in neutral form. Although the differences in the current amplitudes between the transport of

Lys-Gly and Gly-Lys could be due to differences in substrate affinity, the results from the rabbit transporter could explain the excess in transport current observed in Atlantic salmon PepT1b for Lys-Gly.

Moreover, the Lys-Gly dose response experiments highlight the difference in transport kinetics between Atlantic salmon PepT1a and PepT1b. The fitting with the Michaelis-Menten equation allows the computation of the kinetic parameters ($K_{0.5}$ and I_{max}) at each voltage for PepT1b (**Figure 3.17A** and **13.7B**), but not for PepT1a. In this experiment, the current recorded in PepT1a does not reach the saturation (**Figure 3.16A**), and residual *PSS* currents are visible even with perfusion of Lys-Gly 30 mmol/L (**Figure 3.16C**), making the evaluation of the kinetic parameters not reliable. In zebrafish transporters, the comparison between $K_{0.5}$ values at the same experimental conditions (pH 7.6 and at -60 mV) show that PepT1b transports Lys-Gly with an affinity five-fold higher ($K_{0.5}$ 3.5 ± 0.6 mmol/L see Verri et al., 2009) than PepT1a ($K_{0.5}$ 18.35 ± 3.51) (**Table 3.4**). Moreover, when the external pH is increased from 7.5/7.6 to 8.5 the percentage of the positively charged Lys-Gly molecules decreases from 83 to 33% and the kinetic parameters are differently influenced in PepT1b and PepT1a transporters. Zebrafish PepT1b shows a decrease in relative affinity (ratio: ~ 0.2) but an increase in maximal relative current (ratio: ~ 0.6), whereas PepT1a shows an increase in affinity (ratio: ~ 1.6) but the simultaneous change in maximal relative current is only moderate (ratio: ~ 1.1).

Transport data on Lys- and Met- containing substrates have been also evaluated to better investigate the role of each transporter in nutrition. Applying a pulse protocol, the transport current of 1 mmol/L of each dipeptide are measured at pH 6.5 and 7.6 and compared to investigate both voltage and pH dependency (**Figure 3.14**). The same experimental procedure was applied by Margheritis and collaborators in 2013 to collect transport current of zebrafish PepT1b, seabass PepT1 and mammalian transporters (Margheritis et al., 2013). When the results of Atlantic salmon PepT1b are compared with other transporters, the I/V

relationships of Lys-Gly show a similar behavior to that found in zebrafish transporter, whereas the I/V relationships of Met-Lys and Lys-Met appear to be similar to those observed in seabass and mammalian transporters (Margheritis et al., 2013). When the current amplitudes are compared between PepT1a and PepT1b transporters of each species, the highest values are obtained from PepT1b. These results suggest the low involvement of PepT1a in the transport of these important nutritional dipeptides.

Summarizing in PepT1a transporters, dipeptides containing lysine and/or methionine show currents that are smaller than the reference current, for all the tested potentials and pH conditions. Conversely, large currents are shown in Atlantic salmon PepT1b for all the tested substrates with the only exception of Gly-Lys. These currents are influenced by membrane potential and by the position of charge residue in dipeptide.

Particularly in zebrafish PepT1a transporter, the currents elicited by all of the tested substrates are slightly increased by membrane potentials and by different pH conditions. In Atlantic salmon PepT1a, the transport current is augmented by increasing negative potential only in the presence of methionine containing dipeptides with a peculiar pH dependency. In Atlantic salmon PepT1b, large currents are observed in the presence of dipeptides carrying the lysine in N-terminus position at the more negative potentials and at external pH 7.6.

These data on charged substrate have a dual importance. First, these evidences have major importance in animal nutrition being lysine an essential amino acid; secondly, the information about the ability of PepT1 to transport charged amino acid is crucially useful in modelling the steps of translocation of charged peptido-mimetic drugs.

Chapter 5. Conclusions

This thesis work describes the novel evidence that PepT1a-type proteins of teleost fish are functional transporters that work as a proton depended, sodium independent system for the uptake of di- and tripeptides. Similar to the paralogues PepT1b, both zebrafish and Atlantic salmon PepT1a transporters are low affinity and high capacity systems that show kinetic parameters influenced by voltage and external pH. The unique pH dependency of the zebrafish PepT1b transporter is confirmed also for PepT1a. This functional peculiarity strongly supports the use of PepT1 orthologues of zebrafish as tools for a detailed analysis of residues and domains involved in the proton-protein relationships.

Although a cursory comparison shows species-specific conserved features in basic transport function, detailed analysis on steady-state and *PSS* currents show differences between PepT1a and PepT1b transporters of each species that are correlated strictly to the differences in amino acids sequences. These differences emerge analyzing the current response for different externally definable parameters such as substrate concentration, pH and membrane potentials.

Since the transport kinetics are thought to result from a series of molecular rearrangements between multiple conformational states, the results reported here suggest that differences in structural-functional relationships exist between the transporters analyzed in this work.

In this perspective, the functional characterization of teleost fish orthologues represents an important starting point to define better the relation between structure and function of PepT1-type proteins.

Considering the increase in structural information from the crystal structures of bacterial transporters, it is possible to perform a comprehensive analysis of the information collected about this highly conserved family of proteins. This allows

to identify residues that are involved in distinct phases of the transport cycle and to explain also how these residues may be critical in determining the diversified behaviors of PepT1 orthologues.

Moreover, the data about the transport currents elicited by charged substrates or by important nutritional substrates highlight strong differences between PepT1a and PepT1b transporters, giving the opportunity to define the determinants possibly involved in the interaction with charged substrates.

When PepT1a and PepT1b transporters are contemporarily expressed in the same tissue, the functional differences suggest that they might operate synergistically to achieve the optimal absorption of protein degradation products, further implying physiological roles based on the differential interaction with different substrate peptides. Indeed, the expression of PepT1 in the enteroendocrine cells supports the possible physiological role as nutrient detector/sensor.

All data presented in this thesis will be useful not only to study and specify the physiological role(s) in peptide transport and/or sensing in fish, but also to give new insights about unsolved questions on the kinetic mechanism of PepT1-mediated transport. Moreover, the increasing use of teleost fish as animal models in translational research demands deep information on the physiology of these organisms. For instance, the studies of intestinal inflammatory diseases, metabolic disorders and cancers in which PepT1 is involved directly or indirectly, require a detailed knowledge of the function of different orthologues transporters. Additionally, the functional data can support the therapeutic approach because PepT1 is important not only as main route in oral drug delivery but also as pharmacological target. These aspects require a detailed analysis of protein-substrate interactions from the structural as well as kinetic and functional points of view. The comprehension of the molecular basis of the wide substrate recognition provides a powerful template for prodrugs development.

To conclude, the study of PepT1 based on comparative approaches could be useful to better clarify its role in the complex scenario of sensing and absorption of nutrient and drugs.

Bibliography

Alcock, J., Maley, C.C., and Aktipis, C.A. (2014). Is eating behavior manipulated by the gastrointestinal microbiota? Evolutionary pressures and potential mechanisms. Bioessays 36, 940-949.

Amasheh, S., Wenzel, U., Boll, M., Dorn, D., Weber, W., Clauss, W., and Daniel, H. (1997). Transport of charged dipeptides by the intestinal H+/peptide symporter PepT1 expressed in Xenopus laevis oocytes. J Membr Biol 155, 247-256.

Amole, N., and Unniappan, S. (2009). Fasting induces preproghrelin mRNA expression in the brain and gut of zebrafish, Danio rerio. Gen Comp Endocrinol 161, 133-137.

Anderle, P., Nielsen, C.U., Pinsonneault, J., Krog, P.L., Brodin, B., and Sadee, W. (2006). Genetic variants of the human dipeptide transporter PEPT1. J Pharmacol Exp Ther 316, 636-646.

Anderson, C.M., Jevons, M., Thangaraju, M., Edwards, N., Conlon, N.J., Woods, S., Ganapathy, V., and Thwaites, D.T. (2010). Transport of the photodynamic therapy agent 5-aminolevulinic acid by distinct H+-coupled nutrient carriers coexpressed in the small intestine. J Pharmacol Exp Ther 332, 220-228.

Ayyadurai, S., Charania, M.A., Xiao, B., Viennois, E., and Merlin, D. (2013). PepT1 expressed in immune cells has an important role in promoting the immune response during experimentally induced colitis. Lab Invest 93, 888-899.

Bakke, A.M., Nordrum, S., Krogdahl, A., and Buddington, R. (2000). Absorption of glucose, amino acids, and dipeptides by the intestines of Atlantic salmon (Salmo salar L.). Fish Physiology and Biochemistry 22, 33-44.

Balimane, P.V., Tamai, I., Guo, A., Nakanishi, T., Kitada, H., Leibach, F.H., Tsuji, A., and Sinko, P.J. (1998). Direct evidence for peptide transporter (PepT1)-mediated uptake of a nonpeptide prodrug, valacyclovir. Biochem Biophys Res Commun 250, 246-251.

Baron, M., Kim, I.S., Moncada, R., Yan, Y., Campbell, N.R., White, R.M., and Yanai, I. (2018). Cancer archetypes co-opt and adapt the transcriptional programs of existing cellular states. bioRxiv, 396622.

Bates, J.M., Akerlund, J., Mittge, E., and Guillemin, K. (2007). Intestinal alkaline phosphatase detoxifies lipopolysaccharide and prevents inflammation in zebrafish in response to the gut microbiota. Cell Host Microbe 2, 371-382.

Batista, M.R.B., Watts, A., and Jose Costa-Filho, A. (2019). Exploring Conformational Transitions and Free-Energy Profiles of Proton-Coupled Oligopeptide Transporters. J Chem Theory Comput 15, 6433-6443.

Belkaid, Y., and Hand, T.W. (2014). Role of the microbiota in immunity and inflammation. Cell 157, 121-141.

Bhardwaj, R.K., Herrera-Ruiz, D., Eltoukhy, N., Saad, M., and Knipp, G.T. (2006). The functional evaluation of human peptide/histidine transporter 1 (hPHT1) in transiently transfected COS-7 cells. Eur J Pharm Sci 27, 533-542.

Bierwirtz, A., Schwarz, W. (2014). Two-electrode voltage-clamp (TEVC). Conference Proceedings-Biophysikalisches Praktikum Institut fur Biophysik Johann, Wonfgang Goethe-Universitat.

Blanco, A.M., Bertucci, J.I., Ramesh, N., Delgado, M.J., Valenciano, A.I., and Unniappan, S. (2017). Ghrelin Facilitates GLUT2-, SGLT1- and SGLT2-mediated Intestinal Glucose Transport in Goldfish (Carassius auratus). Sci Rep 7, 45024.

Bolger, M.B., Haworth, I.S., Yeung, A.K., Ann, D., von Grafenstein, H., Hamm-Alvarez, S., Okamoto, C.T., Kim, K.J., Basu, S.K., Wu, S., and Lee, V.H. (1998). Structure, function, and molecular modeling approaches to the study of the intestinal dipeptide transporter PepT1. J Pharm Sci 87, 1286-1291.

Boll, M., Markovich, D., Weber, W.M., Korte, H., Daniel, H., and Murer, H. (1994). Expression cloning of a cDNA from rabbit small intestine related to proton-coupled transport of peptides, beta-lactam antibiotics and ACE-inhibitors. Pflugers Arch 429, 146-149.

Bossi, E., Cherubino, F., Margheritis, E., Oyadeyi, A.S., Vollero, A., and Peres, A. (2012). Temperature effects on the kinetic properties of the rabbit intestinal oligopeptide cotransporter PepT1. Pflugers Arch 464, 183-191.

Bossi, E., Fabbrini, M.S., and Ceriotti, A. (2007). Exogenous protein expression in Xenopus oocytes: basic procedures. Methods Mol Biol 375, 107-131.

Bradford, Y.M., Toro, S., Ramachandran, S., Ruzicka, L., Howe, D.G., Eagle, A., Kalita, P., Martin, R., Taylor Moxon, S.A., Schaper, K., and Westerfield, M. (2017). Zebrafish Models of Human Disease: Gaining Insight into Human Disease at ZFIN. ILAR J 58, 4-16.

Brandsch, M., Knutter, I., and Bosse-Doenecke, E. (2008). Pharmaceutical and pharmacological importance of peptide transporters. J Pharm Pharmacol 60, 543-585.

Bretschneider, B., Brandsch, M., and Neubert, R. (1999). Intestinal transport of beta-lactam antibiotics: analysis of the affinity at the H+/peptide symporter (PEPT1), the uptake into Caco-2 cell monolayers and the transepithelial flux. Pharm Res 16, 55-61.

Brodin, B., Nielsen, C.U., Steffansen, B., and Frokjaer, S. (2002). Transport of peptidomimetic drugs by the intestinal Di/tri-peptide transporter, PepT1. Pharmacology & toxicology 90, 285-296.

Broer, S. (2008). Amino acid transport across mammalian intestinal and renal epithelia. Physiol Rev 88, 249-286.

Broer, S., and Broer, A. (2017). Amino acid homeostasis and signalling in mammalian cells and organisms. Biochem J 474, 1935-1963.

Bucking, C., and Schulte, P.M. (2012). Environmental and nutritional regulation of expression and function of two peptide transporter (PepT1) isoforms in a euryhaline teleost. Comp Biochem Physiol A Mol Integr Physiol 161, 379-387.

Buracco, S., Peracino, B., Cinquetti, R., Signoretto, E., Vollero, A., Imperiali, F., Castagna, M., Bossi, E., and Bozzaro, S. (2015). Dictyostelium Nramp1, which is structurally and functionally similar to mammalian DMT1 transporter, mediates phagosomal iron efflux. J Cell Sci 128, 3304-3316.

Buyse, M., Charrier, L., Sitaraman, S., Gewirtz, A., and Merlin, D. (2003). Interferon-gamma increases hPepT1-mediated uptake of di-tripeptides including the bacterial tripeptide fMLP in polarized intestinal epithelia. Am J Pathol 163, 1969-1977.

Carnovali, M., Luzi, L., Banfi, G., and Mariotti, M. (2016). Chronic hyperglycemia affects bone metabolism in adult zebrafish scale model. Endocrine 54, 808-817.

Cesar-Razquin, A., Snijder, B., Frappier-Brinton, T., Isserlin, R., Gyimesi, G., Bai, X., Reithmeier, R.A., Hepworth, D., Hediger, M.A., Edwards, A.M., and Superti-Furga, G. (2015). A Call for Systematic Research on Solute Carriers. Cell 162, 478-487.

Chen, H., Wong, E.A., and Webb, K.E., Jr. (1999). Tissue distribution of a peptide transporter mRNA in sheep, dairy cows, pigs, and chickens. J Anim Sci 77, 1277-1283.

Cheng, Q., Shah, N., Bröer, A., Fairweather, S., Jiang, Y., Schmoll, D., Corry, B., and Bröer, S. (2017). Identification of novel inhibitors of the amino acid transporter B(0) AT1 (SLC6A19), a potential target to induce protein restriction and to treat type 2 diabetes. British journal of pharmacology 174, 468-482.

Chouliaras, G., Panayotou, I., Margoni, D., Mantzou, E., Pervanidou, P., Manios, Y., Chrousos, G.P., and Roma, E. (2013). Circulating leptin and adiponectin and their relation to glucose metabolism in children with Crohn's disease and ulcerative colitis. Pediatr Res 74, 420-426.

Colas, C., Masuda, M., Sugio, K., Miyauchi, S., Hu, Y., Smith, D.E., and Schlessinger, A. (2017). Chemical Modulation of the Human Oligopeptide Transporter 1, hPepT1. Mol Pharm 14, 4685-4693.

Colas, C., Ung, P.M., and Schlessinger, A. (2016). SLC Transporters: Structure, Function, and Drug Discovery. Medchemcomm 7, 1069-1081.

Cole, K.S., and Curtis, H.J. (1941). Membrane Potential of the Squid Giant Axon during Current Flow. J Gen Physiol 24, 551-563.

Con, P., Nitzan, T., and Cnaani, A. (2017). Salinity-Dependent Shift in the Localization of Three Peptide Transporters along the Intestine of the Mozambique Tilapia (Oreochromis mossambicus). Front Physiol 8, 8.

Cossins, A.R., and Crawford, D.L. (2005). Fish as models for environmental genomics. Nat Rev Genet 6, 324-333.

Covitz, K.M., Amidon, G.L., and Sadee, W. (1998). Membrane topology of the human dipeptide transporter, hPEPT1, determined by epitope insertions. Biochemistry 37, 15214-15221.

Cuevas-Sierra, A., Ramos-Lopez, O., Riezu-Boj, J.I., Milagro, F.I., and Martinez, J.A. (2019). Diet, Gut Microbiota, and Obesity: Links with Host Genetics and Epigenetics and Potential Applications. Adv Nutr 10, S17-S30.

Cummings, D.E., and Overduin, J. (2007). Gastrointestinal regulation of food intake. J Clin Invest 117, 13-23.

Dalmasso, G., Nguyen, H.T., Charrier-Hisamuddin, L., Yan, Y., Laroui, H., Demoulin, B., Sitaraman, S.V., and Merlin, D. (2010). PepT1 mediates transport of the proinflammatory bacterial tripeptide L-Ala-{gamma}-D-Glu-meso-DAP in intestinal epithelial cells. Am J Physiol Gastrointest Liver Physiol 299, G687-696.

Daniel, H. (2004). Molecular and integrative physiology of intestinal peptide transport. Annu Rev Physiol 66, 361-384.

Daniel, H., and Kottra, G. (2004). The proton oligopeptide cotransporter family SLC15 in physiology and pharmacology. Pflugers Arch 447, 610-618.

Daniel, H., and Zietek, T. (2015). Taste and move: glucose and peptide transporters in the gastrointestinal tract. Exp Physiol 100, 1441-1450.

Delgado, M.J., Cerda-Reverter, J.M., and Soengas, J.L. (2017). Hypothalamic Integration of Metabolic, Endocrine, and Circadian Signals in Fish: Involvement in the Control of Food Intake. Front Neurosci 11, 354.

Deveau, A.P., Bentley, V.L., and Berman, J.N. (2017). Using zebrafish models of leukemia to streamline drug screening and discovery. Exp Hematol 45, 1-9.

Diakogiannaki, E., Pais, R., Tolhurst, G., Parker, H.E., Horscroft, J., Rauscher, B., Zietek, T., Daniel, H., Gribble, F.M., and Reimann, F. (2013). Oligopeptides stimulate glucagon-like peptide-1 secretion in mice through proton-coupled uptake and the calcium-sensing receptor. Diabetologia 56, 2688-2696.

Doki, S., Kato, H.E., Solcan, N., Iwaki, M., Koyama, M., Hattori, M., Iwase, N., Tsukazaki, T., Sugita, Y., Kandori, H.*, et al.* (2013). Structural basis for dynamic mechanism of proton-coupled symport by the peptide transporter POT. Proc Natl Acad Sci U S A 110, 11343-11348.

Doring, F., Will, J., Amasheh, S., Clauss, W., Ahlbrecht, H., and Daniel, H. (1998). Minimal molecular determinants of substrates for recognition by the intestinal peptide transporter. J Biol Chem 273, 23211-23218.

Du, Y., Tian, C., Wang, M., Huang, D., Wei, W., Liu, Y., Li, L., Sun, B., Kou, L., Kan, Q.*, et al.* (2018). Dipeptide-modified nanoparticles to facilitate oral docetaxel delivery: new insights into PepT1-mediated targeting strategy. Drug delivery 25, 1403-1413.

Egerod, K.L., Engelstoft, M.S., Grunddal, K.V., Nohr, M.K., Secher, A., Sakata, I., Pedersen, J., Windelov, J.A., Fuchtbauer, E.M., Olsen, J.*, et al.* (2012). A major lineage of enteroendocrine cells coexpress CCK, secretin, GIP, GLP-1, PYY, and neurotensin but not somatostatin. Endocrinology 153, 5782-5795.

Farber, S.A., Pack, M., Ho, S.Y., Johnson, I.D., Wagner, D.S., Dosch, R., Mullins, M.C., Hendrickson, H.S., Hendrickson, E.K., and Halpern, M.E. (2001). Genetic analysis of digestive physiology using fluorescent phospholipid reporters. Science 292, 1385-1388.

Farr, G.H., 3rd, Imani, K., Pouv, D., and Maves, L. (2018). Functional testing of a human PBX3 variant in zebrafish reveals a potential modifier role in congenital heart defects. Dis Model Mech 11.

Fei, Y.J., Kanai, Y., Nussberger, S., Ganapathy, V., Leibach, F.H., Romero, M.F., Singh, S.K., Boron, W.F., and Hediger, M.A. (1994). Expression cloning of a mammalian proton-coupled oligopeptide transporter. Nature 368, 563-566.

Fei, Y.J., Sugawara, M., Liu, J.C., Li, H.W., Ganapathy, V., Ganapathy, M.E., and Leibach, F.H. (2000). cDNA structure, genomic organization, and promoter analysis of the mouse intestinal peptide transporter PEPT1. Biochim Biophys Acta 1492, 145-154.

Foster, D.R., Landowski, C.P., Zheng, X., Amidon, G.L., and Welage, L.S. (2009). Interferon-gamma increases expression of the di/tri-peptide transporter, h-PEPT1, and dipeptide transport in cultured human intestinal monolayers. Pharmacol Res 59, 215-220.

Fuentes, R., Letelier, J., Tajer, B., Valdivia, L.E., and Mullins, M.C. (2018). Fishing forward and reverse: Advances in zebrafish phenomics. Mech Dev 154, 296-308.

Ganapathy, M.E., Brandsch, M., Prasad, P.D., Ganapathy, V., and Leibach, F.H. (1995). Differential recognition of beta -lactam antibiotics by intestinal and renal peptide transporters, PEPT 1 and PEPT 2. J Biol Chem 270, 25672-25677.

Gangopadhyay, A., Thamotharan, M., and Adibi, S.A. (2002). Regulation of oligopeptide transporter (Pept-1) in experimental diabetes. Am J Physiol Gastrointest Liver Physiol 283, G133-138.

Gilbert, E.R., Wong, E.A., and Webb, K.E., Jr. (2008). Board-invited review: Peptide absorption and utilization: Implications for animal nutrition and health. J Anim Sci 86, 2135-2155.

Goncalves, A.F., Castro, L.F., Pereira-Wilson, C., Coimbra, J., and Wilson, J.M. (2007). Is there a compromise between nutrient uptake and gas exchange in the gut of Misgurnus anguillicaudatus, an intestinal air-breathing fish? Comp Biochem Physiol Part D Genomics Proteomics 2, 345-355.

Gong, Y., Wu, X., Wang, T., Zhao, J., Liu, X., Yao, Z., Zhang, Q., and Jian, X. (2017). Targeting PEPT1: a novel strategy to improve the antitumor efficacy of doxorubicin in human hepatocellular carcinoma therapy. Oncotarget 8, 40454-40468.

Gourdon, B., Chemin, C., Moreau, A., Arnauld, T., Baumy, P., Cisternino, S., Pean, J.M., and Decleves, X. (2017). Functionalized PLA-PEG nanoparticles targeting intestinal transporter PepT1 for oral delivery of acyclovir. International journal of pharmaceutics 529, 357-370.

Gourdon, B., Chemin, C., Moreau, A., Arnauld, T., Delbos, J.M., Pean, J.M., and Decleves, X. (2018). Influence of PLA-PEG nanoparticles manufacturing process on intestinal transporter PepT1 targeting and oxytocin transport. European journal of pharmaceutics and biopharmaceutics : official journal of Arbeitsgemeinschaft fur Pharmazeutische Verfahrenstechnik eV 129, 122-133.

Guettou, F., Quistgaard, E.M., Raba, M., Moberg, P., Low, C., and Nordlund, P. (2014). Selectivity mechanism of a bacterial homolog of the human drug-peptide transporters PepT1 and PepT2. Nat Struct Mol Biol 21, 728-731.

Habib, A.M., Richards, P., Cairns, L.S., Rogers, G.J., Bannon, C.A., Parker, H.E., Morley, T.C., Yeo, G.S., Reimann, F., and Gribble, F.M. (2012). Overlap of endocrine hormone expression in the mouse intestine revealed by transcriptional profiling and flow cytometry. Endocrinology 153, 3054-3065.

Hagting, A., Kunji, E.R., Leenhouts, K.J., Poolman, B., and Konings, W.N. (1994). The di- and tripeptide transport protein of Lactococcus lactis. A new type of bacterial peptide transporter. J Biol Chem 269, 11391-11399.

Hanahan, D., and Weinberg, R.A. (2011). Hallmarks of cancer: the next generation. Cell 144, 646-674.

Hatef, A., Yufa, R., and Unniappan, S. (2015). Ghrelin O-Acyl Transferase in Zebrafish Is an Evolutionarily Conserved Peptide Upregulated During Calorie Restriction. Zebrafish 12, 327-338.

Havel, P.J. (2001). Peripheral signals conveying metabolic information to the brain: short-term and long-term regulation of food intake and energy homeostasis. Exp Biol Med (Maywood) 226, 963-977.

Hediger, M.A., Clemencon, B., Burrier, R.E., and Bruford, E.A. (2013). The ABCs of membrane transporters in health and disease (SLC series): introduction. Molecular aspects of medicine 34, 95-107.

Hediger, M.A., Coady, M.J., Ikeda, T.S., and Wright, E.M. (1987). Expression cloning and cDNA sequencing of the Na+/glucose co-transporter. Nature 330, 379-381.

Hediger, M.A., Romero, M.F., Peng, J.B., Rolfs, A., Takanaga, H., and Bruford, E.A. (2004). The ABCs of solute carriers: physiological, pathological and therapeutic implications of human membrane transport proteinsIntroduction. Pflugers Arch 447, 465-468.

Hindlet, P., Bado, A., Farinotti, R., and Buyse, M. (2007). Long-term effect of leptin on H+-coupled peptide cotransporter 1 activity and expression in vivo: evidence in leptin-deficient mice. J Pharmacol Exp Ther 323, 192-201.

Hindlet, P., Bado, A., Kamenicky, P., Delomenie, C., Bourasset, F., Nazaret, C., Farinotti, R., and Buyse, M. (2009). Reduced intestinal absorption of dipeptides via PepT1 in mice with diet-induced obesity is associated with leptin receptor down-regulation. J Biol Chem 284, 6801-6808.

Hodgkin, A.L., Huxley, A.F., and Katz, B. (1952). Measurement of current-voltage relations in the membrane of the giant axon of Loligo. J Physiol 116, 424-448.

Hoglund, P.J., Nordstrom, K.J., Schioth, H.B., and Fredriksson, R. (2011). The solute carrier families have a remarkably long evolutionary history with the majority of the human families present before divergence of Bilaterian species. Mol Biol Evol 28, 1531-1541.

Howe, K., Clark, M.D., Torroja, C.F., Torrance, J., Berthelot, C., Muffato, M., Collins, J.E., Humphray, S., McLaren, K., Matthews, L.*, et al.* (2013). The zebrafish reference genome sequence and its relationship to the human genome. Nature 496, 498-503.

Huang, Q., Vera Delgado, J.M., Seni Pinoargote, O.D., and Llaguno, R.A. (2015). Molecular evolution of the Slc15 family and its response to waterborne copper and mercury exposure in tilapia. Aquat Toxicol 163, 140-147.

Hulo, N., Bairoch, A., Bulliard, V., Cerutti, L., De Castro, E., Langendijk-Genevaux, P.S., Pagni, M., and Sigrist, C.J. (2006). The PROSITE database. Nucleic Acids Res 34, D227-230.

Ikeda, T.S., Hwang, E.S., Coady, M.J., Hirayama, B.A., Hediger, M.A., and Wright, E.M. (1989). Characterization of a Na+/glucose cotransporter cloned from rabbit small intestine. J Membr Biol 110, 87-95.

Inui, K., Tomita, Y., Katsura, T., Okano, T., Takano, M., and Hori, R. (1992). H+ coupled active transport of bestatin via the dipeptide transport system in rabbit intestinal brush-border membranes. J Pharmacol Exp Ther 260, 482-486.

Javed, K., Cheng, Q., Carroll, A.J., Truong, T.T., and Bröer, S. (2018). Development of Biomarkers for Inhibition of SLC6A19 (B^0AT1)-A Potential Target to Treat Metabolic Disorders. Int J Mol Sci 19, 3597.

Jiang, Y., Rose, A.J., Sijmonsma, T.P., Broer, A., Pfenninger, A., Herzig, S., Schmoll, D., and Broer, S. (2015). Mice lacking neutral amino acid transporter B(0)AT1 (Slc6a19) have elevated levels of FGF21 and GLP-1 and improved glycaemic control. Molecular metabolism 4, 406-417.

Joshi, S., Tough, I.R., and Cox, H.M. (2013). Endogenous PYY and GLP-1 mediate l-glutamine responses in intestinal mucosa. British Journal of Pharmacology 170, 1092-1101.

Jung, S.H., Kim, Y.S., Lee, Y.R., and Kim, J.S. (2016). High glucose-induced changes in hyaloid-retinal vessels during early ocular development of zebrafish: a short-term animal model of diabetic retinopathy. Br J Pharmacol 173, 15-26.

Kottra, G., and Daniel, H. (2001). Bidirectional electrogenic transport of peptides by the proton-coupled carrier PEPT1 in Xenopus laevis oocytes: its asymmetry and symmetry. J Physiol 536, 495-503.

Kottra, G., Stamfort, A., and Daniel, H. (2002). PEPT1 as a paradigm for membrane carriers that mediate electrogenic bidirectional transport of anionic, cationic, and neutral substrates. J Biol Chem 277, 32683-32691.

Kou, L., Bhutia, Y.D., Yao, Q., He, Z., Sun, J., and Ganapathy, V. (2018). Transporter-Guided Delivery of Nanoparticles to Improve Drug Permeation across Cellular Barriers and Drug Exposure to Selective Cell Types. Frontiers in pharmacology 9, 27.

Kuhre, R.E., Frost, C.R., Svendsen, B., and Holst, J.J. (2015). Molecular mechanisms of glucose-stimulated GLP-1 secretion from perfused rat small intestine. Diabetes 64, 370-382.

Landowski, C.P., Vig, B.S., Song, X., and Amidon, G.L. (2005). Targeted delivery to PEPT1-overexpressing cells: acidic, basic, and secondary floxuridine amino acid ester prodrugs. Mol Cancer Ther 4, 659-667.

Latorre, R., Sternini, C., De Giorgio, R., and Greenwood-Van Meerveld, B. (2016). Enteroendocrine cells: a review of their role in brain-gut communication. Neurogastroenterology and motility : the official journal of the European Gastrointestinal Motility Society 28, 620-630.

Lee, V.H., Chu, C., Mahlin, E.D., Basu, S.K., Ann, D.K., Bolger, M.B., Haworth, I.S., Yeung, A.K., Wu, S.K., Hamm-Alvarez, S., and Okamoto, C.T. (1999). Biopharmaceutics of transmucosal peptide and protein drug administration: role of transport mechanisms with a focus on the involvement of PepT1. J Control Release 62, 129-140.

Letunic, I., Doerks, T., and Bork, P. (2015). SMART: recent updates, new developments and status in 2015. Nucleic Acids Res 43, D257-260.

Liang, R., Fei, Y.J., Prasad, P.D., Ramamoorthy, S., Han, H., Yang-Feng, T.L., Hediger, M.A., Ganapathy, V., and Leibach, F.H. (1995). Human intestinal H+/peptide cotransporter. Cloning, functional expression, and chromosomal localization. J Biol Chem 270, 6456-6463.

Liu, H., Chen, S., Huang, K., Kim, J., Mo, H., Iovine, R., Gendre, J., Pascal, P., Li, Q., Sun, Y.*, et al.* (2016). A High-Content Larval Zebrafish Brain Imaging Method for Small Molecule Drug Discovery. PLoS One 11, e0164645.

Liu, Z., Zhou, Y., Feng, J., Lu, S., Zhao, Q., and Zhang, J. (2013). Characterization of oligopeptide transporter (PepT1) in grass carp (Ctenopharyngodon idella). Comp Biochem Physiol B Biochem Mol Biol 164, 194-200.

Longo, A., Miles, N.W., and Dickstein, R. (2018). Genome Mining of Plant NPFs Reveals Varying Conservation of Signature Motifs Associated With the Mechanism of Transport. Front Plant Sci 9, 1668-1668.

Lyons, J.A., Parker, J.L., Solcan, N., Brinth, A., Li, D., Shah, S.T., Caffrey, M., and Newstead, S. (2014). Structural basis for polyspecificity in the POT family of proton-coupled oligopeptide transporters. EMBO Rep 15, 886-893.

Mackenzie, B., Fei, Y.J., Ganapathy, V., and Leibach, F.H. (1996a). The human intestinal H+/oligopeptide cotransporter hPEPT1 transports differently-charged dipeptides with identical electrogenic properties. Biochim Biophys Acta 1284, 125-128.

Mackenzie, B., Loo, D.D., Fei, Y., Liu, W.J., Ganapathy, V., Leibach, F.H., and Wright, E.M. (1996b). Mechanisms of the human intestinal H+-coupled oligopeptide transporter hPEPT1. J Biol Chem 271, 5430-5437.

Maffia, M., Verri, T., Danieli, A., Thamotharan, M., Pastore, M., Ahearn, G.A., and Storelli, C. (1997). H(+)-glycyl-L-proline cotransport in brush-border membrane vesicles of eel (Anguilla anguilla) intestine. Am J Physiol 272, R217-225.

Mager, S., Naeve, J., Quick, M., Labarca, C., Davidson, N., and Lester, H.A. (1993). Steady states, charge movements, and rates for a cloned GABA transporter expressed in Xenopus oocytes. Neuron 10, 177-188.

Margheritis, E., Terova, G., Oyadeyi, A.S., Renna, M.D., Cinquetti, R., Peres, A., and Bossi, E. (2013). Characterization of the transport of lysine-containing dipeptides by PepT1 orthologs expressed in Xenopus laevis oocytes. Comp Biochem Physiol A Mol Integr Physiol 164, 520-528.

Meredith, D., and Price, R.A. (2006). Molecular modeling of PepT1--towards a structure. J Membr Biol 213, 79-88.

Merlin, D., Si-Tahar, M., Sitaraman, S.V., Eastburn, K., Williams, I., Liu, X., Hediger, M.A., and Madara, J.L. (2001). Colonic epithelial hPepT1 expression occurs in inflammatory bowel disease: transport of bacterial peptides influences expression of MHC class 1 molecules. Gastroenterology 120, 1666-1679.

Mertl, M., Daniel, H., and Kottra, G. (2008). Substrate-induced changes in the density of peptide transporter PEPT1 expressed in Xenopus oocytes. Am J Physiol Cell Physiol 295, C1332-1343.

Michel, M., Page-McCaw, P.S., Chen, W., and Cone, R.D. (2016). Leptin signaling regulates glucose homeostasis, but not adipostasis, in the zebrafish. Proc Natl Acad Sci U S A 113, 3084-3089.

Minhas, G.S., and Newstead, S. (2019). Structural basis for prodrug recognition by the SLC15 family of proton-coupled peptide transporters. Proc Natl Acad Sci U S A 116, 804-809.

Nalbant, P., Boehmer, C., Dehmelt, L., Wehner, F., and Werner, A. (1999). Functional characterization of a Na+-phosphate cotransporter (NaPi-II) from zebrafish and identification of related transcripts. The Journal of physiology 520 Pt 1, 79-89.

Nduati, V., Yan, Y., Dalmasso, G., Driss, A., Sitaraman, S., and Merlin, D. (2007). Leptin transcriptionally enhances peptide transporter (hPepT1) expression and activity via the cAMP-response element-binding protein and Cdx2 transcription factors. J Biol Chem 282, 1359-1373.

Newstead, S. (2015). Molecular insights into proton coupled peptide transport in the PTR family of oligopeptide transporters. Biochim Biophys Acta 1850, 488-499.

Newstead, S. (2017a). Recent advances in understanding proton coupled peptide transport via the POT family. Curr Opin Struct Biol 45, 17-24.

Newstead, S. (2017b). Symmetry and Structure in the POT Family of Proton Coupled Peptide Transporters. Symmetry 9, 85.

Newstead, S., Drew, D., Cameron, A.D., Postis, V.L.G., Xia, X., Fowler, P.W., Ingram, J.C., Carpenter, E.P., Sansom, M.S.P., McPherson, M.J.*, et al.* (2011). Crystal structure of a prokaryotic homologue of the mammalian oligopeptide–proton symporters, PepT1 and PepT2. The EMBO Journal 30, 417-426.

Nordrum, S., Bakke-McKellep, A.M., Krogdahl, A., and Buddington, R.K. (2000). Effects of soybean meal and salinity on intestinal transport of nutrients in Atlantic salmon (Salmo salar L.) and rainbow trout (Oncorhynchus mykiss). Comp Biochem Physiol B Biochem Mol Biol 125, 317-335.

Norton, M., and Murphy, K.G. (2017). Targeting gastrointestinal nutrient sensing mechanisms to treat obesity. Curr Opin Pharmacol 37, 16-23.

Nussberger, S., Steel, A., Trotti, D., Romero, M.F., Boron, W.F., and Hediger, M.A. (1997). Symmetry of H+ binding to the intra- and extracellular side of the H+-coupled oligopeptide cotransporter PepT1. J Biol Chem 272, 7777-7785.

Oehlers, S.H., Flores, M.V., Hall, C.J., Swift, S., Crosier, K.E., and Crosier, P.S. (2011a). The inflammatory bowel disease (IBD) susceptibility genes NOD1 and NOD2 have conserved anti-bacterial roles in zebrafish. Dis Model Mech 4, 832-841.

Oehlers, S.H., Flores, M.V., Okuda, K.S., Hall, C.J., Crosier, K.E., and Crosier, P.S. (2011b). A chemical enterocolitis model in zebrafish larvae that is dependent on microbiota and responsive to pharmacological agents. Dev Dyn 240, 288-298.

Omasits, U., Ahrens, C.H., Muller, S., and Wollscheid, B. (2014). Protter: interactive protein feature visualization and integration with experimental proteomic data. Bioinformatics 30, 884-886.

Parent, L., Supplisson, S., Loo, D.D., and Wright, E.M. (1992). Electrogenic properties of the cloned Na+/glucose cotransporter: I. Voltage-clamp studies. J Membr Biol 125, 49-62.

Parker, J.L., Li, C., Brinth, A., Wang, Z., Vogeley, L., Solcan, N., Ledderboge-Vucinic, G., Swanson, J.M.J., Caffrey, M., Voth, G.A., and Newstead, S. (2017). Proton movement and coupling in the POT family of peptide transporters. Proc Natl Acad Sci U S A 114, 13182-13187.

Parker, J.L., and Newstead, S. (2014). Molecular basis of nitrate uptake by the plant nitrate transporter NRT1.1. Nature 507, 68-72.

Patton, E.E., and Tobin, D.M. (2019). Spotlight on zebrafish: the next wave of translational research. Disease Models & Mechanisms 12, dmm039370.

Paulsen, I.T., and Skurray, R.A. (1994). The POT family of transport proteins. Trends Biochem Sci 19, 404.

Pedretti, A., De Luca, L., Marconi, C., Negrisoli, G., Aldini, G., and Vistoli, G. (2008). Modeling of the intestinal peptide transporter hPepT1 and analysis of its transport capacities by docking and pharmacophore mapping. ChemMedChem 3, 1913-1921.

Phillips, J.B., and Westerfield, M. (2014). Zebrafish models in translational research: tipping the scales toward advancements in human health. Dis Model Mech 7, 739-743.

Ravi, V., and Venkatesh, B. (2008). Rapidly evolving fish genomes and teleost diversity. Curr Opin Genet Dev 18, 544-550.

Renna, M.D., Oyadeyi, A.S., Bossi, E., Kottra, G., and Peres, A. (2011a). Functional and structural determinants of reverse operation in the pH-dependent oligopeptide transporter PepT1. Cell Mol Life Sci 68, 2961-2975.

Renna, M.D., Sangaletti, R., Bossi, E., Cherubino, F., Kottra, G., and Peres, A. (2011b). Unified modeling of the mammalian and fish proton-dependent oligopeptide transporter PepT1. Channels (Austin) 5, 89-99.

Reshkin, S.J., and Ahearn, G.A. (1991). Intestinal glycyl-L-phenylalanine and L-phenylalanine transport in a euryhaline teleost. Am J Physiol 260, R563-569.

Rizzello, A., Romano, A., Kottra, G., Acierno, R., Storelli, C., Verri, T., Daniel, H., and Maffia, M. (2013). Protein cold adaptation strategy via a unique seven-amino acid domain in the icefish (Chionodraco hamatus) PEPT1 transporter. Proc Natl Acad Sci U S A 110, 7068-7073.

Roder, P.V., Geillinger, K.E., Zietek, T.S., Thorens, B., Koepsell, H., and Daniel, H. (2014). The role of SGLT1 and GLUT2 in intestinal glucose transport and sensing. PLoS One 9, e89977.

Roest Crollius, H., and Weissenbach, J. (2005). Fish genomics and biology. Genome research 15, 1675-1682.

Romano, A., Barca, A., Storelli, C., and Verri, T. (2014). Teleost fish models in membrane transport research: the PEPT1(SLC15A1) H+-oligopeptide transporter as a case study. J Physiol 592, 881-897.

Ronnestad, I., Gomes, A.S., Murashita, K., Angotzi, R., Jonsson, E., and Volkoff, H. (2017). Appetite-Controlling Endocrine Systems in Teleosts. Front Endocrinol (Lausanne) 8, 73.

Ronnestad, I., Murashita, K., Kottra, G., Jordal, A.E., Narawane, S., Jolly, C., Daniel, H., and Verri, T. (2010). Molecular cloning and functional expression of atlantic salmon peptide transporter 1 in Xenopus oocytes reveals efficient intestinal uptake of lysine-containing and other bioactive di- and tripeptides in teleost fish. J Nutr 140, 893-900.

Ruusunen, A., Rocks, T., Jacka, F., and Loughman, A. (2019). The gut microbiome in anorexia nervosa: relevance for nutritional rehabilitation. Psychopharmacology (Berl) 236, 1545-1558.

Saito, H., Okuda, M., Terada, T., Sasaki, S., and Inui, K. (1995). Cloning and characterization of a rat H+/peptide cotransporter mediating absorption of beta-lactam antibiotics in the intestine and kidney. J Pharmacol Exp Ther 275, 1631-1637.

Sakata, K., Yamashita, T., Maeda, M., Moriyama, Y., Shimada, S., and Tohyama, M. (2001). Cloning of a lymphatic peptide/histidine transporter. Biochem J 356, 53-60.

Sala-Rabanal, M., Loo, D.D., Hirayama, B.A., Turk, E., and Wright, E.M. (2006). Molecular interactions between dipeptides, drugs and the human intestinal H+ - oligopeptide cotransporter hPEPT1. J Physiol 574, 149-166.

Salmi, T.M., Tan, V.W.T., and Cox, A.G. (2019). Dissecting metabolism using zebrafish models of disease. Biochem Soc Trans 47, 305-315.

Sandoval, I.T., Delacruz, R.G., Miller, B.N., Hill, S., Olson, K.A., Gabriel, A.E., Boyd, K., Satterfield, C., Van Remmen, H., Rutter, J., and Jones, D.A. (2017). A metabolic switch controls intestinal differentiation downstream of Adenomatous polyposis coli (APC). Elife 6.

Sangaletti, R., Terova, G., Peres, A., Bossi, E., Cora, S., and Saroglia, M. (2009). Functional expression of the oligopeptide transporter PepT1 from the sea bass (Dicentrarchus labrax). Pflugers Arch 459, 47-54.

Santoriello, C., and Zon, L.I. (2012). Hooked! Modeling human disease in zebrafish. J Clin Invest 122, 2337-2343.

Sartor, R.B. (2006). Mechanisms of disease: pathogenesis of Crohn's disease and ulcerative colitis. Nat Clin Pract Gastroenterol Hepatol 3, 390-407.

Sawada, K., Terada, T., Saito, H., Hashimoto, Y., and Inui, K. (1999). Effects of glibenclamide on glycylsarcosine transport by the rat peptide transporters PEPT1 and PEPT2. Br J Pharmacol 128, 1159-1164.

Shtraizent, N., DeRossi, C., Nayar, S., Sachidanandam, R., Katz, L.S., Prince, A., Koh, A.P., Vincek, A., Hadas, Y., Hoshida, Y., *et al.* (2017). MPI depletion enhances O-GlcNAcylation of p53 and suppresses the Warburg effect. Elife 6.

Shu, C., Shen, H., Hopfer, U., and Smith, D.E. (2001). Mechanism of intestinal absorption and renal reabsorption of an orally active ace inhibitor: uptake and transport of fosinopril in cell cultures. Drug Metab Dispos 29, 1307-1315.

Sievers, F., Wilm, A., Dineen, D., Gibson, T.J., Karplus, K., Li, W., Lopez, R., McWilliam, H., Remmert, M., Soding, J., *et al.* (2011). Fast, scalable generation of high-quality protein multiple sequence alignments using Clustal Omega. Molecular systems biology 7, 539.

Sitaraman, S., Liu, X., Charrier, L., Gu, L.H., Ziegler, T.R., Gewirtz, A., and Merlin, D. (2004). Colonic leptin: source of a novel proinflammatory cytokine involved in IBD. FASEB J 18, 696-698.

Smith, D.L., Jr., Barry, R.J., Powell, M.L., Nagy, T.R., D'Abramo, L.R., and Watts, S.A. (2013). Dietary protein source influence on body size and composition in growing zebrafish. Zebrafish 10, 439-446.

Soengas, J.L., Cerda-Reverter, J.M., and Delgado, M.J. (2018). Central regulation of food intake in fish: an evolutionary perspective. J Mol Endocrinol 60, R171-R199.

Solcan, N., Kwok, J., Fowler, P.W., Cameron, A.D., Drew, D., Iwata, S., and Newstead, S. (2012). Alternating access mechanism in the POT family of oligopeptide transporters. EMBO J 31, 3411-3421.

Song, F., Hu, Y., Wang, Y., Smith, D.E., and Jiang, H. (2018). Functional Characterization of Human Peptide/Histidine Transporter 1 in Stably Transfected MDCK Cells. Mol Pharm 15, 385-393.

Spanier, B. (2014). Transcriptional and functional regulation of the intestinal peptide transporter PEPT1. J Physiol 592, 871-879.

Spanier, B., and Rohm, F. (2018). Proton Coupled Oligopeptide Transporter 1 (PepT1) Function, Regulation, and Influence on the Intestinal Homeostasis. Compr Physiol 8, 843-869.

Sreedharan, S., Stephansson, O., Schioth, H.B., and Fredriksson, R. (2011). Long evolutionary conservation and considerable tissue specificity of several atypical solute carrier transporters. Gene 478, 11-18.

Steel, A., Nussberger, S., Romero, M.F., Boron, W.F., Boyd, C.A., and Hediger, M.A. (1997). Stoichiometry and pH dependence of the rabbit proton-dependent oligopeptide transporter PepT1. J Physiol 498 (Pt 3), 563-569.

Sun, J., Bankston, J.R., Payandeh, J., Hinds, T.R., Zagotta, W.N., and Zheng, N. (2014). Crystal structure of the plant dual-affinity nitrate transporter NRT1.1. Nature 507, 73-77.

Sykaras, A.G., Demenis, C., Cheng, L., Pisitkun, T., McLaughlin, J.T., Fenton, R.A., and Smith, C.P. (2014). Duodenal CCK cells from male mice express multiple hormones including ghrelin. Endocrinology 155, 3339-3351.

Tai, W., Chen, Z., and Cheng, K. (2013). Expression profile and functional activity of peptide transporters in prostate cancer cells. Mol Pharm 10, 477-487.

Teame, T., Zhang, Z., Ran, C., Zhang, H., Yang, Y., Ding, Q., Xie, M., Gao, C., Ye, Y., Duan, M., and Zhou, Z. (2019). The use of zebrafish (Danio rerio) as biomedical models. Animal Frontiers 9, 68-77.

Terada, T., Sawada, K., Saito, H., Hashimoto, Y., and Inui, K. (2000). Inhibitory effect of novel oral hypoglycemic agent nateglinide (AY4166) on peptide transporters PEPT1 and PEPT2. Eur J Pharmacol 392, 11-17.

Tessadori, F., Roessler, H.I., Savelberg, S.M.C., Chocron, S., Kamel, S.M., Duran, K.J., van Haelst, M.M., van Haaften, G., and Bakkers, J. (2018). Effective CRISPR/Cas9-based nucleotide editing in zebrafish to model human genetic cardiovascular disorders. Dis Model Mech 11.

Thamotharan, M., Bawani, S.Z., Zhou, X., and Adibi, S.A. (1999). Hormonal regulation of oligopeptide transporter pept-1 in a human intestinal cell line. Am J Physiol 276, C821-826.

Tian, J., He, G., Mai, K., and Liu, C. (2015). Effects of postprandial starvation on mRNA expression of endocrine-, amino acid and peptide transporter-, and metabolic enzyme-related genes in zebrafish (Danio rerio). Fish Physiol Biochem 41, 773-787.

Ton, Q.V., Leino, D., Mowery, S.A., Bredemeier, N.O., Lafontant, P.J., Lubert, A., Gurung, S., Farlow, J.L., Foroud, T.M., Broderick, J., and Sumanas, S. (2018). Collagen COL22A1 maintains vascular stability and mutations in COL22A1 are potentially associated with intracranial aneurysms. Dis Model Mech 11.

Valentini, L., Wirth, E.K., Schweizer, U., Hengstermann, S., Schaper, L., Koernicke, T., Dietz, E., Norman, K., Buning, C., Winklhofer-Roob, B.M.*, et al.* (2009). Circulating adipokines and the protective effects of hyperinsulinemia in inflammatory bowel disease. Nutrition 25, 172-181.

Valenzuela, M.J., Caruffo, M., Herrera, Y., Medina, D.A., Coronado, M., Feijoo, C.G., Munoz, S., Garrido, D., Troncoso, M., Figueroa, G., *et al.* (2018). Evaluating the Capacity of Human Gut Microorganisms to Colonize the Zebrafish Larvae (Danio rerio). Frontiers in microbiology 9, 1032.

van de Pol, I., Flik, G., and Gorissen, M. (2017). Comparative Physiology of Energy Metabolism: Fishing for Endocrine Signals in the Early Vertebrate Pool. Front Endocrinol (Lausanne) 8, 36.

Vander Heiden, M.G., Cantley, L.C., and Thompson, C.B. (2009). Understanding the Warburg effect: the metabolic requirements of cell proliferation. Science 324, 1029-1033.

Vavricka, S.R., Musch, M.W., Chang, J.E., Nakagawa, Y., Phanvijhitsiri, K., Waypa, T.S., Merlin, D., Schneewind, O., and Chang, E.B. (2004). hPepT1 transports muramyl dipeptide, activating NF-kappaB and stimulating IL-8 secretion in human colonic Caco2/bbe cells. Gastroenterology 127, 1401-1409.

Vavricka, S.R., Musch, M.W., Fujiya, M., Kles, K., Chang, L., Eloranta, J.J., Kullak-Ublick, G.A., Drabik, K., Merlin, D., and Chang, E.B. (2006). Tumor necrosis factor-alpha and interferon-gamma increase PepT1 expression and activity in the human colon carcinoma cell line Caco-2/bbe and in mouse intestine. Pflugers Arch 452, 71-80.

Verri, T., Barca, A., Pisani, P., Piccinni, B., Storelli, C., and Romano, A. (2017). Di- and tripeptide transport in vertebrates: the contribution of teleost fish models. J Comp Physiol B 187, 395-462.

Verri, T., Kottra, G., Romano, A., Tiso, N., Peric, M., Maffia, M., Boll, M., Argenton, F., Daniel, H., and Storelli, C. (2003). Molecular and functional characterisation of the zebrafish (Danio rerio) PEPT1-type peptide transporter. FEBS Lett 549, 115-122.

Verri, T., Maffia, M., Danieli, A., Herget, M., Wenzel, U., Daniel, H., and Storelli, C. (2000). Characterisation of the H(+)/peptide cotransporter of eel intestinal brush-border membranes. J Exp Biol 203, 2991-3001.

Verri, T., Romano, A., Barca, A., Kottra, G., Daniel, H., and Storelli, C. (2009). Transport of di- and tripeptides in teleost fish intestine. Aquaculture Research 41, 641-653.

Verri, T., Terova, G., Dabrowski, K., and Saroglia, M. (2011). Peptide transport and animal growth: the fish paradigm. Biol Lett 7, 597-600.

Verri, T., Terova, G., Romano, A., Barca, A., Pisani, P., Storelli, C., and Saroglia, M. (2012). The SoLute Carrier (SLC) Family Series in Teleost Fish. In: Functional Genomics in Aquaculture. pp. 219-320.

Viennois, E., Ingersoll, S.A., Ayyadurai, S., Zhao, Y., Wang, L., Zhang, M., Han, M.K., Garg, P., Xiao, B., and Merlin, D. (2016). Critical role of PepT1 in promoting colitis-associated cancer and therapeutic benefits of the anti-inflammatory PepT1-mediated tripeptide KPV in a murine model. Cell Mol Gastroenterol Hepatol 2, 340-357.

Viennois, E., Pujada, A., Zen, J., and Merlin, D. (2018). Function, Regulation, and Pathophysiological Relevance of the POT Superfamily, Specifically PepT1 in Inflammatory Bowel Disease. Compr Physiol 8, 731-760.

Vig, B.S., Stouch, T.R., Timoszyk, J.K., Quan, Y., Wall, D.A., Smith, R.L., and Faria, T.N. (2006). Human PEPT1 pharmacophore distinguishes between dipeptide transport and binding. J Med Chem 49, 3636-3644.

Volff, J.N. (2005). Genome evolution and biodiversity in teleost fish. Heredity (Edinb) 94, 280-294.

Volkoff, H. (2019). Fish as models for understanding the vertebrate endocrine regulation of feeding and weight. Mol Cell Endocrinol 497, 110437.

Volkoff, H., Xu, M., MacDonald, E., and Hoskins, L. (2009). Aspects of the hormonal regulation of appetite in fish with emphasis on goldfish, Atlantic cod and winter flounder: notes on actions and responses to nutritional, environmental and reproductive changes. Comp Biochem Physiol A Mol Integr Physiol 153, 8-12.

Wang, J., Yan, X., Lu, R., Meng, X., and Nie, G. (2017). Peptide transporter 1 (PepT1) in fish: A review. Aquaculture and Fisheries 2.

Wang, P., Lu, Y.Q., Wen, Y., Yu, D.Y., Ge, L., Dong, W.R., Xiang, L.X., and Shao, J.Z. (2013). IL-16 induces intestinal inflammation via PepT1 upregulation in a pufferfish model: new insights into the molecular mechanism of inflammatory bowel disease. J Immunol 191, 1413-1427.

Won, E.T., Douros, J.D., Hurt, D.A., and Borski, R.J. (2016). Leptin stimulates hepatic growth hormone receptor and insulin-like growth factor gene expression in a teleost fish, the hybrid striped bass. Gen Comp Endocrinol 229, 84-91.

Wuensch, T., Schulz, S., Ullrich, S., Lill, N., Stelzl, T., Rubio-Aliaga, I., Loh, G., Chamaillard, M., Haller, D., and Daniel, H. (2013). The peptide transporter PEPT1 is expressed in distal colon in rodents and humans and contributes to water absorption. Am J Physiol Gastrointest Liver Physiol 305, G66-73.

Wuensch, T., Ullrich, S., Schulz, S., Chamaillard, M., Schaltenberg, N., Rath, E., Goebel, U., Sartor, R.B., Prager, M., Buning, C.*, et al.* (2014). Colonic expression of the peptide transporter PEPT1 is downregulated during intestinal inflammation and is not required for NOD2-dependent immune activation. Inflamm Bowel Dis 20, 671-684.

Yamada, T., Katagiri, H., Ishigaki, Y., Ogihara, T., Imai, J., Uno, K., Hasegawa, Y., Gao, J., Ishihara, H., Niijima, A., *et al.* (2006). Signals from intra-abdominal fat modulate insulin and leptin sensitivity through different mechanisms: neuronal involvement in food-intake regulation. Cell metabolism 3, 223-229.

Yamashita, T., Shimada, S., Guo, W., Sato, K., Kohmura, E., Hayakawa, T., Takagi, T., and Tohyama, M. (1997). Cloning and functional expression of a brain peptide/histidine transporter. J Biol Chem 272, 10205-10211.

Yao, Y., Sun, S., Fei, F., Wang, J., Wang, Y., Zhang, R., Wu, J., Liu, L., Liu, X., Cui, Z., *et al.* (2017). Screening in larval zebrafish reveals tissue-specific distribution of fifteen fluorescent compounds. Dis Model Mech 10, 1155-1164.

Yeung, A.K., Basu, S.K., Wu, S.K., Chu, C., Okamoto, C.T., Hamm-Alvarez, S.F., von Grafenstein, H., Shen, W.C., Kim, K.J., Bolger, M.B., *et al.* (1998). Molecular identification of a role for tyrosine 167 in the function of the human intestinal proton-coupled dipeptide transporter (hPepT1). Biochem Biophys Res Commun 250, 103-107.

Zang, L., Maddison, L.A., and Chen, W. (2018). Zebrafish as a Model for Obesity and Diabetes. Front Cell Dev Biol 6, 91.

Zhang, E.Y., Emerick, R.M., Pak, Y.A., Wrighton, S.A., and Hillgren, K.M. (2004a). Comparison of human and monkey peptide transporters: PEPT1 and PEPT2. Mol Pharm 1, 201-210.

Zhang, E.Y., Fu, D.J., Pak, Y.A., Stewart, T., Mukhopadhyay, N., Wrighton, S.A., and Hillgren, K.M. (2004b). Genetic polymorphisms in human proton-dependent dipeptide transporter PEPT1: implications for the functional role of Pro586. J Pharmacol Exp Ther 310, 437-445.

Zhang, Y., Zhang, Y., Sun, K., Meng, Z., and Chen, L. (2019). The SLC transporter in nutrient and metabolic sensing, regulation, and drug development. J Mol Cell Biol 11, 1-13.

Zhu, T., Chen, X.Z., Steel, A., Hediger, M.A., and Smith, D.E. (2000). Differential recognition of ACE inhibitors in Xenopus laevis oocytes expressing rat PEPT1 and PEPT2. Pharm Res 17, 526-532.

Ziegler, T.R., Fernandez-Estivariz, C., Gu, L.H., Bazargan, N., Umeakunne, K., Wallace, T.M., Diaz, E.E., Rosado, K.E., Pascal, R.R., Galloway, J.R., *et al.* (2002). Distribution of the H+/peptide transporter PepT1 in human intestine: up-regulated expression in the colonic mucosa of patients with short-bowel syndrome. Am J Clin Nutr 75, 922-930.

Zietek, T., and Daniel, H. (2015). Intestinal nutrient sensing and blood glucose control. Curr Opin Clin Nutr Metab Care 18, 381-388.

Zietek, T., and Rath, E. (2016). Inflammation Meets Metabolic Disease: Gut Feeling Mediated by GLP-1. Front Immunol 7, 154.

Zietek, T., Rath, E., Haller, D., and Daniel, H. (2015). Intestinal organoids for assessing nutrient transport, sensing and incretin secretion. Sci Rep 5, 16831.

Zucchelli, M., Torkvist, L., Bresso, F., Halfvarson, J., Hellquist, A., Anedda, F., Assadi, G., Lindgren, G.B., Svanfeldt, M., Janson, M.*, et al.* (2009). PepT1 oligopeptide transporter (SLC15A1) gene polymorphism in inflammatory bowel disease. Inflamm Bowel Dis 15, 1562-1569.

Supplementary Material

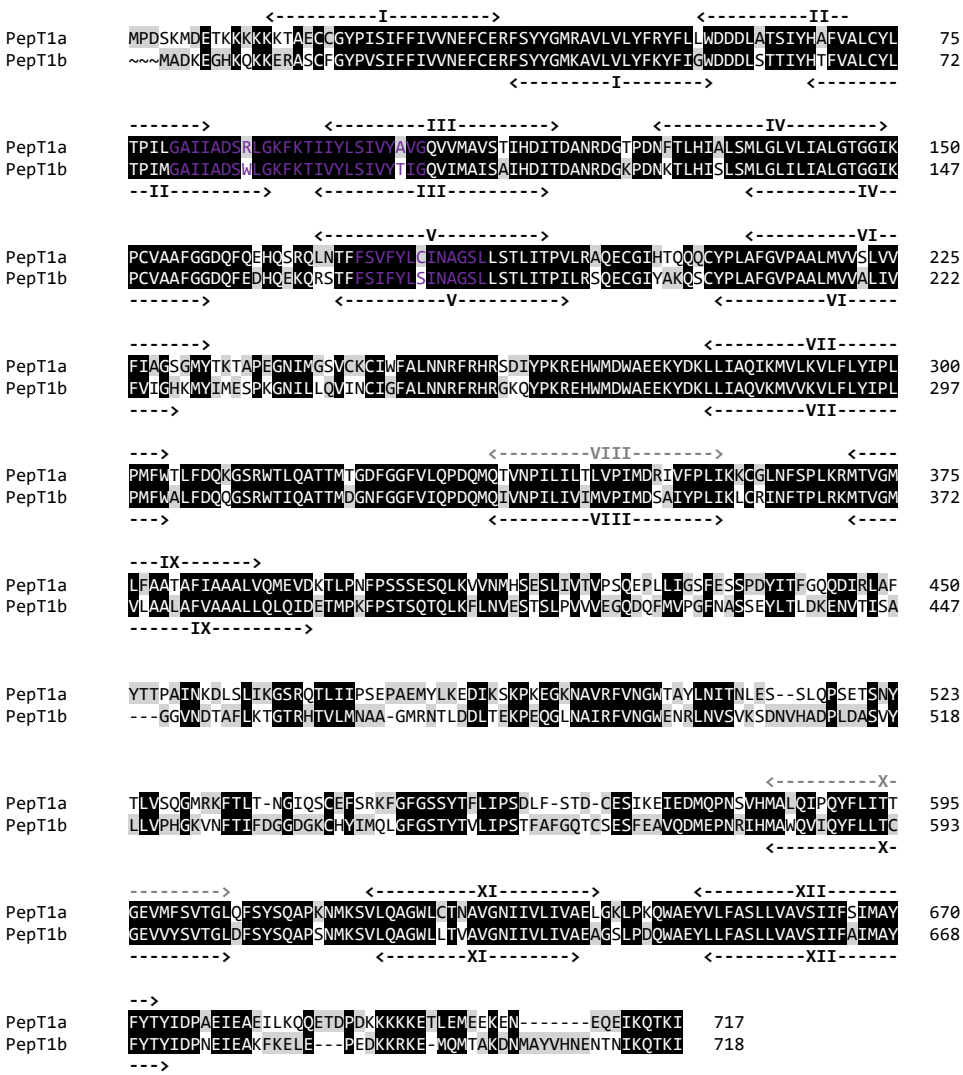

Figure S.1 Pairwise alignment between zebrafish PepT1a (Slc15a1a) and PepT1b (Slc15a1b) amino acid sequences obtained by using Clustal Omega (https://www.ebi.ac.uk/Tools/msa/clustalo/)(Sievers et al., 2011) and edited using GeneDoc 2.7 software. The predicted (https://prosite.expasy.org/scanprosite/) (Hulo et al., 2006) conserved PTR2 family proton/oligopeptide symporters signatures (in zebrafish PepT1a, motif 1 - PROSITE pattern PS01022 - amino acid residues 80-104; and motif 2 - PROSITE pattern PS01023 - amino acid residues 173-185) are colored in purple. In the amino acid sequence, putative transmembrane domains are named I to XII. Weak predicted transmembrane domains (in zebrafish PepT1a, transmembrane domains VIII and X) are colored in gray.

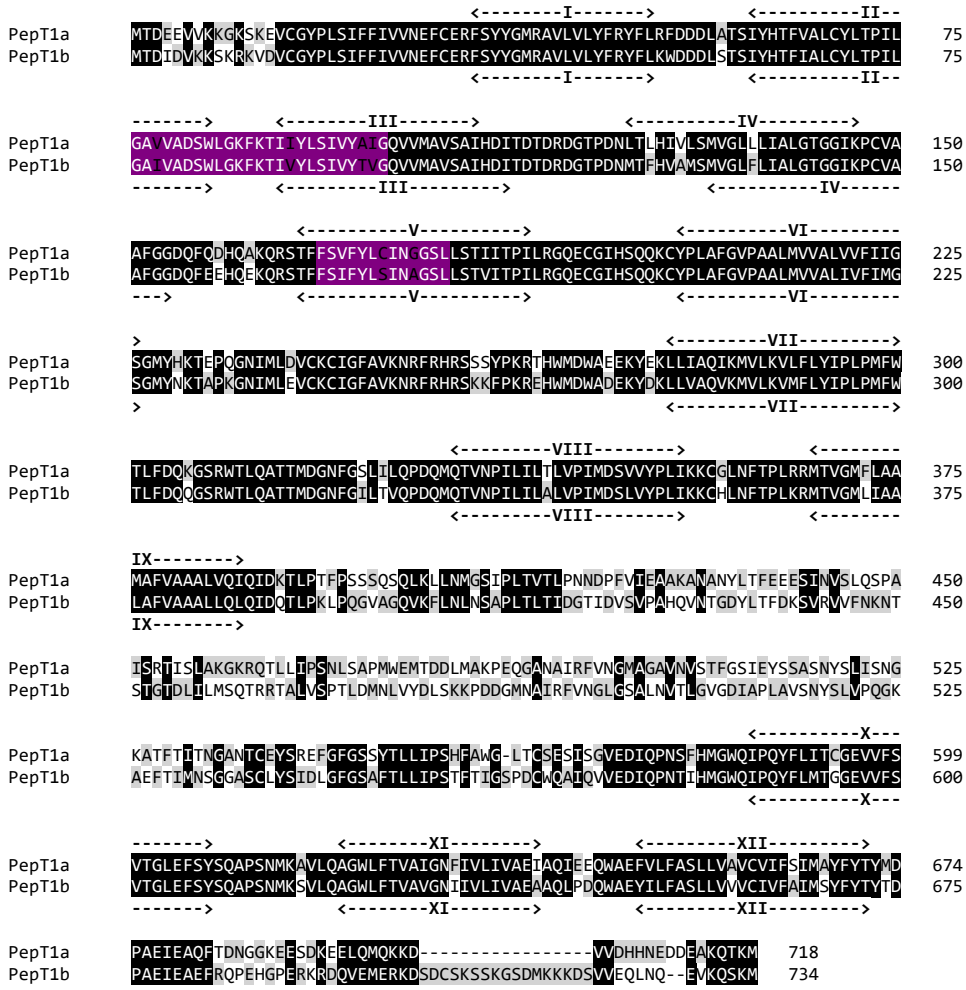

Figure S.2 Pairwise alignment between Atlantic salmon PepT1a (Slc15a1a) and PepT1b (Slc15a1b) amino acid sequences obtained by using Clustal Omega (https://www.ebi.ac.uk/Tools/msa/clustalo/) (Sievers et al., 2011) and edited using GeneDoc 2.7 software. The predicted (https://prosite.expasy.org/scanprosite/) (Hulo et al., 2006) conserved PTR2 family proton/oligopeptide symporters signatures (in Atlantic salmon PepT1a, motif 1 - PROSITE pattern PS01022 - amino acid residues 76-100; and motif 2 - PROSITE pattern PS01023 - amino acid residues 169-181) are colored in purple. In the amino acid sequence, putative transmembrane domains are named I to XII.